

# Neural Dynamic Data Valuation

Zhangyong Liang<sup>a</sup>, Huanhuan Gao<sup>\*b</sup>, and Ji Zhang<sup>\*c</sup>

This manuscript was compiled on June 13, 2024

Data constitute the foundational component of the data economy and its marketplaces. Efficient and fair data valuation has emerged as a topic of significant interest. Many methods based on marginal contribution have shown promising results in various downstream tasks. However, they are well known to be computationally expensive as they require training a large number of utility functions, which are used to evaluate the usefulness or value of a given dataset for a specific purpose. As a result, it has been recognized as infeasible to apply these methods to a data marketplace involving large-scale datasets. Consequently, a critical issue arises: how can the re-training of the utility function be avoided? To address this issue, we propose a novel data valuation method from the perspective of optimal control, named the neural dynamic data valuation (NDDV). Our method has solid theoretical interpretations to accurately identify the data valuation via the sensitivity of the optimal control state. In addition, we implement a data re-weighting strategy to capture the unique features of data points, ensuring fairness through the interaction between data points and the mean-field states. Notably, our method requires only training once to estimate the value of all data points, significantly improving the computational efficiency. We conduct comprehensive experiments using different datasets and tasks. The results demonstrate that the proposed NDDV method outperforms the existing state-of-the-art data valuation methods in accurately identifying data points with either high or low values and is more computationally efficient.

data economy | data marketplace | data valuation | marginal contribution | optimal control

Data has become a valuable asset in the modern data-driven economy, and it is considered a form of property in data marketplaces (1, 2). Each dataset possesses an individual value, which helps facilitate data sharing, exchange, and reuse among various entities, such as businesses, organizations, and researchers. The value of data is influenced by a wide range of factors, including the size of the dataset, the dynamic changes in the data marketplace, the decision-making processes that rely on the data, and the inherent noise or errors within the data itself. These factors can significantly impact the usefulness and reliability of the data for different applications.

Quantifying the value of data, which is termed data valuation, is crucial for establishing a fair and efficient data marketplace. By accurately assessing the value of datasets, buyers and sellers can engage in informed transactions, leading to the formation of rational data products. This process of buying and selling data based on its assessed value is known as data pricing (3). Effective data pricing strategies enable data owners to receive fair compensation for their data while allowing data consumers to acquire valuable datasets that align with their needs and budget.

However, accurately and fairly assessing the value of data in real-world scenarios remains a fundamental challenge. The complex interplay of various factors, such as market dynamics, data quality, and the specific context in which the data is used, makes it difficult to develop a universal valuation framework. Moreover, ensuring fairness in data valuation is essential to prevent bias and discrimination against certain data owners or types of data. Another significant challenge is the computational efficiency of data valuation methods when dealing with large datasets, which are prevalent in many real-world applications. Traditional data valuation methods often struggle to scale effectively to massive datasets, making it difficult to assess the value of data in a timely and cost-effective manner. Addressing these challenges requires the development of sophisticated data valuation methods that can account for the complex nature of data value, promote equitable practices in data marketplaces, and efficiently handle large-scale datasets.

Contribution-based methods for data valuation aim to quantify the value of individual data points by measuring their impact on the performance of a machine learning model. These methods typically assess the marginal contribution of each data point to the model's performance, which can be used as a proxy for its value.

## Significance Statement

Data is a form of property, and it is the fuel that powers the data economy and marketplaces. However, efficiently and fairly evaluating data value remains a significant challenge, and existing marginal contribution-based methods face computational challenges due to requiring training numerous models. Utilizing the optimal control theory, we view data valuation as a dynamic optimization process and propose a neural dynamic data valuation method. Our method implements a data re-weighting strategy to capture the unique features of data points, ensuring fairness through the interaction between data points and mean-field states. Furthermore, the training is required only once to obtain the value of all data points, which significantly improves the computational efficiency of data valuation problems.

Author affiliations: <sup>a</sup>National Center for Applied Mathematics, Tianjin University, Tianjin 300072, PR China; <sup>b</sup>School of Mechanical and Aerospace Engineering, Jilin University, Changchun 130025, PR China; <sup>c</sup>School of Mathematics, Physics and Computing, University of Southern Queensland, Australia

The authors declare no competing interests.

<sup>1</sup>Correspondence and requests for materials should be addressed. Email: gao.huanhuan@jlu.edu.cn, ji.zhang@unisuq.edu.au.

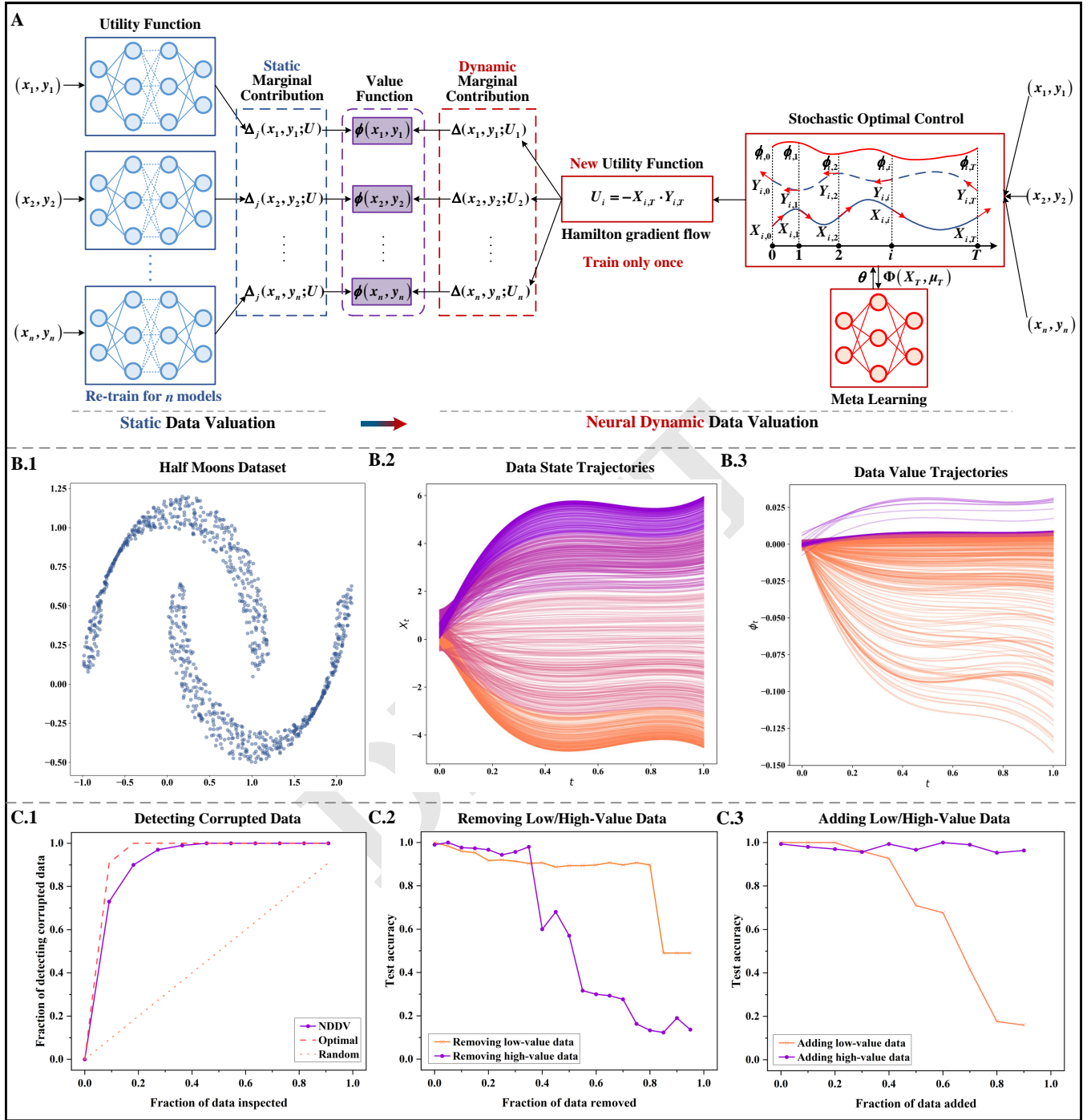


**Fig. 1. Neural dynamic data valuation schematic and results.** (A) shows a comparison between the NDDV method and existing data valuation methods. It is evident that the NDDV method transforms the static composite calculation method of existing data valuation into a dynamic optimization process, defining a new utility function and dynamic marginal contribution. Compared to existing data valuation methods, the NDDV method requires only one training session to determine the value of all data points, significantly enhancing computational efficiency. Taking the half-moons dataset illustrated in Panel (B.1) as an example, we demonstrate some results of the NDDV method to indicate its effectiveness. Panels (B.2), (B.3) display the trajectories of data states and values over time, revealing the relationship between the dynamic characteristics of the data and their intrinsic values. Panels (C.1), (C.2), (C.3) display the effectiveness of the NDDV method in three typical data valuation experiments: detecting corrupted data, removing low/high-value data, and adding low/high-value data.

A standard contribution-based data valuation method involves assessing the impact of adding or removing data points on model performance by calculating their marginal contributions. One of the earliest methods proposed for computing marginal contributions is the leave-one-out (LOO) method. This method entails removing a specific piece of data from the entire dataset and using the difference in model performance before and after its removal as the marginal contribution (4, 5). However, the leave-one-out (LOO) method has several limitations. Firstly, it requires retraining the model for each data point, which can be computationally expensive, especially for large datasets. Secondly, the LOO method may not capture the interactions between data points, as it only considers the impact of removing a single data point at a time, potentially overlooking the synergistic or antagonistic effects among data points.

Another class of methods calculates the Shapley value based on cooperative game theory (6), which distributes the average marginal contributions fairly as the value of the data points (7–9). The Shapley-based data valuation methods have been widely applied in various domains, such as high-quality data mining, data marketplace design, and medical image screening, due to their ability to provide a fair and theoretically grounded valuation. However, these methods require the prior setting of utility functions and estimate marginal contributions through the exponential combination of training numerous models, leading to high computational costs in the data valuation process. To address this issue, a series of improved approximation algorithms have been proposed to reduce the computational burden while maintaining valuation accuracy. The use of  $k$ -Nearest Neighbors (10) or linear models (11) for data valuation has somewhat enhanced valuation efficiency but struggles with high-dimensional data. Then, a data valuation method employing a linearly sparse LASSO model has been proposed (12), which improves sampling efficiency under the assumption of sparsity. However, it requires additional training in the LASSO model and performs poorly in identifying low-quality data. Another recent development is the out-of-bag (OOB) estimation method (13), introduced for efficient data valuation problems. Although it reduces the number of models to be trained, it still requires training numerous models when faced with new data points.

Recent developments in marginal contribution-based data valuation methods have focused on capturing the interaction characteristics among data points by calculating marginal contributions through the removal or addition of data points and averaging the model performance differences across all combinations. However, this method raises a fundamental question: is every outcome of the exponential level of combinatorial calculations genuinely essential? Given the goal of capturing the average impact of data points within the dataset, it may be more efficient to directly model the interactions between the data points and the mean-field.

To address the question raised, we propose **Neural Dynamic Data Valuation (NDDV)**, a novel data valuation method that reformulates the classical valuation criteria in terms of stochastic optimal control in continuous time, as illustrated in Fig. 1. This reformulation involves expressing the traditional valuation methods, such as marginal contribution-based approaches, using the framework of stochastic optimal control theory. The NDDV method obtains the optimal representation

of data points in a latent space, which we refer to as the optimal state of data points, through dynamic interactions between data point states and the mean-field state. The NDDV method leads to a novel method for calculating marginal contributions, where the optimal state of data points captures the essential characteristics and relationships among data points that contribute to their value within the dataset.

Our method establishes a connection with the marginal contribution calculation based on cooperative game theory, which focuses on the contribution of individual data entities to a coalition of data points in the context of data valuation. Instead of calculating the marginal contribution of each data point separately, the NDDV method, by leveraging the mean-field approximation and the optimal state of data points, explores the potential for a more efficient and unified method to data valuation. This unified method aims to compute the overall value of the dataset and then redistribute the contributions among the individual data points, taking into account their optimal states and interactions with the mean-field state.

The proposed NDDV method reformulates the data valuation paradigm from the perspective of optimal control. Existing data valuation methods based on marginal contributions adopt a discrete combinatorial computation model, which only accounts for the static interactions among data points. In contrast, under mean-field optimal control, data points undergo a continuous optimization process to derive mean-field optimal control strategies. This method facilitates the manifestation of the value of data points through their interactions with the mean-field state, thereby capturing the dynamic interplay among data points. By considering the continuous optimization process and the interactions between data points and the mean-field state, this method provides a more comprehensive and dynamic representation of data value compared to the static and discrete nature of traditional marginal contribution-based methods.

**Our Contributions.** This paper has the following three contributions:

- We propose a new data valuation method from the perspective of stochastic optimal control, formulating data valuation as a continuous-time optimization process.
- We develop a novel marginal contribution metric that captures the impact of data through the sensitivity of its optimal control state.
- The proposed NDDV method requires only a single training session, thereby avoiding the need for repetitive training of the utility function and significantly enhancing computational efficiency.

## Related Works

**Dynamics and Optimal Control Theory.** The dynamical perspective, viewing Deep Neural Networks (DNNs) as continuous-time dynamical systems, has provided new insights into their architecture and training processes (14). This method equates the propagating rule in deep residual networks with a one-step discretization of the forward Euler scheme on an ordinary differential equation (ODE), enhancing numerical approximations in residual blocks (15, 16). Furthermore, the deep continuum limit allows for transport analysis using Wasserstein

geometry (17). This analogy extends to optimization and control mechanisms in algorithms, promoting new mean-field optimal control problem frameworks for reinterpreting supervised learning methodologies (18, 19). Inspired by control theory, new training algorithms have been developed (20–22). A similar analysis can be applied to stochastic gradient descent (SGD) by viewing it as a stochastic dynamical system. Most previous discussions on implicit bias formulate SGD as stochastic Langevin dynamics (23). Recent studies also consider other stochastic models like Lévy processes (24). Stability analyses of Gram matrix dynamics induced by DNNs indicate global optimality (25, 26), leading to optimal adaptive strategies for tuning hyper-parameters in SGD, such as learning rate, momentum, and batch size (27, 28).

**Data Valuation.** Existing data valuation methods, such as LOO (5), DataShapley (7, 29), BetaShapley (30), DataBanzhaf (31), InfluenceFunction (32) and so on, generally require knowledge of the underlying learning algorithms and are known for their substantial computational demands. Notably, the work by (10) proposes a  $k$ -Nearest Neighbor classifier as a learning-agnostic proxy model for data valuation. Still, it is less effective and efficient than the NDDV method in distinguishing data quality. Alternatively, measuring the utility of a dataset by the volume (33) provides an algorithm-agnostic calculation but fails to detect label errors. Assessing data points with the Shapley value is still costly for large datasets. Moreover, the work by (34) introduces a learning-agnostic data valuation method using class-wise Wasserstein distances, yet it relies on a validation set and has limitations in assessing fairness. Recently, a method based on the out-of-bag estimate is computationally efficient and outperforms existing methods (13). Despite its advantages, this method is constrained by the sequential dependency of weak learners in boosting, limiting its direct applicability to downstream tasks. Marginal contribution-based methods have been studied and applied to various machine learning problems, including feature attribution (35, 36), model explanation (37, 38), and collaborative learning (39, 40). Among these works, the Shapley value is one of the most widely used marginal contribution-based methods, and many alternative methods have been studied by relaxing some of the underlying fair division axioms (41, 42). Additionally, some methods are independent of marginal contributions. For instance, in the data valuation literature, a data value estimator model using reinforcement learning is proposed by (43). This method combines data valuation with model training using reinforcement learning. However, it measures data usage likelihood, not the impact on model quality.

To our knowledge, optimal control has not yet been exploited for data valuation problems. The proposed NDDV method diverges from existing methods in several key aspects. First, we construct a data valuation framework from the perspective of optimal control, marking a pioneering endeavor in this field. Second, whereas most data valuation methods rely on calculating marginal contributions within cooperative games, necessitating repetitive training of a predefined utility function, our method derives control strategies from a continuous time optimization process. The gradient of the Hamiltonian concerning the control states serves as the marginal contribution, representing a novel attempt at data valuation problems. Finally, we transform the interactions

among data points into interactions between data points and the mean-field state, thereby circumventing the need for exponential combinatorial computations.

## Problem Formulation and Preliminaries

In this section, we formally describe the data valuation problem. Then, we review the concept of marginal contribution-based data valuation.

In various downstream tasks, data valuation aims to fairly assign model performance scores to each data point, reflecting the contribution of individual data points. Let  $[N] = \{1, \dots, N\}$  denotes a training set of size  $n$ . We define the training dataset as  $\mathcal{D} = (x_i, y_i)_{i=1}^N$ , where each pair  $(x_i, y_i)$  consists of an input  $x_i$  from the input space  $\mathcal{X} \subset \mathbb{R}^d$  and a corresponding label  $y_i$  from the label space  $\mathcal{Y} \subset \mathbb{R}$ , pertaining to the  $i$ -th data point. To measure the contributions of data points, we define a utility function  $U : 2^N \rightarrow \mathbb{R}$ , which takes a subset of the training dataset  $\mathcal{D}$  as input and outputs the performance score that is trained on that subset. In classification tasks, for instance, a common choice for  $U$  is the test classification accuracy of an empirical risk minimizer trained on a subset of  $\mathcal{D}$ . Formally, we set  $U(S) = \text{metric}(\mathcal{A}(S))$ , where  $\mathcal{A}$  denotes a base model trained on the dataset  $S$ , and  $\text{metric}$  represents the metric function for evaluating the performance of  $\mathcal{A}$ , e.g., the accuracy of a finite hold-out validation set. When  $S = \{\}$  is the empty set,  $U(S)$  is set to be the performance of the best constant model by convention. The utility function is influenced by the selection of learning algorithms and a specific class. However, this dependency is omitted in our discussion, prioritizing the comparative analysis of data value formulations instead. For a set  $S$ , we denote its power set by  $2^S$  and its cardinality by  $|S|$ . We set  $[j] := \{1, \dots, j\}$  for  $j \in \mathbb{N}$ .

A standard method for quantifying data values is the marginal contribution, which measures the average change in a utility function when a particular datum is removed from a subset of the entire dataset  $\mathcal{D}$ . We denote the data value of data point  $(x_i, y_i) \in \mathcal{D}$  computed from  $U$  as  $\phi(x_i, y_i; U)$ . The following sections review well-known notions of data value.

**Loo Metric.** A simple data value measure is the LOO metric, which calculates the change in model performance when the data point  $(x_i, y_i)$  is excluded from the training set  $N$

$$\phi_{\text{loo}}(x_i, y_i; U) \triangleq U(N) - U(N \setminus (x_i, y_i)). \quad [1]$$

The LOO metric quantifies the impact of removing a specific data point  $(x_i, y_i)$  from the entire dataset  $\mathcal{D}$ . This metric incorporates Cook’s distance and the approximate empirical influence function to measure changes. However, it is known to be computationally feasible, but it often assigns erroneous values that are close to zero (44).

**Static Marginal Contribution.** Existing standard data valuation methods can be expressed as a function of the marginal contribution. For a specific utility function  $U$  and  $j \in [N]$ , the marginal contribution of  $(x_i, y_i) \in \mathcal{D}$  with respect to  $[j]$  data points is defined as follows

$$\Delta_j(x_i, y_i; U) \triangleq \frac{1}{\binom{N-1}{j-1}} \sum_{S \in \mathcal{D} \setminus (x_i, y_i)} U(S \cup (x_i, y_i)) - U(S), \quad [2]$$

where  $\mathcal{D}^{\setminus(x_i, y_i)} = \{S \subseteq \mathcal{D} \setminus (x_i, y_i) : |S| = j - 1\}$ . Eq.2 is a combination to calculate the error in adding  $(x_i, y_i)$ , which is a static metric.

**Shapley Value Metric.** The Shapley value metric is considered the most widely studied data valuation scheme, originating from cooperative game theory. At a high level, it appraises each point based on the average utility change caused by adding the point into different subsets. The Shapley value of a data point  $i$  is defined as

$$\phi_{\text{Shap}}(x_i, y_i; U) \triangleq \frac{1}{N} \sum_{j=1}^N \Delta_j(x_i, y_i; U). \quad [3]$$

As its extension, Beta Shapley is proposed by is expressed as a weighted mean of marginal contributions

$$\phi_{\text{Beta}}(x_i, y_i; U) \triangleq \sum_{j=1}^N \beta_j \Delta_j(x_i, y_i; U). \quad [4]$$

where  $\beta = (\beta_1, \dots, \beta_n)$  is a predefined weight vector such that  $\sum_{j=1}^N \beta_j = 1$  and  $\beta_j \geq 0$  for all  $j \in [N]$ . A functional form of Eq.4 is also known as semi-values.

Shapley value metric is empirically more effective than the LOO metric in many downstream tasks such as mislabeled data detection in classification settings (7, 30). However, their computational complexity is well known to be expensive, making it infeasible to apply to large datasets (29, 31, 45). As a result, most existing data valuation methods have focused on small datasets, *e.g.*,  $n \leq 1000$ .

### NDDV: A Dynamic Data Valuation Notion

Existing methods are often formulated as a player valuation problem in cooperative game theory. The fundamental problem in cooperative game theory is to assign essential vectors to all players. A standard method for quantifying data values is to use the marginal contribution as in Eq.2. The marginal contribution-based method considers the interactions among data points, ensuring a fair distribution of contributions of each data point. This static combinatorial computation method measures the average change in a utility function as data points are added or removed, which is achieved by iterating through all possible combinations among the data points, resulting in an exponential level of computational cost. Despite a series of efforts to reduce the computational burden of calculating marginal contributions, the challenge of avoiding repetitive training of the utility function remains difficult to overcome.

**Learning Stochastic Dynamics from Data.** To address this issue, we concentrate on learning stochastic dynamics from data, emphasizing the interactions among data points and avoiding inefficient pairwise combinatorial gaming. In fact, data points often exist in the form of coalitions influenced by collective decisions, and this influence can be essentially considered as a utility function. The interactions among data points under such conditions tend to be dynamic and stochastic (see Fig.2). Furthermore, data points evolve over time to get optimal control trajectories by maximizing coalition gains. Aiming at that target, we construct the stochastic dynamics of data points as a stochastic optimal control process (more details in SI Appendix 1).

The following minimization of the stochastic control problem is considered, involving a cost function with naive partial information. We define the stochastic optimal control as follows

$$\mathcal{L}(\psi) \triangleq \mathbb{E} \left[ \int_0^T R(X_t, \psi_t) dt + \Phi(X_T) \right], \quad [5]$$

where  $\psi : [0, T] \rightarrow \Psi \subset \mathbb{R}^p$  is the stochastic control parameters and  $X_t = (X_{1,t}, \dots, X_{N,t}) \in \mathbb{R}^{d \times N}$  is the data state for all  $t \in [0, T]$ . Then,  $\Phi : \mathbb{R}^d \rightarrow \mathbb{R}$  is the terminal cost function, corresponding to the loss term in traditional machine learning tasks.  $R : \mathbb{R}^d \times \Psi \rightarrow \mathbb{R}$  is the running cost function, playing a role in regularization. Eq.5 subjects to the following stochastic dynamical system

$$\begin{cases} dX_t = b(X_t, \psi_t) dt + \sigma dW_t, & t \in [0, T], \\ X_0 = x, \end{cases} \quad [6]$$

where  $b : \mathbb{R}^d \times \Psi \rightarrow \mathbb{R}^d$  is the drift function, primarily embodying a combination of a linear transformation followed by a non-linear function applied element-wise.  $\sigma : \mathbb{R} \rightarrow \mathbb{R}$  and  $W_t : \mathbb{R}^d \rightarrow \mathbb{R}^d$  are the diffusion function and the standard Wiener process, respectively. Moreover,  $\sigma$  and  $dW_t$  (the differential of  $W_t$ ) remain identical constants for all  $t$ . The control equation of Eq.6 is the Forward Stochastic Differential Equations (FSDEs).

The stochastic optimal control problem is often stated by the Stochastic Maximum Principle (SMP)(46, 47). The SMP finds the optimal control strategy by maximizing the Hamiltonian. In this optimization process, a gradient concerning control can be derived through the adjoint process of state dynamics, resulting in a gradient descent format.

We define the Hamiltonian  $H : [0, T] \times \mathbb{R}^d \times \mathbb{R}^d \times \Psi \rightarrow \mathbb{R}$  as

$$\mathcal{H}(X_t, Y_t, Z_t, \psi_t) \triangleq b(X_t, \psi_t) \cdot Y_t + \text{tr}(\sigma^\top Z_t) - R(X_t, \psi_t). \quad [7]$$

The adjoint equation is then given by the Backward Stochastic Differential Equations (BSDEs)

$$\begin{cases} dY_t = -\nabla_x \mathcal{H}(X_t, Y_t, \psi_t) dt + Z_t dW_t, & t \in [0, T], \\ Y_T = -\nabla_x \Phi(X_T), \end{cases} \quad [8]$$

where the terminal condition  $Y_T$  is an optimally controlled path for Eq.5. Then, Eq.6 and Eq.8 are combined to the framework of Forward-Backward Stochastic Differential Equation (FBSDE) of the McKean-Vlasov type. The Hamiltonian maximization condition is

$$\mathcal{H}(X_t^*, Y_t^*, Z_t^*, \psi_t^*) \geq \mathcal{H}(X_t^*, Y_t^*, Z_t^*, \psi), \quad [9]$$

In the SMP (Eq.6-9), the necessary conditions are established for the optimal solution of Eq.6. Here, the method of successive approximations (MSA) (48, 49) based on alternating propagation and optimization steps, is employed as our training strategy. We convert Eq.9 into an iterative form of the MSA, as follows

$$\psi_t^{k+1} = \arg \max_{\psi} \mathcal{H}(X_t^k, Y_t^k, Z_t^k, \psi), \quad [10]$$

The numerical process in Eq.10 is repeated until convergence as outlined in Alg.1. However,  $\psi_t^{k+1}$  may diverge if the arg-max step is executed, leading to the dominance by non-negative

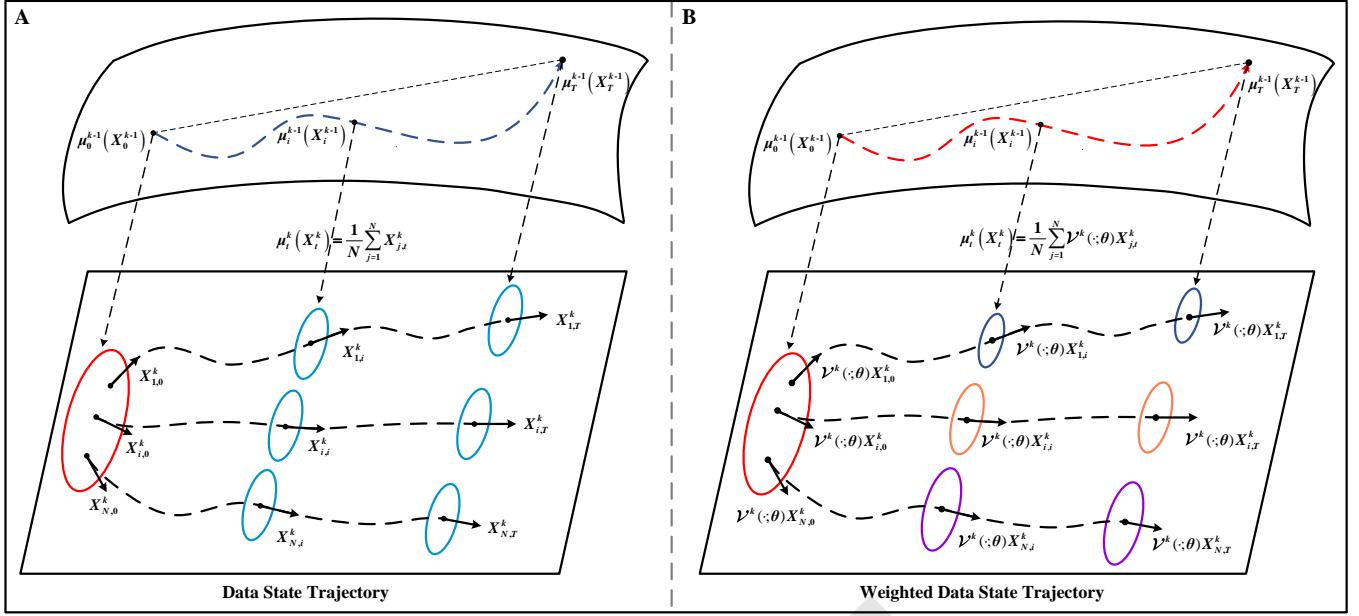


**Fig. 2. Learning data stochastic dynamic schematic.** (A) In stochastic optimal control, data points get their optimal state trajectories via dynamic interactions with the mean-field state. (B) Within the data re-weighting strategy, data points are characterized by heterogeneity. In this scenario, data points dynamically interact with the weighted mean-field state, thereby determining their optimal state trajectories.

penalty terms (49). A straightforward solution is to gradually adjust the arg-max step appropriately, ensuring that the updates remain feasible. Specifically, if  $\psi$  is differentiable, one can replace the arg-max step with a steepest ascent step

$$\psi_t^{k+1} = \psi_t^k + \alpha \nabla_{\psi} \mathcal{H}(X_t^k, Y_t^k, Z_t^k, \psi_t^k), \quad [11]$$

In fact, there is an interesting relationship of Eq.11 with classical gradient descent for back-propagation (49), as follows

$$\begin{aligned} \nabla_{\psi} \mathcal{L}(\psi_t) &= \nabla_{X_{t+1}} \Phi(X_T) \cdot \nabla_{\psi} X_{t+1} + \nabla_{\psi} R(\psi_t) \\ &= -Y_{t+1} \cdot \nabla_{\psi} X_{t+1} + \nabla_{\psi} R(\psi_t) \\ &= -\nabla_{\psi} \mathcal{H}(X_t, Y_t, Z_t, \psi_t), \end{aligned}$$

where  $X_{t+1}$  and  $X_{t+1}$  is

$$\begin{cases} X_t = X_0 + \int_0^t b(X_s, \psi_s) ds + \int_0^t \sigma dW_s, \\ Y_t = Y_0 - \int_0^t \nabla_x \mathcal{H}(X_s, Y_s, \psi_s) ds + \int_0^t Z_s dW_s, \end{cases} \quad [12]$$

Hence, Eq.11 is simply the gradient descent step

$$\psi_t^{k+1} = \psi_t^k - \alpha \nabla_{\psi} \mathcal{L}(\psi_t^k). \quad [13]$$

**Data Points Re-weighting Strategy.** To enhance the heterogeneity of data points, we employ a strategy of assigning weights to highlight the importance of individual ones. We introduce a novel SDE model for data valuation in which the weighted mean-field states are considered, and this is referred as the weighted control function for it represents the attention of each data point on different inference weights. The proofs of this issue can be found in SI Appendix 2.

Here, the meta-weighting method (50) derived from the Stackelberg game (51) is applied. The meta-network of our method, acting as the leader, makes decisions and disseminates

meta-weights across individual data points. Imposing meta-weight function  $\mathcal{V}(\Phi_i(\psi); \theta)$  on the  $i$ -th data point terminal cost, where  $\theta$  represents the hyper-parameters in the meta-network, the stochastic control formulation in Eq.5 can be modified as follows

$$\mathcal{L}(\psi; \theta) = \frac{1}{N} \sum_{i=1}^N \left[ \sum_{t=0}^{T-1} R_i(\psi_t) + \mathcal{V}(\Phi_i(\psi_T); \theta) \Phi_i(\psi_T) \right]. \quad [14]$$

where  $\mathcal{V}(\Phi_i(\psi); \theta)$  is approximated via a multi-layer perceptron (MLP) network with only one hidden layer containing a few nodes. Each hidden node utilizes the ReLU activation function, and the output is activated by the Sigmoid function to guarantee the output is located in the interval of  $[0, 1]$ . In SI Appendix 2.A, we provide the proof of convergence for Eq.14. It is evident that the training loss  $\mathcal{L}$  progressively converges to 0 through a gradient descent scheme.

Generally, the meta-dataset for meta-network requires a small, unbiased dataset with clean labels and balanced data distribution. The meta loss is

$$\ell(\psi(\theta)) = \frac{1}{M} \sum_{i=1}^M \ell_i(\psi(\theta)), \quad [15]$$

where the gradient of the meta loss  $\ell$  converges to a small number, meeting the convergence criteria (see SI Appendix 2.B for a more detailed explanation).

The optimal parameter  $\psi^*$  and  $\theta^*$  are obtained by minimizing the following

$$\begin{cases} \psi^*(\theta) = \arg \min_{\psi} \mathcal{L}(\psi; \theta), \\ \theta^* = \arg \min_{\theta} \ell(\psi^*(\theta)), \end{cases} \quad [16]$$

Yielding the optimal  $\psi^*$  and  $\theta^*$  requires two nested loops of optimization. Here, we adopt an online strategy to update

$\psi^*$  and  $\theta^*$  through a single optimization loop, respectively, to guarantee the efficiency of the algorithm. The bi-optimization proceeds in three sequential steps to update parameters. One can represent the gradient descent for back-propagation through the gradient of the Hamiltonian concerning weights

$$\begin{cases} \hat{\psi}^k = \psi^k + \frac{\alpha}{N} \sum_{i=1}^N \nabla_{\psi} \mathcal{H}_i(\psi, \mathcal{V}(\Phi_i(\psi_T^k); \theta))|_{\psi^k}, \\ \theta^{k+1} = \theta^k - \frac{\beta}{M} \sum_{i=1}^M \nabla_{\theta} \ell_i(\hat{\psi}^k(\theta))|_{\theta^k}, \\ \psi^{k+1} = \psi^k + \frac{\alpha}{N} \sum_{i=1}^N \nabla_{\psi} \mathcal{H}_i(\psi, \mathcal{V}(\Phi_i(\psi_T^k); \theta^{k+1}))|_{\psi^k}, \end{cases} \quad [17]$$

where  $\alpha$  and  $\beta$  are the step size. The parameters  $\hat{\psi}^k$ ,  $\theta^{k+1}$  and  $\psi^{k+1}$  are updated as delineated in Eq.17, where the flow form is expressed as

$$\begin{array}{ccccccc} \Phi(\psi_T^k) & \xrightarrow{\mathcal{V}(\cdot; \theta)} & \theta^k & \longrightarrow & \theta^{k+1} & \xrightarrow{\hat{\psi}^k} & \ell(\hat{\psi}^k(\theta^{k+1})) \\ \uparrow & & & & \downarrow & & \\ \psi_T^k & \longrightarrow & \hat{\psi}^k & & \psi^{k+1} & \longrightarrow & \mathcal{L}(\psi^{k+1}, \theta^{k+1}) \end{array}$$

The update of the meta parameters  $\theta^{k+1}$  in Eq.17 by backpropagation can be rewritten as

$$\theta^{k+1} = \theta^k + \frac{\alpha\beta}{n} \sum_{j=1}^n \left( \frac{1}{m} \sum_{i=1}^m G_{ij} \right) \frac{\partial \mathcal{V}(\mathcal{L}_j(\psi^k); \theta)}{\partial \theta} \bigg|_{\theta^k}, \quad [18]$$

where the derivation of  $G_{ij}$  can be found in SI Appendix 2.C. The coefficient  $\frac{1}{m} \sum_{i=1}^m G_{ij}$  on the  $j$ -th gradient term measures the similarity between a data point's gradient from training loss and the average gradient from meta loss in the mini-batch. If aligned closely, the data point's weight is likely to increase to show its effectiveness; otherwise, it may decrease.

**Mean-field Interactions.** Motivated by the cooperative game theory, existing methods provide seemingly robust mathematical justifications. However, the fair division axioms underpinning the Shapley value remain untested statistically, raising fundamental questions about their suitability in machine learning problems (42, 52). Moreover, it is not necessary for data points to iterate through all combinations to engage in the game. In fact, each data point has an optimal control strategy, optimized through dynamic interactions among others.

We consider a class of stochastic dynamics characterized with interactions among data points which are defined by functions of average individual state characteristics. Specifically, the data state  $X_t$ , with its  $N$  components  $X_{i,t}$ , represents the individual state of each data point ( $x_i, y_i$ ). A typical interaction capturing the symmetry is depicted by models where the dynamics of the individual state  $X_{i,t}$  unfold. Those are described by coupled stochastic differential equations of the following form

$$dX_{i,t} = \frac{1}{N} \sum_{j=1}^N b(X_{i,t}, X_{j,t}, \psi_{i,t}) dt + \sigma dW_{i,t}, \quad [19]$$

For a given admissible control  $\psi_{i,t}$ , we write  $X_{i,t}$  for the unique solution to Eq.19. The problem is to control the process to minimize the expectation optimally.

For the sake of simplicity, we assume that each process  $X_{i,t}$  is uni-variate. Otherwise, the notations become more involved

while the results remain essentially the same. The present discussion can accommodate models where the volatility  $\sigma$  is a function with the same structure as the function  $b$ . We refrain from considering this level of generality to keep the notations to a reasonable level. We use the notation  $\psi_t = (\psi_{1,t}, \dots, \psi_{N,t})$  for the control strategies. Notice that the stochastic dynamics Eq.19 can be rewritten in the form

$$dX_{i,t} = b(X_{i,t}, \mu_t, \psi_{i,t}) dt + \sigma dW_{i,t}, \quad [20]$$

The function  $b$  which encompasses the time, the individual state, the empirical distribution over individual states for the data points and the control, is defined as follows

$$b(X_t, \mu_t, \psi_t) = \int_{\mathbb{R}} b(X_t, X'_t, \psi_t) d\mu_t(X'_t), \quad [21]$$

where the measure  $\mu_t$  is defined as the empirical distribution of the data points states, i.e.

$$\mu_t \triangleq \frac{1}{N} \sum_{i=1}^N \delta_{X_{i,t}}, \quad [22]$$

Interactions given by functions in the form Eq.21 are called linear (order 1). We employ the function  $b$  into Eq.19, giving that the interaction between the individual states is of the form

$$\frac{1}{N^2} \sum_{j,k=1}^N b(X_{i,t}, X_{j,t}, X_{k,t}, \psi_{i,t}),$$

where the function  $b$  could be rewritten in the form

$$b(X_t, \mu_t, \psi_t) = \int_{\mathbb{R}} b(X_t, X'_t, X''_t, \psi_t) d\psi(X'_t) d\mu_t(X''_t). \quad [23]$$

Interactions of the form shown in Eq.23 are called quadratic. Given the frozen flow of measures  $\mu$ , the stochastic optimization problem is a standard stochastic control problem whose solution can be solved by the SMP.

Generally, it is understood that the stochastic control exhibits mean-field interactions when the dynamics of an individual state, as described by the coefficients of the stochastic differential equation, are influenced solely by the empirical distribution of other individual states, which implies that the interaction is entirely nonlinear according to its definition above.

To summarize the aforementioned issue, the mean-field interactions consist of minimizing simultaneously the costs in the following form

$$\mathcal{L}(\psi) = \mathbb{E} \left[ \int_0^T R(X_t, \mu_t, \psi_t) dt + \Phi(X_T, \mu_T) \right], \quad [24]$$

It is important to highlight that, due to the considerations of symmetry, we select  $R$  and  $\Phi$  to be the same for all data points.

For clarity, the focus is restricted to equilibria given by Markovian control strategies in the closed-loop feedback form

$$\psi_t = (\psi^1(X_t), \dots, \psi^N(X_t)), \quad t \in [0, T], \quad [25]$$

for some deterministic functions  $\psi_1, \dots, \psi_N$  of time and the state of the system. The strategies are categorized as distributed ones. This categorization means the control function  $\psi_i$ , associated with the data point  $(x_i, y_i)$ , relies

solely on  $X_{i,t}$ . Here,  $X_{i,t}$  represents the individual state of the data point  $(x_i, y_i)$ . It is independent of the overall system state  $X_t$ . In other words, we request that.

$$\psi_{i,t} = \psi(X_{i,t}), \quad i = 1, \dots, N, \quad [26]$$

Furthermore, due to the symmetry of the setup, the search for the equilibria is limited to scenarios where all data points use the same feedback strategy function, as the following

$$\psi_1(X_{1,t}) = \dots = \psi_N(X_{N,t}) = \psi(X_t), \quad t \in [0, T], \quad [27]$$

Here,  $\psi$  is identified as a deterministic function. With the involvement of a finite number of data points, it is assumed that each one anticipates other participants who have already selected their optimal control strategies. That means  $\psi_{1,t} = \psi(X_{1,t})$ ,  $\dots$ ,  $\psi_{i-1,t} = \psi(X_{i-1,t})$ ,  $\psi_{i+1,t} = \psi(X_{i+1,t})$ ,  $\dots$ ,  $\psi_{N,t} = \psi(X_{N,t})$ , and under this assumption, solving the optimization problem

$$\psi_i = \arg \min_{\psi} \mathcal{L}(\psi(X_{i,t})), \quad [28]$$

Additionally, it is important to note that the assumption of symmetry leads to the restriction to optimal strategies where  $\psi_1 = \psi_2 = \dots = \psi_N$ . Due to the system's exchangeability property, the individual characteristics of data points are not easily highlighted. To emphasize the non-exchangeability of optimal control strategies, the data points re-weighting is introduced. So, one can solve the weighted stochastic control problem

$$\mathcal{L}(\psi) = \mathbb{E} \left[ \int_0^T R(X_t, \mu_t, \psi_t) dt + \mathcal{V}(\Phi(\psi_T); \theta) \Phi(X_T, \mu_T) \right], \quad [29]$$

subject to the following mean-field dynamical system

$$dX_t = b(X_t, \mu_t, \psi_t) dt + \sigma dW_t. \quad [30]$$

Revisiting Eq.2, the marginal contribution primarily reflects a form of "average". To obtain the optimal control strategy for data points, complex mean-field models require a certain degree of simplification. In fact, the capability of the marginal distribution  $\mu_t$  to represent the average state of data points during the interactions can achieve an approximation of the marginal contribution in mean-field interactions. Inspired by the mean-field linear quadratic control theory, we have reformulated the marginal contribution format based cooperative games into a state control marginal contribution.

In Eq.30, the drift term within the context of the mean-field linear quadratic control can be simplified to

$$b(X_t, \mu_t, \psi_t) = a(\mu_t - X_t) + \psi_t, \quad [31]$$

where  $a$  is the positive constant. At this stage, the marginal distribution embodies the empirical average of the data state. Consequently, Eq.22 can be succinctly reformulated as follows

$$\mu_t = \frac{1}{N} \sum_{i=1}^N X_{i,t}. \quad [32]$$

where Eq.32 does not account for the heterogeneity among data points, as shown in Fig.2.(A). To emphasize the contribution of individual data points, the weighted of  $\mu_t$  should be considered

$$\mu_t = \frac{1}{N} \sum_{i=1}^N \mathcal{V}(\Phi(X_{i,T}; \mu_T)) X_{i,t}. \quad [33]$$

Fig.2.(B) shows data points dynamically interact with the weighted mean-field state of Eq.33. It is evident that the weighted optimal state trajectories capture the characteristics of individual data points' states.

In the following, we interact the control states of the data points with the control states endowed with authority, explicitly formulating the drift term of the control equation as

$$dX_t = [a(\mu_t - X_t) + \psi_t] dt + \sigma dW_t, \quad [34]$$

Applying Eq.34 into Eq.5, the discrete-time analogue of the weighted stochastic control problem is

$$\begin{aligned} \min_{\psi, \theta} \frac{1}{N} \sum_{i=1}^N \left[ \sum_{t=0}^{T-1} R_i(\psi_t) + \mathcal{V}(\Phi_i(\psi_T); \theta) \Phi_i(\psi_T) \right], \\ \text{s.t. } X_{i,t+1} = X_{i,t} + [a(\mu_t - X_{i,t}) + \psi_t] \Delta t + \sigma \Delta W. \end{aligned} \quad [35]$$

where  $\Delta t$  and  $\Delta W$  represent the uniform partitioning of the interval  $[0, T]$ .

Based on this, we define the discrete mean-field Hamiltonian in Eq.7 as

$$\begin{aligned} \mathcal{H}_i(X_{i,t}, Y_{i,t}, Z_{i,t}, \mu_t, \psi_t) = [a(\mu_t - X_{i,t}) + \psi_t] \cdot Y_{i,t} \\ + \sigma^\top Z_{i,t} - R(X_{i,t}, \mu_t, \psi_t). \end{aligned} \quad [36]$$

Then, we transform Eq.35 into the discrete-time format of the SMP to maximize the mean-field Hamiltonian  $\mathcal{H}_i$  in Eq.36. The necessary conditions can be written as follows

$$\begin{cases} X_{i,t+1}^* = X_{i,t}^* + [a(\mu_t^* - X_{i,t}^*) + \psi_t^*] \Delta t + \sigma \Delta W, \\ Y_{i,t+1}^* = Y_{i,t}^* - \nabla_x \mathcal{H}_i(X_{i,t}^*, Y_{i,t}^*, Z_{i,t}^*, \mu_t^*, \psi_t^*) \Delta t + Z_{i,t}^* \Delta W, \\ X_0^* = x, \quad Y_T^* = -\nabla_x (\mathcal{V}(\Phi_i(\psi_T); \theta) \Phi_i(X_{i,T}^*, \mu_T^*)), \\ \mathbb{E} [\mathcal{H}_i(X_{i,t}^*, Y_{i,t}^*, Z_{i,t}^*, \mu_t^*, \psi_t^*)] \geq \mathbb{E} [\mathcal{H}_i(X_{i,t}^*, Y_{i,t}^*, Z_{i,t}^*, \mu_t^*, \psi)]. \end{cases} \quad [37]$$

where Eq.37 describes the trajectory of a random variable that is completely determined by random variables. The proof for the error estimation of the weighted mean-field MSA is provided in SI Appendix 3.

**Data State Utility Function.** To perform data valuation from the perspective of stochastic dynamics, a natural choice is to redefine the utility function. The NDDV method captures the dynamic characteristics of data points through a continuous dynamical system. We establish a connection between data point states and their marginal contributions. For stochastic optimal control problems, the optimality conditions from SMP relate the sensitivities of a cost function to the adjoint variables, which is used in sensitivity analysis to estimate the influence of parameters (53, 54).

Inspired by the recent work on propagating importance scores (55), we define the individual data state utility function  $U_i(S)$  as follow

$$\begin{aligned} U_i(S) &= X_{i,T} \cdot \frac{\partial \mathcal{L}(\psi)}{\partial X_{i,T}} \\ &= X_{i,T} \cdot \nabla_x \Phi(X_{i,T}, \mu_T) \\ &= -X_{i,T} \cdot Y_{i,T}, \end{aligned} \quad [38]$$

where Eq.38 highlights the maximization of utility scores under the condition of minimal control state differences, see SI Appendix 4.A for further details. Moreover, it becomes evident that a single training suffices to obtain all data state utility functions  $U(S) = (U_1(S), U_2(S), \dots, U_n(S))$ .



**Dynamic Marginal Contribution.** Under optimal control, the data points to be evaluated obtain their respective optimal control strategies, with the value of each data point being determined by its sensitivity to the coalition’s revenue.

We can compute the value of a data point based on the calibrated sensitivity of the coalition’s cost to the final state of the data point

$$\Delta(x_i, y_i; U_i) = U_i(S) - \sum_{j \in \{1, \dots, N\} \setminus i} \frac{U_j(S)}{N-1}, \quad [39]$$

Similar to Eq.2, Eq.39 also reflects the changes in the utility function upon removing or adding data points.

Notably, Eq.39 distinguishes itself by representing the average change in the utility function and comparing individual state utility scores with others. Furthermore, it emphasizes the stochastic dynamic properties of data points, herein named the dynamic marginal contribution. The error analysis between Eq.39 and Eq.2 is presented in [SI Appendix 4.B](#).

**Dynamic Data Valuation Metric.** Learning stochastic dynamics from data reveals individual optimal control strategies through effective interactions, eliminating the need to iterate over all data points for averaging marginal contributions. The value of a data point  $(x_i, y_i)$  is equivalent to its marginal contribution, which is expressed as

$$\phi(x_i, y_i; U_i) = \Delta(x_i, y_i; U_i). \quad [40]$$

Eq.40 can be interpreted as a measure of the data point’s contribution to the terminal cost.  $\phi(x_i, y_i; U_i)$  can be either positive or negative, indicating that the evolution of the data state towards this point would increase or decrease the terminal cost, respectively.

## Experiments

In this section, we evaluate the NDDV method through three experiments: elapsed time comparison, corrupted data detection, and data points removal/addition. These experiments are designed to assess the computational efficiency, accuracy in identifying mislabeled data, and the impact of data values on model training, following the evaluation protocols commonly adopted in previous studies (7, 34, 43). The experiments demonstrate the superior computational efficiency of the NDDV method, the effectiveness of the NDDV method in accurately identifying mislabeled or corrupted data points, and the effectiveness of the NDDV method in improving model performance by selectively removing detrimental (low-value) data points and adding beneficial (high-value) ones. Details of these experiments are provided in [SI Appendix 5](#).

**Experimental Setup.** We use six datasets that are publicly available in OpenDataVal (56), many of which were used in existing works (7, 30). We compare NDDV with the following eight methods: LOO (5), DataShapley (7), BetaShapley (30), DataBanzhaf (31), InfluenceFunction (32), KNNShapley (10), AME (12), and Data-OOB (13). To make our comparison fair, we use the same number or a greater number of utility functions for existing data valuation methods compared to the NDDV method (see [SI Appendix 5](#) for a more detailed explanation).

We apply a standard normalization procedure to each dataset, ensuring that each feature has zero mean and unit

standard deviation. Next, we divide the normalized dataset into four distinct subsets: training, validation, test, and meta. The training subset is used to train the models, while the validation subset is employed to evaluate the utility functions for the existing data valuation methods. The NDDV method utilizes only a smaller subset of the training data and does not require the validation subset, as it operates independently of the utility functions. The test subset is reserved for evaluating the test accuracy during the point removal experiments, providing an unbiased assessment of the model’s performance on unseen data. The meta subset is utilized for meta-learning purposes, such as hyperparameter tuning or model selection. We fix the sizes of the validation, test, and meta subsets at 10%, 30%, and 10% of the training size, respectively. For the training subset, we consider two different sizes: 1,000 and 10,000 data points.

**Elapsed Time Comparison.** To compare the runtime performance, we focus on several data valuation methods with good computational efficiency, including InfluenceFunction, KNNShapley, AME, Data-OOB, and NDDV. In contrast, other methods like LOO, DataShapley, BetaShapley, and DataBanzhaf exhibit lower computational efficiency and are evaluated under scenarios with fewer data points. Detailed results and analysis of these methods can be found in the supplementary material ([SI Appendix 5.F](#)). First, we synthesized a binary classification dataset under a standard Gaussian distribution and sample five sets of data points with varying sizes. The set of data point sizes  $n$  is then chosen as  $\{1.0 \times 10^4, 5.0 \times 10^4, 1.0 \times 10^5, 5.0 \times 10^5, 1.0 \times 10^6\}$ , representing a wide range of dataset scales. We consider three different data feature dimensions  $d$ , specifically  $\{5, 50, 500\}$ , which correspond to three groups of time comparison experiments. To expedite the running time, we set the batch size to 1,000. The influence of batch size on the running time of all methods is presented in [SI Appendix 5.I](#).

Fig.3 presents the runtime curves of different data valuation methods as the number of data points increases in various  $d$  settings. The results clearly highlight the superior computational efficiency of the NDDV method compared to other approaches. AME and Data-OOB exhibit lower computational efficiency due to their requirement of training numerous base models. KNNShapley demonstrates high computational efficiency for small datasets due to its closed-form nature, which allows for quick computation of data values without the need for iterative training. However, as  $n$  increases, its efficiency diminishes significantly, which becomes particularly noticeable when  $n$  reaches or exceeds  $1.0 \times 10^5$ . This decline stems from the substantial memory requirements for sorting data points for each validation instance.

As for the algorithmic complexity, the computational complexity of NDDV is  $\mathcal{O}(kn/b)$  where  $k$  is the number of times the meta-learning model is trained,  $n$  is the number of data points, and  $b$  is the batch size for training. For KNNShapley, the complexity is  $\mathcal{O}(n^2 \log(n))$  when the number of data points in the validation dataset is  $\mathcal{O}(n)$ ; AME is  $\mathcal{O}(kn/b)$ ; Data-OOB is  $\mathcal{O}(Bdn \log(n))$  where  $B$  is the number of trees and  $d$  is the number of features. Therefore, it can be observed that NDDV exhibits linear complexity. Overall, NDDV is highly efficient, and it takes less than half an hour when  $(n, d) = (10^6, 500)$ .

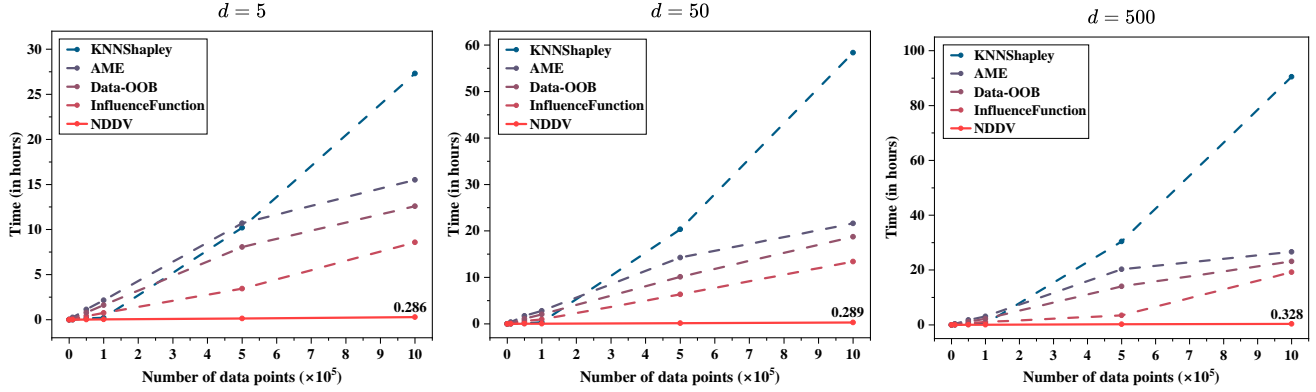


Fig. 3. Elapsed time comparison between NDDV and existing efficient methods. We employ a synthetic binary classification dataset, illustrated with feature dimensions of (left)  $d = 5$ , (middle)  $d = 50$  and (right)  $d = 500$ . As the number of data points increases, the NDDV method exhibits significantly lower elapsed time than other methods.

**Corrupted Data Detection.** In real-world scenarios, training datasets often contain noisy data points with corrupted labels or features, which can significantly degrade model performance. Assigning low values to these noisy data points is crucial for mitigating their negative impact and improving the overall quality of the dataset. In this subsection, we focus on detecting label noisy data points in six datasets from Tab.S1. To evaluate the ability of different data valuation methods to detect corrupted data, we synthesize label noise on the training datasets by introducing perturbations. Specifically, we randomly select a subset of the training data points and flip their labels, simulating a label noise rate of 10%. The training sample size is set to  $n \in \{1,000, 10,000\}$ . However, due to the low computational efficiency of LOO, DataShapley, BetaShapley, and DataBanzhaf, we compute their results only for the smaller sample size of  $n = 1,000$ . After conducting data valuation, we use the  $k$ -means clustering algorithm to divide the value of data points into two clusters based on the mean. The cluster with the lower mean is considered to be the identification of corrupted data points.

As shown in Tab.1, the F1-scores for various data valuation methods are presented, showcasing their performance under the influence of mislabeled data points across six datasets.

Overall, the NDDV method outperforms the existing methods, demonstrating its superiority in detecting corrupted data points. Moreover, Fig.4 (first column) illustrates the capability of NDDV to achieve optimal results in this task. The NDDV method exhibits remarkable performance in converging towards optimal (ground truth) results compared to the currently high-performing methods such as KNNShapley, AME, Data-OOB, and InfluenceFunction. We also explore the impact of introducing various levels of label and feature noise on its performance. In SI Appendix 5.G and SI Appendix 5.H, we systematically vary the noise rates and evaluate how the NDDV method handles these challenging scenarios. Impressively, the NDDV method maintains its superior performance even in the presence of increasing levels of label and feature noise.

**Removing and Adding Data with High/Low Value.** This subsection presents experiments conducted on the six datasets to evaluate the impact of removing and adding data points on model performance, as described in (7, 13). The experiments aim to assess the effectiveness of different data valuation methods in identifying the values of data points and their contribution to the model’s performance. In the removal experiment, data points are sequentially removed from the

Table 1. F1-score of different data valuation methods on the six datasets when (left)  $n = 1000$  and (right)  $n = 10000$ . The mean and standard deviation of the F1-score are derived from 5 independent experiments. The highest and second-highest results are highlighted in bold and underlined, respectively.

Dataset	$n = 1000$									$n = 10000$			
	LOO	Data Shapley	Beta Shapley	Data Banzhaf	Influence Function	KNN Shapley	AME	Data -OOB	NDDV	KNN Shapley	AME	Data -OOB	NDDV
2dplanes	0.17±	0.17±	0.19±	0.18±	0.21±	0.34±	0.18±	0.60±	<b>0.67±</b>	0.37±	0.010±	0.71±	<b>0.79±</b>
	0.003	0.005	0.003	0.009	0.005	0.007	0.009	0.007	0.005	0.004	0.012	0.002	0.005
electricity	0.18±	0.20±	0.20±	0.35±	0.17±	0.24±	0.18±	0.35±	<b>0.39±</b>	0.32±	0.01±	0.38±	<b>0.44±</b>
	0.004	0.004	0.006	0.002	0.003	0.006	0.010	0.002	0.002	0.001	0.009	0.003	0.002
bbc	0.19±	0.16±	0.18±	0.14±	0.16±	0.33±	0.18±	0.78±	<b>0.90±</b>	0.52±	0.01±	0.73±	<b>0.85±</b>
	0.004	0.004	0.003	0.005	0.002	0.008	0.009	0.004	0.002	0.005	0.010	0.002	0.006
IMDB	0.18±	0.16±	0.17±	0.18±	0.16±	0.21±	0.18±	<b>0.42±</b>	<u>0.26±</u>	0.29±	0.18±	0.48±	<b>0.52±</b>
	0.002	0.004	0.003	0.002	0.009	0.008	0.011	0.005	0.007	0.002	0.012	0.002	0.003
STL10	0.14±	0.17±	0.16±	0.17±	0.18±	0.25±	0.01±	0.53±	<b>0.85±</b>	0.16±	0.01±	0.77	<b>0.91±</b>
	0.006	0.004	0.002	0.005	0.009	0.007	0.009	0.003	0.008	0.009	0.012	0.002	0.003
CIFAR10	0.18±	0.19±	0.20±	0.17±	0.18±	0.24±	0.01±	0.40±	<b>0.59±</b>	0.27±	0.01±	0.46±	<b>0.58±</b>
	0.004	0.003	0.005	0.002	0.007	0.004	0.008	0.004	0.004	0.009	0.010	0.001	0.004

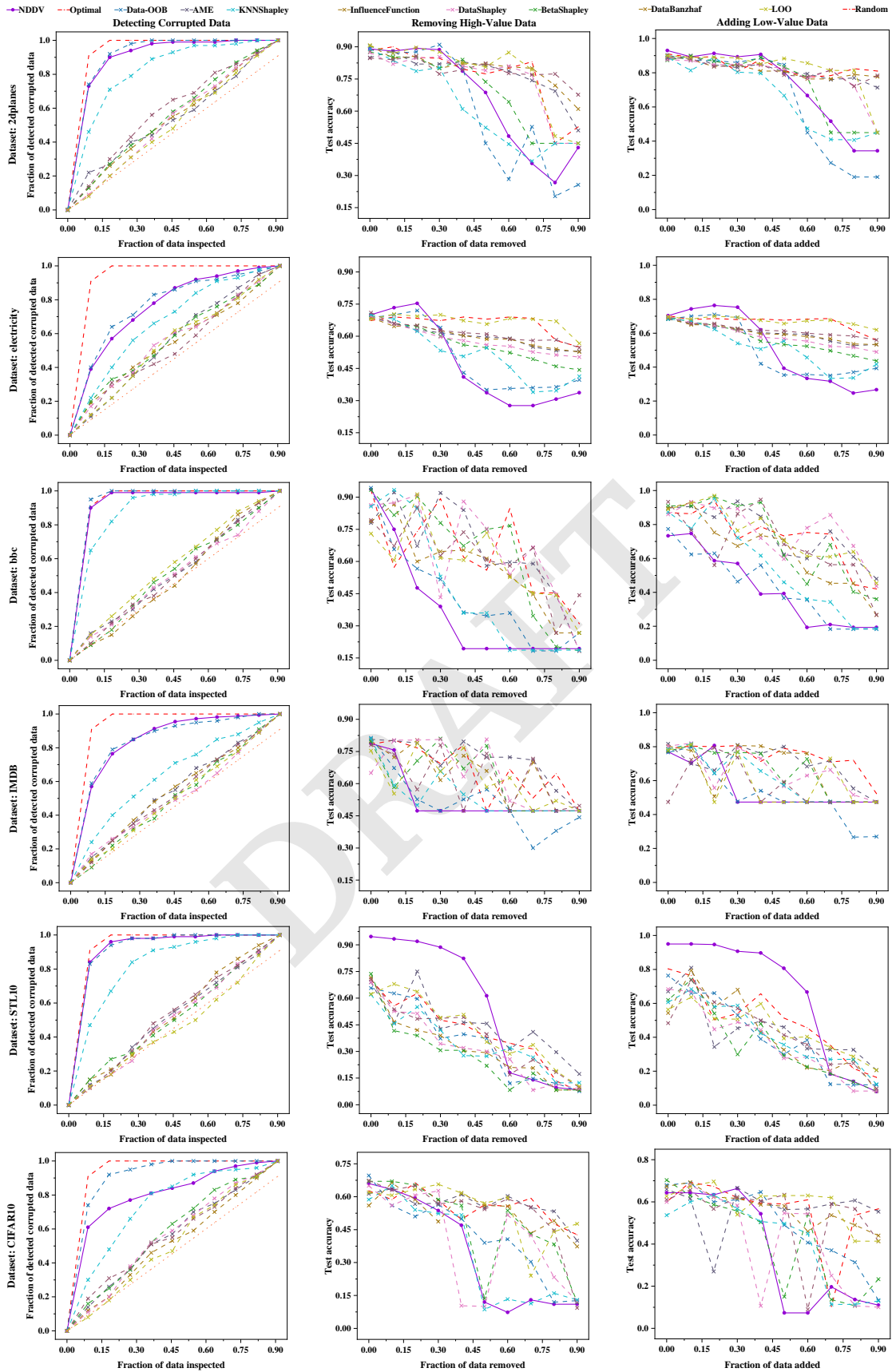


Fig. 4. Data valuation experiments on six datasets with 10% label noisy rate. (First column) Detecting corrupted data experiment. (Second column) Removing high-value data experiment. (Third column) Adding low-value data experiment.

training set based on their assigned values, starting from the highest value and progressing towards the lowest value. Conversely, in the addition experiment, data points are incrementally added to the training set based on their assigned values, starting from the lowest value and moving towards the highest value. After each removal or addition step, the base model is re-trained using the updated training set, and its test accuracy is evaluated using a fixed holdout dataset. In all experiments, we fix the number of training data points at 1,000, validation data points at 100, and test data points at 300, with 100 metadata points.

Fig.4 (second column) illustrates the performance changes of different data valuation methods after removing the most valuable data points. It can be observed that the test accuracy curve corresponding to the NDDV method effectively decreases in all datasets, indicating its ability to identify and prioritize the most influential data points. In contrast, Fig.S3 depicts the impact of removing the least valuable data points on performance by different data valuation methods. The results show that removing the least valuable data points has a less significant impact on performance compared to removing the most valuable data points, and the NDDV method's effectiveness in removing the least valuable data points is comparable to that of most existing methods. AME tends to have a random baseline in test accuracy due to the LASSO model, which may limit its effectiveness in identifying valuable data points. KNNShapley performs worse in removing high-value data points due to its local characteristic, which fails to capture the margin from a classification boundary. Data-OOB shows the worst performance in removing low-value data points, indicating a lack of sensitivity towards low-quality data. Overall, the results demonstrate that the NDDV method exhibits the fastest model performance decrease when removing high-value data points and the slowest model performance decline when adding low-value data points, reflecting the NDDV method's superiority in data valuation.

Similar to the data removal experiment, Fig.4 (third columns) and Fig.S4 demonstrate the test accuracy curves of different data valuation methods in the data point addition experiment. The experiments show that adding high-value data points boosts test accuracy above the random baseline while adding low-value points leads to a decrease. This observation highlights the effectiveness of the data valuation methods in identifying the impact of adding high and low-value data points. Among the existing works, Data-OOB exhibits the best performance in identifying the impact of adding

high and low-value data points. LOO, on the other hand, shows a slightly better performance than the random baseline. Compared to Data-OOB, the NDDV method demonstrates similar performance in most cases.

## Conclusion

In this paper, we propose a novel data valuation method from a new perspective of optimal control. Unlike existing works, we formulate data valuation as an optimization process of optimal control, thereby eliminating the need for re-training utility functions. In addition, we propose a novel marginal contribution metric that captures the impact of data points via the sensitivity of their optimal control state. Through comprehensive experiments, we demonstrate that the NDDV method significantly improves computational efficiency while ensuring the accurate identification of high and low-value data points for model training.

Our work represents a novel attempt with several research avenues worthy of further exploration:

- Extending the NDDV method to handle data valuation in dynamic and uncertain data marketplaces is an important research direction, as it can provide more robust and adaptive valuation techniques in real-world scenarios.
- Data transactions frequently occur across data markets, and applying the NDDV method to datasets originating from multiple sources or incorporating the method into a framework that can handle multiple datasets simultaneously represents an exciting direction.
- Adapting the NDDV method to analyze multimodal data, which involves integrating data from various modalities, such as text, images, and audio, presents a valuable application of interest.

## Materials and Methods

The code used for conducting experiments can be available at <https://github.com/liangzhangyong/NDDV>

**ACKNOWLEDGMENTS.** We appreciate the constructive feedback provided by the anonymous reviewers, which has greatly helped in refining the presentation. Additionally, We gratefully acknowledge the financial support from the National Natural Science Foundation of China (12202157).

1. A Agarwal, M Dahleh, T Sarkar, A marketplace for data: An algorithmic solution in *Proceedings of the 2019 ACM Conference on Economics and Computation*. pp. 701–726 (2019).
2. Z Tian, et al., Private data valuation and fair payment in data marketplaces. *arXiv preprint arXiv:2210.08723* (2022).
3. J Pei, A survey on data pricing: from economics to data science. *IEEE Transactions on Knowledge Data Eng.* **34**, 4586–4608 (2020).
4. RD Cook, S Weisberg, *Residuals and influence in regression*. (New York: Chapman and Hall), (1982).
5. PW Koh, P Liang, Understanding black-box predictions via influence functions in *International Conference on Machine Learning*. (PMLR), pp. 1885–1894 (2017).
6. LS Shapley, A value for n-person games. *Contributions to Theory Games* **2**, 307–317 (1953).
7. A Ghorbani, J Zou, Data shapley: Equitable valuation of data for machine learning in *International conference on machine learning*. (PMLR), pp. 2242–2251 (2019).
8. A Ghorbani, M Kim, J Zou, A distributional framework for data valuation in *International Conference on Machine Learning*. (PMLR), pp. 3535–3544 (2020).
9. S Schoch, H Xu, Y Ji, Cs-shapley: class-wise shapley values for data valuation in classification. *Adv. Neural Inf. Process. Syst.* **35**, 34574–34585 (2022).
10. R Jia, et al., Efficient task-specific data valuation for nearest neighbor algorithms. *arXiv preprint arXiv:1908.08619* (2019).
11. Y Kwon, MA Rivas, J Zou, Efficient computation and analysis of distributional shapley values in *International Conference on Artificial Intelligence and Statistics*. (PMLR), pp. 793–801 (2021).
12. J Lin, et al., Measuring the effect of training data on deep learning predictions via randomized experiments in *International Conference on Machine Learning*. (PMLR), pp. 13468–13504 (2022).
13. Y Kwon, J Zou, Data-oob: out-of-bag estimate as a simple and efficient data value in *International Conference on Machine Learning*. (PMLR), pp. 18135–18152 (2023).
14. E Weinan, A proposal on machine learning via dynamical systems. *Commun. Math. Stat.* **1**, 1–11 (2017).
15. K He, X Zhang, S Ren, J Sun, Deep residual learning for image recognition in *Proceedings of the IEEE conference on computer vision and pattern recognition*. pp. 770–778 (2016).
16. Y Lu, A Zhong, Q Li, B Dong, Beyond finite layer neural networks: Bridging deep architectures and numerical differential equations in *International Conference on Machine Learning*. (PMLR), pp. 3276–3285 (2018).
17. S Sonoda, N Murata, Transport analysis of infinitely deep neural network. *J. Mach. Learn. Res.* **20**, 1–52 (2019).

18. B Hu, L Lessard, Control interpretations for first-order optimization methods in *2017 American Control Conference (ACC)*. (IEEE), pp. 3114–3119 (2017).
19. J Han, Q Li, et al., A mean-field optimal control formulation of deep learning. *Res. Math. Sci.* **6**, 1–41 (2019).
20. Q Li, L Chen, C Tai, E Weinan, Maximum principle based algorithms for deep learning. *J. Mach. Learn. Res.* **18**, 1–29 (2018).
21. Q Li, S Hao, An optimal control approach to deep learning and applications to discrete-weight neural networks in *International Conference on Machine Learning*. (PMLR), pp. 2985–2994 (2018).
22. D Zhang, T Zhang, Y Lu, Z Zhu, B Dong, You only propagate once: Accelerating adversarial training via maximal principle. *Adv. neural information processing systems* **32** (2019).
23. GA Pavliotis, *Stochastic processes and applications: diffusion processes, the Fokker-Planck and Langevin equations*. (Springer) Vol. 60, (2014).
24. U Simsekli, L Sagun, M Gurbuzbalaban, A tail-index analysis of stochastic gradient noise in deep neural networks in *International Conference on Machine Learning*. (PMLR), pp. 5827–5837 (2019).
25. SS Du, X Zhai, B Póczos, A Singh, Gradient descent provably optimizes over-parameterized neural networks. *arXiv preprint arXiv:1810.02054* (2018).
26. S Du, J Lee, H Li, L Wang, X Zhai, Gradient descent finds global minima of deep neural networks in *International conference on machine learning*. (PMLR), pp. 1675–1685 (2019).
27. Q Li, C Tai, E Weinan, Stochastic modified equations and adaptive stochastic gradient algorithms in *International Conference on Machine Learning*. (PMLR), pp. 2101–2110 (2017).
28. J An, J Lu, L Ying, Stochastic modified equations for the asynchronous stochastic gradient descent. *Inf. Inference: A J. IMA* **9**, 851–873 (2020).
29. R Jia, et al., Towards efficient data valuation based on the shapley value in *The 22nd International Conference on Artificial Intelligence and Statistics*. (PMLR), pp. 1167–1176 (2019).
30. Y Kwon, J Zou, Beta shapley: a unified and noise-reduced data valuation framework for machine learning. *arXiv preprint arXiv:2110.14049* (2021).
31. T Wang, R Jia, Data banzha: A data valuation framework with maximal robustness to learning stochasticity. *arXiv preprint arXiv:2205.15466* (2022).
32. V Feldman, C Zhang, What neural networks memorize and why: Discovering the long tail via influence estimation. *Adv. Neural Inf. Process. Syst.* **33**, 2881–2891 (2020).
33. X Xu, Z Wu, CS Foo, BKH Low, Validation free and replication robust volume-based data valuation. *Adv. Neural Inf. Process. Syst.* **34**, 10837–10848 (2021).
34. HA Just, et al., Lava: Data valuation without pre-specified learning algorithms. *arXiv preprint arXiv:2305.00054* (2023).
35. SM Lundberg, SI Lee, A unified approach to interpreting model predictions. *Adv. neural information processing systems* **30** (2017).
36. I Covert, S Lundberg, SI Lee, Explaining by removing: A unified framework for model explanation. *J. Mach. Learn. Res.* **22**, 1–90 (2021).
37. J Stier, G Gianini, M Granitzer, K Ziegler, Analysing neural network topologies: a game theoretic approach. *Procedia Comput. Sci.* **126**, 234–243 (2018).
38. A Ghorbani, JY Zou, Neuron shapley: Discovering the responsible neurons. *Adv. Neural Inf. Process. Syst.* **33**, 5922–5932 (2020).
39. RHL Sim, Y Zhang, MC Chan, BKH Low, Collaborative machine learning with incentive-aware model rewards in *International Conference on Machine Learning*. (PMLR), pp. 8927–8936 (2020).
40. X Xu, et al., Gradient driven rewards to guarantee fairness in collaborative machine learning. *Adv. Neural Inf. Process. Syst.* **34**, 16104–16117 (2021).
41. A Benmerzoug, M de Benito Delgado, [re] if you like shapley then you'll love the core in *ML Reproducibility Challenge 2022*. (2023).
42. B Rozemberczki, et al., The shapley value in machine learning. *arXiv preprint arXiv:2202.05594* (2022).
43. J Yoon, S Arik, T Pfister, Data valuation using reinforcement learning in *International Conference on Machine Learning*. (PMLR), pp. 10842–10851 (2020).
44. S Basu, P Pope, S Feizi, Influence functions in deep learning are fragile. *arXiv preprint arXiv:2006.14651* (2020).
45. Y Bachrach, et al., Approximating power indices: theoretical and empirical analysis. *Auton. Agents Multi-Agent Syst.* **20**, 105–122 (2010).
46. HJ Kushner, On the stochastic maximum principle: Fixed time of control. *J. Math. Analysis Appl.* **11**, 78–92 (1965).
47. H Kushner, Necessary conditions for continuous parameter stochastic optimization problems. *SIAM J. on Control.* **10**, 550–565 (1972).
48. FL Chernousko, A Lyubushin, Method of successive approximations for solution of optimal control problems. *Optim. Control. Appl. Methods* **3**, 101–114 (1982).
49. Q Li, L Chen, C Tai, E Weinan, Maximum principle based algorithms for deep learning. *J. Mach. Learn. Res.* **18**, 1–29 (2018).
50. J Shu, et al., Meta-weight-net: Learning an explicit mapping for sample weighting. *Adv. neural information processing systems* **32** (2019).
51. H Von Stackelberg, SH Von, *The theory of the market economy*. (Oxford University Press), (1952).
52. IE Kumar, S Venkatasubramanian, C Scheidegger, S Friedler, Problems with shapley-value-based explanations as feature importance measures in *International Conference on Machine Learning*. (PMLR), pp. 5491–5500 (2020).
53. R Serban, AC Hindmarsh, Ccodes: the sensitivity-enabled ode solver in sundials in *International Design Engineering Technical Conferences and Computers and Information in Engineering Conference*. Vol. 47438, pp. 257–269 (2005).
54. JB Jørgensen, Adjoint sensitivity results for predictive control, state-and parameter-estimation with nonlinear models in *2007 European Control Conference (ECC)*. (IEEE), pp. 3649–3656 (2007).
55. A Shrikumar, P Greenside, A Kundaje, Learning important features through propagating activation differences in *International conference on machine learning*. (PMLR), pp. 3145–3153 (2017).
56. K Jiang, W Liang, JY Zou, Y Kwon, Opendataval: a unified benchmark for data valuation. *Adv. Neural Inf. Process. Syst.* **36** (2023).
57. M Feurer, et al., Openml-python: an extensible python api for openml. *J. Mach. Learn. Res.* **22**, 1–5 (2021).
58. J Gama, P Medas, G Castillo, P Rodrigues, Learning with drift detection in *Advances in Artificial Intelligence–SBIA 2004: 17th Brazilian Symposium on Artificial Intelligence, Sao Luis, Maranhao, Brazil, September 29–October 1, 2004. Proceedings 17*. (Springer), pp. 286–295 (2004).
59. D Greene, P Cunningham, Practical solutions to the problem of diagonal dominance in kernel document clustering in *Proceedings of the 23rd international conference on Machine learning*. pp. 377–384 (2006).
60. A Maas, et al., Learning word vectors for sentiment analysis in *Proceedings of the 49th annual meeting of the association for computational linguistics: Human language technologies*. pp. 142–150 (2011).
61. A Coates, A Ng, H Lee, An analysis of single-layer networks in unsupervised feature learning in *Proceedings of the fourteenth international conference on artificial intelligence and statistics*. (JMLR Workshop and Conference Proceedings), pp. 215–223 (2011).
62. A Krizhevsky, et al., Learning multiple layers of features from tiny images. (Citeseer), (2009).

## Supporting Information

### 1. The Axioms of Existing Data Valuation Method

The popularity of the Shapley value is attributable to the fact that it is the unique data value notion satisfying the following five common axioms (36), as follow

- **Efficiency:** The values add up to the difference in value between the grand coalition and the empty coalition:  $\sum_{i \in N} \phi(x_i, y_i; U) = U(N) - U(\emptyset)$ ;
- **Symmetry:** if  $U(S \cup (x_i, y_i)) = U(S \cup (x_j, y_j))$  for all  $S \in N \setminus \{(x_i, y_i), (x_j, y_j)\}$ , then  $\phi(x_i, y_i; U) = \phi(x_j, y_j; U)$ ;
- **Dummy:** if  $U(S \cup (x_i, y_i)) = U(S)$  for all  $S \in N \setminus (x_i, y_i)$ , then it makes 0 marginal contribution, so the value of the data point  $(x_i, y_i)$  should be  $\phi(x_i, y_i; U) = 0$ ;
- **Additivity:** For two utility functions  $U_1, U_2$  and arbitrary  $\alpha_1, \alpha_2 \in \mathbb{R}$ , the total contribution of a data point  $(x_i, y_i)$  is equal to the sum of its contributions when combined:  $\phi((x_i, y_i); \alpha_1 U_1(S) + \alpha_2 U_2(S)) = \alpha_1 \phi(x_i, y_i; U_1(S)) + \alpha_2 \phi(x_i, y_i; U_2(S))$ ;
- **Marginalism:** For two utility functions  $U_1, U_2$ , if each data point has the identical marginal impact, they receive same valuation:  $U_1(S \cup (x_i, y_i)) - U_1(S) = U_2(S \cup (x_i, y_i)) - U_2(S)$  holds for all  $((x_i, y_i); S)$ , then it holds that  $\phi(x_i, y_i; U_1) = \phi(x_i, y_i; U_2)$ .

### 2. Details of Learning Stochastic Dynamic

**A. Basic MSA.** In this subsection, we illustrate the iterative update process of the basic MSA in Alg.1, comprising the state equation, the costate equation, and the maximization of the Hamiltonian.

---

#### Algorithm 1 Basic MSA

---

- 1: **Initialize**  $\psi^0 = \{\psi_t^0 \in \Psi : t = 0 \dots, T-1\}$ .
- 2: **for**  $k = 0$  **to**  $K$  **do**
- 3:   Solve the forward SDE:

$$dX_t^k = b(X_t^k, \psi_t^k)dt + \sigma dW_t, \quad X_0^k = x,$$

- 4:   Solve the backward SDE:

$$dY_t^k = -\nabla_x \mathcal{H}(X_t^k, Y_t^k, \psi_t^k)dt + Z_t^k dW_t, \quad Y_T^k = -\nabla_x \Phi(X_T^k),$$

- 5:   For each  $t \in [0, T-1]$ , update the state control  $\psi_t^{k+1}$ :

$$\psi_t^{k+1} = \arg \max_{\psi \in \Psi} \mathcal{H}(X_t^k, Y_t^k, Z_t^k, \psi).$$


---

### 3. Derivation of Re-weighting Strategy

#### A. Convergence Proof of The Training Loss.

**Lemma 1.** Let  $(a_n)_{n \leq 1}, (b_n)_{n \leq 1}$  be two non-negative real sequences such that the series  $\sum_{i=1}^{\infty} a_n$  diverges, the series  $\sum_{i=1}^{\infty} a_n b_n$  converges, and there exists  $K > 0$  such that  $|b_{n+1} - b_n| \leq K a_n$ . Then the sequences  $(b_n)_{n \leq 1}$  converges to 0.

**Theorem 1.** Assume the training loss function  $\mathcal{L}$  is Lipschitz smooth with constant  $L$ , and  $\mathcal{V}(\cdot)$  is differential with a  $\delta$ -bounded gradient and twice differential with its Hessian bounded by  $\mathcal{B}$ , and  $\mathcal{L}$  have  $\rho$ -bounded gradients concerning training/metadata points. Let the learning rate  $\alpha^k$  satisfies  $\alpha^k = \min\{1, \frac{k}{T}\}$ , for some  $k > 0$ , such that  $\frac{k}{T} < 1$ , and  $\beta^k, 1 \leq k \leq K$  is a monotone descent sequence,  $\beta^k = \min\{\frac{1}{L}, \frac{c}{\sigma\sqrt{T}}\}$  for some  $c > 0$ , such that  $\frac{\sigma\sqrt{T}}{c} \geq L$  and  $\sum_{k=1}^{\infty} \beta^k \leq \infty, \sum_{k=1}^{\infty} (\beta^k)^2 \leq \infty$ . Then

$$\lim_{k \rightarrow \infty} \mathbb{E}[\|\nabla \mathcal{L}(\psi^k; \theta^{k+1})\|_2^2] = 0. \quad [41]$$

*Proof.* It is easy to conclude that  $\alpha^k$  satisfy  $\sum_{k=0}^{\infty} \alpha^k = \infty, \sum_{k=0}^{\infty} (\alpha^k)^2 < \infty$ . Recall the update of  $\psi$  in each iteration as follows

$$\psi^{k+1} = \psi^k + \frac{\alpha}{N} \sum_{i=1}^N \nabla_{\psi} \mathcal{H}_i(\psi, \mathcal{V}(\Phi_i(\psi_T^k); \theta^{k+1}))|_{\psi^k}. \quad [42]$$

It can be written as

$$\psi^{k+1} = \psi^k + \alpha^k \nabla \mathcal{H}(\psi^k; \theta^{k+1})|_{v^k}, \quad [43]$$

where  $\nabla \mathcal{H}(\psi^k; \theta) = -\nabla \mathcal{L}(\psi^k; \theta)$ . Since the mini-batch  $v^k$  is drawn uniformly at random, we can rewrite the update equation as:

$$\psi^{k+1} = \psi^k + \alpha^k [\nabla \mathcal{H}(\psi^k; \theta^{k+1}) + v^k], \quad [44]$$

where  $v^k = \nabla \mathcal{H}(\psi^k; \theta^{k+1})|_{\Upsilon^k} - \nabla \mathcal{H}(\psi^k; \theta^{k+1})$ . Note that  $v^k$  is i.i.d. random variable with finite variance since  $\Upsilon^k$  are drawn i.i.d. with a finite number of samples. Furthermore,  $\mathbb{E}[v^k] = 0$ , since samples are drawn uniformly at random, and  $\mathbb{E}[\|v^k\|_2^2] \leq \sigma^2$ .

The Hamiltonian  $\mathcal{H}(\psi; \theta)$  defined in Eq.36 can be easily checked to be Lipschitz-smooth with constant  $L$ , and have  $\rho$ -bounded gradients concerning training data. Observe that

$$\begin{aligned} & \mathcal{H}(\psi^{k+1}; \theta^{k+2}) - \mathcal{H}(\psi^k; \theta^{k+1}) \\ &= \{ \mathcal{H}(\psi^{k+1}; \theta^{k+2}) - \mathcal{H}(\psi^{k+1}; \theta^{k+1}) \} + \{ \mathcal{H}(\psi^{k+1}; \theta^{k+1}) - \mathcal{H}(\psi^k; \theta^{k+1}) \}. \end{aligned} \quad [45]$$

For the first term,

$$\begin{aligned} & \mathcal{H}(\psi^{k+1}; \theta^{k+2}) - \mathcal{H}(\psi^{k+1}; \theta^{k+1}) \\ &= \frac{1}{N} \sum_{i=1}^N \sum_{t=0}^{T-1} \{ [ \mathcal{V}(\Phi_i(\psi_T^k); \theta^{k+2}) - \mathcal{V}(\Phi_i(\psi_T^k); \theta^{k+1}) ] [ b(\psi_t^k) Y_t(\psi_t^k) + \sigma Z_t(\psi_t^k) ] - R_i(\psi_t^k) \} \\ &\leq \frac{1}{N} \sum_{i=1}^N \sum_{t=0}^{T-1} \left\{ \left\langle \left. \frac{\partial \mathcal{V}(\Phi_i(\psi_T^k); \theta)}{\partial \theta} \right|_{\theta^k}, \theta^{k+1} - \theta^k \right\rangle + \frac{\delta}{2} \|\theta^{k+1} - \theta^k\|_2^2 \left[ b(\psi_t^k) Y_t(\psi_t^k) + \sigma Z_t(\psi_t^k) \right] - R_i(\psi_t^k) \right\} \\ &= \frac{1}{N} \sum_{i=1}^N \sum_{t=0}^{T-1} \left\{ \left\langle \left. \frac{\partial \mathcal{V}(\Phi_i(\psi_T^k); \theta)}{\partial \theta} \right|_{\theta^k}, -\beta^k [ \nabla \ell(\hat{\psi}^k(\theta^k)) + \xi^k ] \right\rangle + \frac{\delta \beta_k^2}{2} \|\nabla \ell(\hat{\psi}^k(\theta^k)) + \xi^k\|_2^2 \left[ b(\psi_t^k) Y_t(\psi_t^k) + \sigma Z_t(\psi_t^k) \right] - R_i(\psi_t^k) \right\} \\ &= \frac{1}{N} \sum_{i=1}^N \sum_{t=0}^{T-1} \left\{ \left\langle \left. \frac{\partial \mathcal{V}(\Phi_i(\psi_T^k); \theta)}{\partial \theta} \right|_{\theta^k}, -\beta^k [ \nabla \ell(\hat{\psi}^k(\theta^k)) + \xi^k ] \right\rangle + \frac{\delta \beta_k^2}{2} \|\nabla \ell(\hat{\psi}^k(\theta^k)) + \xi^k\|_2^2 \left[ b(\psi_t^k) Y_t(\psi_t^k) + \sigma Z_t(\psi_t^k) \right] - R_i(\psi_t^k) \right\} \\ &= \frac{1}{N} \sum_{i=1}^N \sum_{t=0}^{T-1} \left\{ \left\langle \left. \frac{\partial \mathcal{V}(\Phi_i(\psi_T^k); \theta)}{\partial \theta} \right|_{\theta^k}, -\beta^k [ \nabla \ell(\hat{\psi}^k(\theta^k)) + \xi^k ] \right\rangle + \frac{\delta (\beta^k)^2}{2} (\|\nabla \ell(\hat{\psi}^k(\theta^k))\|_2^2 + \|\xi^k\|_2^2 \right. \\ &\quad \left. + 2 \langle \nabla \ell(\hat{\psi}^k(\theta^k)), \xi^k \rangle) \left[ b(\psi_t^k) Y_t(\psi_t^k) + \sigma Z_t(\psi_t^k) \right] - R_i(\psi_t^k) \right\} \end{aligned} \quad [46]$$

For the second term,

$$\begin{aligned} & \mathcal{H}(\psi^{k+1}; \theta^{k+1}) - \mathcal{H}(\psi^k; \theta^{k+1}) \\ &\leq \langle \nabla \mathcal{H}(\psi^k; \theta^{k+1}), \psi^{k+1} - \psi^k \rangle + \frac{L}{2} \|\psi^{k+1} - \psi^k\|_2^2 \\ &= \langle \nabla \mathcal{H}(\psi^k; \theta^{k+1}), -\alpha^k [ \nabla \mathcal{L}(\psi^k; \theta^{k+1}) + v^k ] \rangle + \frac{L(\alpha^k)^2}{2} \|\nabla \mathcal{H}(\psi^k; \theta^{k+1}) + v^k\|_2^2 \\ &= -(\alpha^k - \frac{L(\alpha^k)^2}{2}) \|\nabla \mathcal{H}(\psi^k; \theta^{k+1})\|_2^2 + \frac{L(\alpha^k)^2}{2} \|v^k\|_2^2 - (\alpha^k - L(\alpha^k)^2) \langle \nabla \mathcal{H}(\psi^k; \theta^{k+1}), v^k \rangle. \end{aligned} \quad [47]$$

Therefore, we have

$$\mathcal{H}(\psi^{k+1}; \theta^{k+2}) - \mathcal{H}(\psi^k; \theta^{k+1}) \leq \frac{1}{N} \sum_{i=1}^N \left\{ \left\langle \left. \frac{\partial \mathcal{V}(\Phi_i(\psi^k); \theta)}{\partial \theta} \right|_{\theta^k}, -\beta^k [ \nabla \ell(\hat{\psi}^k(\theta^k)) + \xi^k ] \right\rangle + \right. \quad [48]$$

$$\left. + \frac{\delta (\beta^k)^2}{2} (\|\nabla \ell(\hat{\psi}^k(\theta^k))\|_2^2 + \|\xi^k\|_2^2 + 2 \langle \nabla \ell(\hat{\psi}^k(\theta^k)), \xi^k \rangle) \right\} \Phi_i(\psi^k) \quad [49]$$

$$- (\alpha^k - \frac{L(\alpha^k)^2}{2}) \|\nabla \mathcal{H}(\psi^k; \theta^{k+1})\|_2^2 + \frac{L(\alpha^k)^2}{2} \|v^k\|_2^2 - (\alpha^k - L(\alpha^k)^2) \langle \nabla \mathcal{H}(\psi^k; \theta^{k+1}), v^k \rangle. \quad [50]$$

Taking expectation of both sides of (47) and since  $\mathbb{E}[\xi^k] = 0, \mathbb{E}[v^k] = 0$ , we have

$$\begin{aligned} & \mathbb{E} [ \mathcal{H}(\psi^{k+1}; \theta^{k+2}) ] - \mathbb{E} [ \mathcal{H}(\psi^k; \theta^{k+1}) ] \leq \mathbb{E} \frac{1}{N} \sum_{i=1}^N \mathcal{H}_i(\psi^k) \left\{ \left\langle \left. \frac{\partial \mathcal{V}(\Phi_i(\psi^k); \theta)}{\partial \theta} \right|_{\theta^k}, -\beta^k [ \nabla \ell(\hat{\psi}^k(\theta^k)) ] \right\rangle + \right. \\ & \left. + \frac{\delta (\beta^k)^2}{2} (\|\nabla \ell(\hat{\psi}^k(\theta^k))\|_2^2 + \|\xi^k\|_2^2) \right\} - \alpha^k \mathbb{E} [ \|\nabla \mathcal{H}(\psi^k; \theta^{k+1})\|_2^2 ] + \frac{L(\alpha^k)^2}{2} \{ \mathbb{E} [ \|\nabla \mathcal{H}(\psi^k; \theta^{k+1})\|_2^2 ] + \mathbb{E} [ \|v^k\|_2^2 ] \} \end{aligned}$$

Summing up the above inequalities over  $k = 1, \dots, \infty$  in both sides, we obtain

$$\begin{aligned} & \sum_{k=1}^{\infty} \alpha^k \mathbb{E} [ \|\nabla \mathcal{H}(\psi^k; \theta^{k+1})\|_2^2 ] + \sum_{k=1}^{\infty} \beta^k \mathbb{E} \frac{1}{N} \sum_{i=1}^N \|\mathcal{H}_i(\psi^k)\| \left\| \left. \frac{\partial \mathcal{V}(\Phi_i(\psi^k); \theta)}{\partial \theta} \right|_{\theta^k} \cdot \|\nabla \ell(\hat{\psi}^k(\theta^k))\| \right. \\ & \leq \sum_{k=1}^{\infty} \frac{L(\alpha^k)^2}{2} \{ \mathbb{E} [ \|\nabla \mathcal{H}(\psi^k; \theta^{k+1})\|_2^2 ] + \mathbb{E} [ \|v^k\|_2^2 ] \} + \mathbb{E} [ \mathcal{H}(\psi^1; \theta^2) ] - \lim_{T \rightarrow \infty} \mathbb{E} [ \mathcal{H}(\psi^{k+1}; \theta^{k+2}) ] \\ & + \sum_{k=1}^{\infty} \frac{\delta (\beta^k)^2}{2} \left\{ \frac{1}{n} \sum_{i=1}^N \|\mathcal{H}_i(\psi^k)\| (\mathbb{E} \|\nabla \ell(\hat{\psi}^k(\theta^k))\|_2^2 + \mathbb{E} \|\xi^k\|_2^2) \right\} \\ & \leq \sum_{k=1}^{\infty} \frac{L(\alpha^k)^2}{2} \{ \rho^2 + \sigma^2 \} + \mathbb{E} [ \mathcal{H}^{tr}(\psi^1; \theta^2) ] + \sum_{k=1}^{\infty} \frac{\delta (\beta^k)^2}{2} \{ M(\rho^2 + \sigma^2) \} \leq \infty. \end{aligned}$$

The last inequality holds since  $\sum_{k=0}^{\infty} (\alpha^k)^2 < \infty$ ,  $\sum_{k=0}^{\infty} (\beta^k)^2 < \infty$ , and  $\frac{1}{N} \sum_{i=1}^N \|\mathcal{H}_i(\psi^k)\| \leq M$  for limited number of data points' loss is bounded. Thus we have

$$\sum_{k=1}^{\infty} \alpha^k \mathbb{E}[\|\nabla \mathcal{H}(\psi^k; \theta^{k+1})\|_2^2] + \sum_{k=1}^{\infty} \beta^k \mathbb{E} \frac{1}{n} \sum_{i=1}^n \|\mathcal{H}_i(\psi^k)\| \left\| \frac{\partial \mathcal{V}(\Phi_i(\psi^k); \theta)}{\partial \theta} \right\|_{\theta^k} \|\cdot\| \cdot \|\nabla \ell(\hat{\psi}^k(\theta^k))\| \leq \infty. \quad [51]$$

Since

$$\begin{aligned} & \sum_{k=1}^{\infty} \beta^k \mathbb{E} \frac{1}{N} \sum_{i=1}^N \|\mathcal{H}_i(\psi^k)\| \left\| \frac{\partial \mathcal{V}(\Phi_i(\psi^k); \theta)}{\partial \theta} \right\|_{\theta^k} \|\cdot\| \cdot \|\nabla \ell(\hat{\psi}^k(\theta^k))\| \\ & \leq M \delta \rho \sum_{k=1}^{\infty} \beta^k \leq \infty, \end{aligned} \quad [52]$$

which implies that  $\sum_{k=1}^{\infty} \alpha^k \mathbb{E}[\|\nabla \mathcal{H}(\psi^k; \theta^{k+1})\|_2^2] < \infty$ . By Lemma 1, to substantiate  $\lim_{t \rightarrow \infty} \mathbb{E}[\|\nabla \mathcal{H}(\psi^k; \theta^{k+1})\|_2^2] = 0$ , since  $\sum_{k=0}^{\infty} \alpha^k = \infty$ , it only needs to prove

$$\left| \mathbb{E}[\|\nabla \mathcal{H}(\psi^{k+1}; \theta^{k+2})\|_2^2] - \mathbb{E}[\|\nabla \mathcal{H}(\psi^k; \theta^{k+1})\|_2^2] \right| \leq C \alpha^k, \quad [53]$$

for some constant  $C$ . Based on the inequality

$$|(\|a\| + \|b\|)(\|a\| - \|b\|)| \leq \|a + b\| \|a - b\|,$$

we then have

$$\begin{aligned} & \left| \mathbb{E}[\|\nabla \mathcal{H}(\psi^{k+1}; \theta^{k+2})\|_2^2] - \mathbb{E}[\|\nabla \mathcal{H}(\psi^k; \theta^{k+1})\|_2^2] \right| \\ & = \left| \mathbb{E} \left[ (\|\nabla \mathcal{H}(\psi^{k+1}; \theta^{k+2})\|_2 + \|\nabla \mathcal{H}(\psi^k; \theta^{k+1})\|_2) (\|\nabla \mathcal{H}(\psi^{k+1}; \theta^{k+2})\|_2 - \|\nabla \mathcal{H}(\psi^k; \theta^{k+1})\|_2) \right] \right| \\ & \leq \mathbb{E} \left[ \left( \|\nabla \mathcal{H}(\psi^{k+1}; \theta^{k+2})\|_2 + \|\nabla \mathcal{H}(\psi^k; \theta^{k+1})\|_2 \right) \left| \|\nabla \mathcal{H}(\psi^{k+1}; \theta^{k+2})\|_2 - \|\nabla \mathcal{H}(\psi^k; \theta^{k+1})\|_2 \right| \right] \\ & \leq \mathbb{E} \left[ \left\| \nabla \mathcal{H}(\psi^{k+1}; \theta^{k+2}) + \nabla \mathcal{H}(\psi^k; \theta^{k+1}) \right\|_2 \left\| \nabla \mathcal{H}(\psi^{k+1}; \theta^{k+2}) - \nabla \mathcal{H}(\psi^k; \theta^{k+1}) \right\|_2 \right] \\ & \leq \mathbb{E} \left[ \left( \|\nabla \mathcal{H}(\psi^{k+1}; \theta^{k+2})\|_2 + \|\nabla \mathcal{H}(\psi^k; \theta^{k+1})\|_2 \right) \|\nabla \mathcal{H}(\psi^{k+1}; \theta^{k+2}) - \nabla \mathcal{H}(\psi^k; \theta^{k+1})\|_2 \right] \\ & \leq 2L\rho \mathbb{E} \left[ \|\psi^{k+1}, \theta^{k+2}\|_2 - \|\psi^k, \theta^{k+1}\|_2 \right] \\ & \leq 2L\rho \alpha_k \beta_k \mathbb{E} \left[ \left\| \nabla \mathcal{H}(\psi^k; \theta^{k+1}) + v^k, \nabla \ell(\theta^{k+1}) + \xi^{k+1} \right\|_2 \right] \\ & \leq 2L\rho \alpha_k \beta_k \mathbb{E} \left[ \sqrt{\|\nabla \mathcal{H}(\psi^k; \theta^{k+1}) + v^k\|_2^2} + \sqrt{\|\nabla \ell(\theta^{k+1}) + \xi^{k+1}\|_2^2} \right] \\ & \leq 2L\rho \alpha_k \beta_k \sqrt{\mathbb{E} \left[ \|\nabla \mathcal{H}(\psi^k; \theta^{k+1}) + v^k\|_2^2 \right] + \mathbb{E} \left[ \|\nabla \ell(\theta^{k+1}) + \xi^{k+1}\|_2^2 \right]} \\ & \leq 2L\rho \alpha_k \beta_k \sqrt{\mathbb{E} \left[ \|\nabla \mathcal{H}(\psi^k; \theta^{k+1})\|_2^2 \right] + \mathbb{E} \left[ \|v^k\|_2^2 \right] + \mathbb{E} \left[ \|\xi^{k+1}\|_2^2 \right] + \mathbb{E} \left[ \|\nabla \ell(\theta^{k+1})\|_2^2 \right]} \\ & \leq 2L\rho \alpha^k \beta^k \sqrt{2\sigma^2 + 2\rho^2} \\ & \leq 2\sqrt{2(\sigma^2 + \rho^2)} L\rho \beta^k \alpha^k. \end{aligned} \quad [54]$$

According to the above inequality, we can conclude that our algorithm can achieve

$$\lim_{k \rightarrow \infty} \mathbb{E} \left[ \|\nabla \mathcal{H}(\psi^k; \theta^{k+1})\|_2^2 \right] = 0. \quad [55]$$

The proof is completed.  $\square$

**B. Convergence Proof of The Meta Loss.** Assume that we have a small amount of meta dataset with  $M$  data points  $\{(x'_i, y'_i), 1 \leq i \leq M\}$  with clean labels, and the meta loss is Eq.15. Let's suppose we have another  $N$  training data points,  $\{(x_i, y_i), 1 \leq i \leq N\}$ , where  $M \ll N$ , and the training loss is Eq.14.

**Lemma 2.** Assume the meta loss function  $\ell$  is Lipschitz smooth with constant  $L$ , and  $\mathcal{V}(\cdot)$  is differential with a  $\delta$ -bounded gradient and twice differential with its Hessian bounded by  $\mathcal{B}$ . The loss function has  $\rho$ -bounded gradients concerning metadata points. Then, the gradient of  $\theta$  concerning meta loss  $\ell$  is Lipschitz continuous.

*Proof.* The gradient of  $\theta$  with respect to meta loss  $\ell_i$  can be written as:

$$\begin{aligned} & \nabla_{\theta} \ell_i(\hat{\psi}^k(\theta)) \Big|_{\theta^k} \\ & = \frac{-\alpha}{n} \sum_{j=1}^n \left( \frac{\partial \ell_i(\hat{\psi})}{\partial \hat{\psi}} \Big|_{\hat{\psi}^k}^T \frac{\partial \Phi_j(\psi)}{\partial \psi} \Big|_{\psi^k} \right) \frac{\partial \mathcal{V}(\Phi_j(\psi^k); \theta)}{\partial \theta} \Big|_{\theta^k}. \end{aligned} \quad [56]$$

Let  $\mathcal{V}_j(\theta) = \mathcal{V}(\Phi_j(\psi^k); \theta)$  and  $G_{ij}$  being defined in Eq.75. Taking gradient of  $\theta$  in both sides of Eq.56, we have

$$\nabla_{\theta^2}^2 \ell_i(\hat{\psi}^k(\theta)) \Big|_{\theta^k} = \frac{-\alpha}{n} \sum_{j=1}^n \left[ \frac{\partial}{\partial \theta} (G_{ij}) \Big|_{\theta^k} \frac{\partial \mathcal{V}_j(\theta)}{\partial \theta} \Big|_{\theta^k} + (G_{ij}) \frac{\partial^2 \mathcal{V}_j(\theta)}{\partial \theta^2} \Big|_{\theta^k} \right].$$



For the first term on the right-hand side, we have that

$$\begin{aligned}
& \left\| \frac{\partial}{\partial \theta} (G_{ij}) \Big|_{\theta^k} \frac{\partial \mathcal{V}_j(\theta)}{\partial \theta} \Big|_{\theta^k} \right\| \leq \delta \left\| \frac{\partial}{\partial \hat{\psi}} \left( \frac{\partial \ell_i(\hat{\psi})}{\partial \theta} \Big|_{\theta^k} \right) \Big|_{\hat{\psi}^k} \frac{\partial \mathcal{L}_j(\psi)}{\partial \psi} \Big|_{\psi^k} \right\| \\
&= \delta \left\| \frac{\partial}{\partial \hat{\psi}} \left( \frac{\partial \ell_i(\hat{\psi})}{\partial \hat{\psi}} \Big|_{\hat{\psi}^k} - \frac{\alpha}{n} \sum_{m=1}^n \frac{\partial \mathcal{L}_m(\psi)}{\partial \psi} \Big|_{\psi^k} \frac{\partial \mathcal{V}_k(\theta)}{\partial \theta} \Big|_{\theta^k} \right) \Big|_{\hat{\psi}^k} \frac{\partial \mathcal{L}_j(\psi)}{\partial \psi} \Big|_{\psi^k} \right\| \\
&= \delta \left\| \left( \frac{\partial^2 \ell_i(\hat{\psi})}{\partial \hat{\psi}^2} \Big|_{\hat{\psi}^k} - \frac{\alpha}{n} \sum_{m=1}^n \frac{\partial \mathcal{L}_m(\psi)}{\partial \psi} \Big|_{\psi^k} \frac{\partial \mathcal{V}_m(\theta)}{\partial \theta} \Big|_{\theta^k} \right) \Big|_{\hat{\psi}^k} \frac{\partial \mathcal{L}_j(\psi)}{\partial \psi} \Big|_{\psi^k} \right\| \leq \alpha L \rho^2 \delta^2,
\end{aligned} \tag{57}$$

since  $\left\| \frac{\partial^2 \ell_i(\hat{\psi})}{\partial \hat{\psi}^2} \Big|_{\hat{\psi}^k} \right\| \leq L$ ,  $\left\| \frac{\partial \Phi_j(\psi)}{\partial \psi} \Big|_{\psi^k} \right\| \leq \rho$ ,  $\left\| \frac{\partial \mathcal{V}_j(\theta)}{\partial \theta} \Big|_{\theta^k} \right\| \leq \delta$ . For the second term, we have

$$\left\| (G_{ij}) \frac{\partial^2 \mathcal{V}_j(\theta)}{\partial \theta^2} \Big|_{\theta^k} \right\| = \left\| \frac{\partial \ell_i(\hat{\psi})}{\partial \hat{\psi}} \Big|_{\hat{\psi}^k} \frac{\partial \mathcal{L}_j(\psi)}{\partial \psi} \Big|_{\psi^k} \frac{\partial^2 \mathcal{V}_j(\theta)}{\partial \theta^2} \Big|_{\theta^k} \right\| \leq \mathcal{B} \rho^2, \tag{58}$$

since  $\left\| \frac{\partial \ell_i(\hat{\psi})}{\partial \hat{\psi}} \Big|_{\hat{\psi}^k} \right\| \leq \rho$ ,  $\left\| \frac{\partial^2 \mathcal{V}_j(\theta)}{\partial \theta^2} \Big|_{\theta^k} \right\| \leq \mathcal{B}$ . Combining the above two inequalities Eq.57 and 58, we have

$$\left\| \nabla_{\theta^2}^2 \ell_i(\hat{\psi}^k(\theta)) \Big|_{\theta^k} \right\| \leq \alpha \rho^2 (\alpha L \delta^2 + \mathcal{B}). \tag{59}$$

Define  $L_V = \alpha \rho^2 (\alpha L \delta^2 + \mathcal{B})$ , based on Lagrange mean value theorem, we have:

$$\|\nabla \ell(\hat{\psi}^k(\theta_1)) - \nabla \ell(\hat{\psi}^k(\theta_2))\| \leq L_V \|\theta_1 - \theta_2\|, \text{ for arbitrary } \theta_1, \theta_2, \tag{60}$$

where  $\nabla \ell(\hat{\psi}^k(\theta_1)) = \nabla_{\theta} \ell_i(\hat{\psi}^k(\theta)) \Big|_{\theta_1}$ .  $\square$

**Theorem 2.** Assume the meta loss function  $\ell$  is Lipschitz smooth with constant  $L$ , and  $\mathcal{V}(\cdot)$  is differential with a  $\delta$ -bounded gradient and twice differential with its Hessian bounded by  $\mathcal{B}$ , and  $\ell$  have  $\rho$ -bounded gradients concerning metadata points. Let the learning rate  $\alpha^k$  satisfies  $\alpha^k = \min\{1, \frac{k}{T}\}$ , for some  $k > 0$ , such that  $\frac{k}{T} < 1$ , and  $\beta^k, 1 \leq k \leq K$  is a monotone descent sequence,  $\beta^1 = \min\{\frac{1}{L}, \frac{c}{\sigma\sqrt{T}}\}$  for some  $c > 0$ , such that  $\frac{\sigma\sqrt{T}}{c} \geq L$  and  $\sum_{t=1}^{\infty} \beta_t \leq \infty, \sum_{t=1}^{\infty} \beta_t^2 \leq \infty$ . Then meta network can achieve  $\mathbb{E}[\|\nabla \ell(\hat{\psi}^k(\theta^k))\|_2^2] \leq \epsilon$  in  $\mathcal{O}(1/\epsilon^2)$  steps. More specifically,

$$\min_{0 \leq k \leq K} \mathbb{E}[\|\nabla \ell(\hat{\psi}^k(\theta^k))\|_2^2] \leq \mathcal{O}\left(\frac{C}{\sqrt{T}}\right), \tag{61}$$

where  $C$  is some constant independent of the convergence process,  $\sigma$  is the variance of randomly drawing uniformly mini-batch data points.

*Proof.* The update of  $\theta$  in  $k$ -th iteration is as follows

$$\theta^{k+1} = \theta^k - \frac{\beta}{m} \sum_{i=1}^m \nabla_{\theta} \ell_i(\hat{\psi}^k(\theta)) \Big|_{\theta^k}. \tag{62}$$

This can be written as:

$$\theta^{k+1} = \theta^k - \beta^k \nabla \ell(\hat{\psi}^k(\theta^k)) \Big|_{\Xi^k}. \tag{63}$$

Since the mini-batch  $\Xi^k$  is drawn uniformly from the entire dataset, we can rewrite the update equation as

$$\theta^{k+1} = \theta^k - \beta^k [\nabla \ell(\hat{\psi}^k(\theta^k)) + \xi^k], \tag{64}$$

where  $\xi^k = \nabla \ell(\hat{\psi}^k(\theta^k)) \Big|_{\Xi^k} - \nabla \ell(\hat{\psi}^k(\theta^k))$ . Note that  $\xi^k$  are i.i.d random variables with finite variance since  $\Xi^k$  are drawn i.i.d with a finite number of samples. Furthermore,  $\mathbb{E}[\xi^k] = 0$ , since samples are drawn uniformly at random. Observe that

$$\begin{aligned}
& \ell(\hat{\psi}^{k+1}(\theta^{k+1})) - \ell(\hat{\psi}^k(\theta^k)) \\
&= \left\{ \ell(\hat{\psi}^{k+1}(\theta^{k+1})) - \ell(\hat{\psi}^k(\theta^{k+1})) \right\} + \left\{ \ell(\hat{\psi}^k(\theta^{k+1})) - \ell(\hat{\psi}^k(\theta^k)) \right\}.
\end{aligned} \tag{65}$$

By Lipschitz smoothness of meta loss function  $\ell$ , we have

$$\begin{aligned}
& \ell(\hat{\psi}^{k+1}(\theta^{k+1})) - \ell(\hat{\psi}^k(\theta^{k+1})) \\
& \leq \langle \nabla \ell(\hat{\psi}^k(\theta^{k+1})), \hat{\psi}^{k+1}(\theta^{k+1}) - \hat{\psi}^k(\theta^{k+1}) \rangle + \frac{L}{2} \|\hat{\psi}^{k+1}(\theta^{k+1}) - \hat{\psi}^k(\theta^{k+1})\|_2^2
\end{aligned}$$

Since  $\hat{\psi}^{k+1}(\theta^{k+1}) - \hat{\psi}^k(\theta^{k+1}) = -\frac{\alpha^k}{n} \sum_{i=1}^n \mathcal{V}(\Phi_i(\psi^{k+1}); \theta^{k+1}) \nabla_{\psi} \Phi_i(\psi) \Big|_{\psi^{k+1}}$  according to Eq.17, we have

$$\|\ell(\hat{\psi}^{k+1}(\theta^{k+1})) - \ell(\hat{\psi}^k(\theta^{k+1}))\| \leq \alpha^k \rho^2 + \frac{L(\alpha^k)^2}{2} \rho^2 = \alpha^k \rho^2 \left(1 + \frac{\alpha^k L}{2}\right) \tag{66}$$

Since  $\left\| \frac{\partial \Phi_j(\psi)}{\partial \psi} \Big|_{\psi^k} \right\| \leq \rho$ ,  $\left\| \frac{\partial \ell_i(\hat{\psi})}{\partial \hat{\psi}} \Big|_{\hat{\psi}^k} \right\| \leq \rho$ .

By Lipschitz continuity of  $\nabla\ell(\hat{\psi}^k(\theta))$  according to Lemma 2, we can obtain the following

$$\begin{aligned}
& \ell(\hat{\psi}^k(\theta^{k+1})) - \ell(\hat{\psi}^k(\theta^k)) \\
& \leq \langle \nabla\ell(\hat{\psi}^k(\theta^k)), \theta^{k+1} - \theta^k \rangle + \frac{L}{2} \|\theta^{k+1} - \theta^k\|_2^2 \\
& = \langle \nabla\ell(\hat{\psi}^k(\theta^k)), -\beta^k[\nabla\ell(\hat{\psi}^k(\theta^k)) + \xi^k] \rangle + \frac{L(\beta^k)^2}{2} \|\nabla\ell(\hat{\psi}^k(\theta^k)) + \xi^k\|_2^2 \\
& = -(\beta^k - \frac{L(\beta^k)^2}{2}) \|\nabla\ell(\hat{\psi}^k(\theta^k))\|_2^2 + \frac{L(\beta^k)^2}{2} \|\xi^k\|_2^2 - (\beta^k - L(\beta^k)^2) \langle \nabla\ell(\hat{\psi}^k(\theta^k)), \xi^k \rangle.
\end{aligned} \tag{67}$$

Thus Eq.65 satisfies

$$\begin{aligned}
\ell(\hat{\psi}^{k+1}(\theta^{k+1})) - \ell(\hat{\psi}^k(\theta^k)) & \leq \alpha^k \rho^2 (1 + \frac{\alpha^k L}{2}) - (\beta^k - \frac{L(\beta^k)^2}{2}) \|\nabla\ell(\hat{\psi}^k(\theta^k))\|_2^2 \\
& \quad + \frac{L(\beta^k)^2}{2} \|\xi^k\|_2^2 - (\beta^k - L(\beta^k)^2) \langle \nabla\ell(\hat{\psi}^k(\theta^k)), \xi^k \rangle.
\end{aligned} \tag{68}$$

Rearranging the terms, we can obtain

$$\begin{aligned}
(\beta^k - \frac{L(\beta^k)^2}{2}) \|\nabla\ell(\hat{\psi}^k(\theta^k))\|_2^2 & \leq \alpha^k \rho^2 (1 + \frac{\alpha^k L}{2}) + \ell(\hat{\psi}^k(\theta^k)) - \ell(\hat{\psi}^{k+1}(\theta^{k+1})) \\
& \quad + \frac{L(\beta^k)^2}{2} \|\xi^k\|_2^2 - (\beta^k - L(\beta^k)^2) \langle \nabla\ell(\hat{\psi}^k(\theta^k)), \xi^k \rangle.
\end{aligned} \tag{69}$$

Summing up the above inequalities and rearranging the terms, we can obtain

$$\begin{aligned}
& \sum_{k=1}^K (\beta^k - \frac{L(\beta^k)^2}{2}) \|\nabla\ell(\hat{\psi}^k(\theta^k))\|_2^2 \\
& \leq \ell(\hat{\psi}^1(\theta^1)) - \ell(\hat{\psi}^{K+1}(\theta^{K+1})) + \sum_{k=1}^K \alpha^k \rho^2 (1 + \frac{\alpha^k L}{2}) - \sum_{k=1}^K (\beta^k - L(\beta^k)^2) \langle \nabla\ell(\hat{\psi}^k(\theta^k)), \xi^k \rangle + \frac{L}{2} \sum_{k=1}^K (\beta^k)^2 \|\xi^k\|_2^2 \\
& \leq \ell(\hat{\psi}^1(\theta^1)) + \sum_{k=1}^K \alpha^k \rho^2 (1 + \frac{\alpha^k L}{2}) - \sum_{k=1}^K (\beta^k - L(\beta^k)^2) \langle \nabla\ell(\hat{\psi}^k(\theta^k)), \xi^k \rangle + \frac{L}{2} \sum_{k=1}^K (\beta^k)^2 \|\xi^k\|_2^2,
\end{aligned} \tag{70}$$

Taking expectations with respect to  $\xi^K$  on both sides of Eq.70, we can then obtain:

$$\sum_{k=1}^K (\beta^k - \frac{L(\beta^k)^2}{2}) \mathbb{E}_{\xi^K} \|\nabla\ell(\hat{\psi}^k(\theta^k))\|_2^2 \leq \ell(\hat{\psi}^1(\theta^1)) + \sum_{k=1}^K \alpha^k \rho^2 (1 + \frac{\alpha^k L}{2}) + \frac{L\sigma^2}{2} \sum_{k=1}^K (\beta^k)^2, \tag{71}$$

since  $\mathbb{E}_{\xi^K} \langle \nabla\ell(\theta^k), \xi^k \rangle = 0$  and  $\mathbb{E}[\|\xi^k\|_2^2] \leq \sigma^2$ , where  $\sigma^2$  is the variance of  $\xi^k$ . Furthermore, we can deduce that

$$\begin{aligned}
& \min_k \mathbb{E} [\|\nabla\ell(\hat{\psi}^k(\theta^k))\|_2^2] \\
& \leq \frac{\sum_{k=1}^K (\beta^k - \frac{L(\beta^k)^2}{2}) \mathbb{E}_{\xi^K} \|\nabla\ell(\hat{\psi}^k(\theta^k))\|_2^2}{\sum_{k=1}^K (\beta^k - \frac{L(\beta^k)^2}{2})} \\
& \leq \frac{1}{\sum_{k=1}^K (2\beta^k - L(\beta^k)^2)} \left[ 2\ell(\hat{\psi}^1(\theta^1)) + \sum_{k=1}^K \alpha^k \rho^2 (2 + \alpha^k L) + L\sigma^2 \sum_{k=1}^K (\beta^k)^2 \right] \\
& \leq \frac{1}{\sum_{k=1}^K \beta^k} \left[ 2\ell(\hat{\psi}^1(\theta^1)) + \sum_{k=1}^K \alpha^k \rho^2 (2 + \alpha^k L) + L\sigma^2 \sum_{k=1}^K (\beta^k)^2 \right] \\
& \leq \frac{1}{K\beta^k} \left[ 2\ell(\hat{\psi}^1(\theta^1)) + \alpha^1 \rho^2 T(2 + L) + L\sigma^2 \sum_{k=1}^K (\beta^k)^2 \right] \\
& = \frac{2\ell(\hat{\psi}^1(\theta^1))}{K} \frac{1}{\beta^k} + \frac{2\alpha^1 \rho^2 (2 + L)}{\beta^k} + \frac{L\sigma^2}{K} \sum_{k=1}^K \beta^k \\
& \leq \frac{2\ell(\hat{\psi}^1(\theta^1))}{K} \frac{1}{\beta^k} + \frac{2\alpha^1 \rho^2 (2 + L)}{\beta^k} + L\sigma^2 \beta^k \\
& = \frac{\ell(\hat{\psi}^1(\theta^1))}{K} \max\{L, \frac{\sigma\sqrt{K}}{c}\} + \min\{1, \frac{k}{K}\} \max\{L, \frac{\sigma\sqrt{T}}{c}\} \rho^2 (2 + L) + L\sigma^2 \min\{\frac{1}{L}, \frac{c}{\sigma\sqrt{T}}\} \\
& \leq \frac{\sigma\ell(\hat{\psi}^1(\theta^1))}{c\sqrt{K}} + \frac{k\sigma\rho^2(2+L)}{c\sqrt{K}} + \frac{L\sigma c}{\sqrt{K}} \\
& = \mathcal{O}(\frac{1}{\sqrt{K}}).
\end{aligned} \tag{72}$$

The third inequality holds for  $\sum_{k=1}^K (2\beta^k - L(\beta^k)^2) \geq \sum_{k=1}^K \beta^k$ . Therefore, we can conclude that our algorithm can always achieve  $\min_{0 \leq k \leq K} \mathbb{E}[\|\nabla \ell(\theta^k)\|_2^2] \leq \mathcal{O}(\frac{1}{\sqrt{K}})$  in  $K$  steps, and this finishes our proof of Theorem 2.  $\square$

**C. Derivation of The Update Details for Meta Parameters.** Recall the updated equation of the parameters of data points re-weighting strategy as follows

$$\theta^{k+1} = \theta^k - \beta \frac{1}{m} \sum_{i=1}^m \nabla_{\theta} \ell_i(\hat{\psi}^k(\theta)) \Big|_{\theta^k}. \quad [73]$$

The computation of Eq.73 in the paper by backpropagation can be understood by the following derivation

$$\begin{aligned} & \frac{1}{m} \sum_{i=1}^m \nabla_{\theta} \ell_i(\hat{\psi}^k(\theta)) \Big|_{\theta^k} \\ &= \frac{1}{m} \sum_{i=1}^m \frac{\partial \ell_i(\hat{\psi})}{\partial \hat{\psi}(\theta)} \Big|_{\hat{\psi}^k} \sum_{j=1}^n \frac{\partial \hat{\psi}^k(\theta)}{\partial \mathcal{V}(\Phi_j(\psi^k); \theta)} \frac{\partial \mathcal{V}(\Phi_j(\psi^k); \theta)}{\partial \theta} \Big|_{\theta^k} \\ &= \frac{-\alpha}{n * m} \sum_{i=1}^m \frac{\partial \ell_i(\hat{\psi})}{\partial \hat{\psi}} \Big|_{\hat{\psi}^k} \sum_{j=1}^n \frac{\partial \Phi_j(\psi)}{\partial \psi} \Big|_{\psi^k} \frac{\partial \mathcal{V}(\Phi_j(\psi^k); \theta)}{\partial \theta} \Big|_{\theta^k} \\ &= \frac{-\alpha}{n} \sum_{j=1}^n \left( \frac{1}{m} \sum_{i=1}^m \frac{\partial \ell_i(\hat{\psi})}{\partial \hat{\psi}} \Big|_{\hat{\psi}^k}^T \frac{\partial \Phi_j(\psi)}{\partial \psi} \Big|_{\psi^k} \right) \frac{\partial \mathcal{V}(\Phi_j(\psi^k); \theta)}{\partial \theta} \Big|_{\theta^k}. \end{aligned} \quad [74]$$

Let

$$G_{ij} = \frac{\partial \ell_i(\hat{\psi})}{\partial \hat{\psi}} \Big|_{\hat{\psi}^k}^T \frac{\partial \Phi_j(\psi)}{\partial \psi} \Big|_{\psi^k}, \quad [75]$$

by substituting Eq.74 into Eq. (73), we can get:

$$\theta^{k+1} = \theta^k + \frac{\alpha\beta}{n} \sum_{j=1}^n \left( \frac{1}{m} \sum_{i=1}^m G_{ij} \right) \frac{\partial \mathcal{V}(\Phi_j(\psi^k); \theta)}{\partial \theta} \Big|_{\theta^k}. \quad [76]$$

## 4. Detailed Description of the Weighted Mean-Field MSA

**A. Weighted Mean-field MSA.** In this subsection, we illustrate the iterative update process of the weighted mean-field MSA in Alg.2, comprising the state equation, the costate equation, and the maximization of the Hamiltonian.

---

### Algorithm 2 Weighted Mean-field MSA

---

- 1: **Initialize**  $\psi^0 = \{\psi_t^0 \in \Psi : t = 0 \dots, T-1\}$ .
- 2: **for**  $k = 0$  **to**  $K$  **do**
- 3:     Solve the forward SDE:

$$dX_t^k = [a(\mu_t - X_t^k) + \psi_t^k] dt + \sigma dW_t, \quad X_0^k = x,$$

- 4:     Solve the backward SDE:

$$dY_t^k = -\nabla_x \mathcal{H}(X_t^k, Y_t^k, \psi_t^k) dt + Z_t^k dW_t, \quad Y_T^k = -\mathcal{V}(\Phi(\psi_T^k); \theta) \nabla_x \Phi(X_T^k),$$

- 5:     For each  $t \in [0, T-1]$ , update the state control  $\psi_t^{k+1}$ :

$$\psi_t^{k+1} = \arg \max_{\psi \in \Psi} \mathcal{H}(X_t^k, Y_t^k, \psi).$$


---

**B. Error Estimate for the Weighted Mean-Field MSA.** In this section, we derive a rigorous error estimate for the weighted mean-field MSA, aiding in comprehending its stochastic dynamic. Let us now make the following assumptions:

**Assumption 1.** The terminal cost function  $\Phi$  in Eq.35 is twice continuously differentiable, with  $\Phi$  and  $\nabla \Phi$  satisfying a Lipschitz condition. There is a constant  $K \geq 0$  such that  $\forall X_T, X'_T \in \mathbb{R}, \forall \psi_T \in \Psi$

$$|\Phi(X_T, \mu_T) - \Phi(X'_T, \mu_T)| + \|\nabla \Phi(X_T, \mu_T) - \nabla \Phi(X'_T, \mu_T)\| \leq K \left\| \frac{X_T - X'_T}{\mathcal{V}(\Phi(\psi_T); \theta)} \right\|$$

**Assumption 2.** From Eq.35, The running cost function  $R$  and the drift function  $b$  are jointly continuous in  $t$  and twice continuously differentiable in  $X_t$ , with  $b, \nabla_x b, R, \nabla_x R$  satisfying Lipschitz conditions in  $X_t$  uniformly in  $t$  and  $\psi_t$ . Since  $\sigma$  is constant, it has no effect on the error estimate. There exists  $K \geq 0$  such that  $\forall x \in \mathbb{R}^d, \forall \psi_t \in \Psi, \forall t \in [0, T-1]$

$$\|b(X_t, \phi_t) - b(X'_t, \phi_t)\| + \|\nabla_x b(X_t, \phi_t) - \nabla_x b(X'_t, \phi_t)\| + |R(X_t, \phi_t) - R(X'_t, \phi_t)| + \|\nabla_x R(X_t, \phi_t) - \nabla_x R(X'_t, \phi_t)\| \leq K \|X_t - X'_t\|$$

With these assumptions, we provide the following error estimate for weighted mean-field MSA.

**Lemma 3.** *Suppose Assumptions 2 and 1 hold. Then for arbitrary admissible controls  $\psi$  and  $\psi'$  there exists a constant  $C > 0$  such that*

$$\begin{aligned}
\mathcal{L}(\psi) - \mathcal{L}(\psi') &\leq - \sum_{i=1}^N \sum_{t=0}^{T-1} [\mathcal{H}(X_{i,t}, Y_{i,t}, P_{i,t}, \psi_t) - H(X_{i,t}, Y_{i,t}, P_{i,t}, \psi'_t)] \\
&\quad + \frac{C}{N} \sum_{i=1}^N \sum_{t=0}^{T-1} \|b(X_{i,t}, Y_{i,t}, P_{i,t}, \psi_t) - b(X_{i,t}, Y_{i,t}, P_{i,t}, \psi'_t)\|^2 \\
&\quad + \frac{C}{N} \sum_{i=1}^N \sum_{t=0}^{T-1} \|\nabla_x b(X_{i,t}, Y_{i,t}, P_{i,t}, \psi_t) - \nabla_x b(X_{i,t}, Y_{i,t}, P_{i,t}, \psi'_t)\|^2, \\
&\quad + \frac{C}{N} \sum_{i=1}^N \sum_{t=0}^{T-1} \|\nabla_x R(X_{i,t}, Y_{i,t}, P_{i,t}, \psi_t) - \nabla_x R(X_{i,t}, Y_{i,t}, P_{i,t}, \psi'_t)\|^2,
\end{aligned} \tag{77}$$

The proof follows a discrete Gronwall's lemma.

**Lemma 4.** *Let  $K \geq 0$  and  $u_t, w_t$ , be non-negative real valued sequences satisfying*

$$u_{t+1} \leq K u_t + w_t,$$

for  $t = 0, \dots, T-1$ . Then, we have for all  $t = 0, \dots, T$ ,

$$u_t \leq \max(1, K^t) \left( u_0 + \sum_{s=0}^{t-1} w_s \right).$$

*Proof.* We prove by induction the inequality

$$u_t \leq \max(1, K^t) \left( u_0 + \sum_{s=0}^{t-1} w_s \right),$$

from which the lemma follows immediately. The case  $t = 0$  is trivial. Suppose the above is true for some  $t$ , we have

$$\begin{aligned}
u_{t+1} &\leq K u_t + w_t \\
&\leq K \max(1, K^t) \left( u_0 + \sum_{s=0}^{t-1} w_s \right) + w_t \\
&\leq \max(1, K^{t+1}) \left( u_0 + \sum_{s=0}^{t-1} w_s \right) + \max(1, K^{t+1}) w_t \\
&= \max(1, K^{t+1}) \left( u_0 + \sum_{s=0}^t w_s \right).
\end{aligned}$$

This proves Eq. (B) and hence the lemma.  $\square$

Let us now commence the proof of a preliminary lemma that estimates the magnitude of  $Y_t$  for arbitrary  $\psi \in \Psi$ . Hereafter,  $C$  will be stand for arbitrary generic constant that does not depend on  $\psi, \psi'$  and  $S$  (batch size) but may depend on other fixed quantities such as  $T$  and the Lipschitz constants  $K$  in Assumption 1-2. Also, the value of  $C$  is allowed to change to another constant value with the same dependencies from line to line to reduce notational clutter.

**Lemma 5.** *There exists a constant  $C > 0$  such that for each  $t = 0, \dots, T$  and  $\psi \in \Psi$ , we have*

$$\|Y_{i,t}\| \leq \frac{C}{N}.$$

for all  $i = 1, \dots, N$ .

*Proof.* First, notice that  $Y_{i,t} = -\frac{1}{N} \nabla \Phi(X_{i,t})$  and so by Assumption 1, we have

$$\|Y_{i,t}\| = \frac{1}{N} \|\nabla \Phi(X_{i,t})\| \leq \frac{K}{N}.$$

Now, for each  $0 \leq t < T$ , we have by Assumption 2 in the main text,

$$\begin{aligned}
\|Y_{i,t}\| &= \|\nabla_x \mathcal{H}(X_{i,t}, Y_{i,t+1}, \psi'_t)\| \\
&\leq \|\nabla_x b(X_{i,t}, \psi'_t)^T Y_{i,t+1}\| + \frac{1}{N} \|\nabla_x R(X_{i,t}, \psi_t)\| \\
&\leq K \|Y_{i,t+1}\| + \frac{K}{N}
\end{aligned}$$

Using Lemma 4 with  $t \rightarrow T - t$ , we get

$$\|Y_{i,t}\| \leq \max(1, K^T) \left( \frac{K}{N} + \frac{TK}{N} \right) = \frac{C}{N}.$$

□

We are now ready to prove Theorem 3.

*Proof.* Recall the Hamiltonian definition

$$\mathcal{H}_i(X_t, Y_t, Z_t, \mu_t, \psi_t) = [a(\mu_t - X_t) + \psi_t] \cdot Y_t + \sigma^\top Z_t - R(X_t, \mu_t, \psi_t).$$

Let us define the quantity

$$I(X_t, Y_t, \psi) := \sum_{t=0}^{T-1} [Y_{t+1} \cdot X_{t+1} - \mathcal{H}(X_t, Y_{t+1}, \psi_t) - R(X_t, \psi_t)]$$

Then, we consider the following linearized form

$$\begin{aligned} b(X_{t+1}, \psi_{t+1}) &= b(X_t, \psi_t) + \nabla_x b(X_t, \psi_t)(\psi_t - X_t) \\ &= [a(\mu_t - X_t) + \psi_t] + \nabla_x [a(\mu_t - X_t) + \psi_t](\psi_t - X_t), \end{aligned} \quad [78]$$

From Eq. 78, we know that  $I(X_t, Y_t, \psi) = 0$  for arbitrary  $i = 1, \dots, N$  and  $\psi \in \Psi$ . Let us now fix some sample  $i$  and obtain corresponding estimates. We have

$$\begin{aligned} 0 &= I(X_t, Y_t, \psi) - I(X'_t, Y'_t, \psi') \\ &= \sum_{i=1}^N \sum_{t=0}^{T-1} [Y_{i,t+1} \cdot X_{i,t+1} - Y'_{i,t+1} \cdot X'_{i,t+1}] \\ &\quad - \sum_{i=1}^N \sum_{t=0}^{T-1} [\mathcal{H}_i(X_{i,t}, Y_{i,t+1}, \psi_t) - \mathcal{H}_i(X'_{i,t}, Y'_{i,t+1}, \psi'_t)] \\ &\quad - \frac{1}{N} \sum_{i=1}^N \sum_{t=0}^{T-1} [R_i(X_{i,t}, \psi_t) - R_i(X'_{i,t}, \psi'_t)] \end{aligned} \quad [79]$$

We can rewrite the first term on the right-hand side as

$$\begin{aligned} &\sum_{i=1}^N \sum_{t=0}^{T-1} [Y_{i,t+1} \cdot X_{i,t+1} - Y'_{i,t+1} \cdot X'_{i,t+1}] \\ &= \sum_{i=1}^N \sum_{t=0}^{T-1} [Y_{i,t+1} \cdot \Delta X_{i,t+1} + X_{i,t+1} \cdot \Delta Y_{i,t+1} - \Delta X_{i,t+1} \cdot \Delta Y_{i,t+1}], \end{aligned} \quad [80]$$

where we have defined  $\Delta X_{i,t} := X_{i,t} - X'_{i,t}$  and  $\Delta Y_{i,t} := Y_{i,t} - Y'_{i,t}$ . We may simplify further by observing that  $\Delta X_{i,0} = 0$ , and so

$$\begin{aligned} &\sum_{i=1}^N \sum_{t=0}^{T-1} [Y_{i,t+1} \cdot \Delta X_{i,t+1} + X_{i,t+1} \cdot \Delta Y_{i,t+1}] \\ &= \sum_{i=1}^N \left\{ Y_{i,T} \cdot \Delta X_{i,T} + \sum_{t=0}^{T-1} [Y_{i,t} \cdot \Delta X_{i,t} + X_{i,t+1} \cdot \Delta Y_{i,t+1}] \right\} \\ &= \sum_{i=1}^N \left\{ Y_{i,T} \cdot \Delta X_{i,T} + \sum_{t=0}^{T-1} [\nabla_x \mathcal{H}_i(X_{i,t}, Y_{i,t+1}, \psi'_t) \cdot \Delta X_{i,t} + \nabla_y \mathcal{H}_i(X_{i,t}, Y_{i,t+1}, \psi'_t) \cdot \Delta Y_{i,t+1}] \right\} \end{aligned}$$

By defining the extended vector  $P_{i,t} := (X_{i,t}, Y_{i,t+1})$  and  $P'_{i,t} := (X'_{i,t}, Y'_{i,t+1})$ , we can rewrite this as

$$\sum_{i=1}^N \sum_{t=0}^{T-1} [Y_{i,t+1} \cdot \Delta X_{i,t+1} + X_{i,t+1} \cdot \Delta Y_{i,t+1}] = \sum_{i=1}^N \left\{ Y_{i,T} \cdot \Delta X_{i,T} + \sum_{t=0}^{T-1} \nabla_p \mathcal{H}_i(P_{i,t}, \psi_t) \cdot \Delta P_{i,t} \right\} \quad [81]$$

Similarly, we also have

$$\begin{aligned}
& \sum_{i=1}^N \sum_{t=0}^{T-1} \Delta X_{i,t+1} \cdot \Delta Y_{i,t+1} \\
&= \frac{1}{2} \sum_{i=1}^N \sum_{t=0}^{T-1} [\Delta X_{i,t+1} \cdot \Delta Y_{i,t+1} + \Delta X_{i,t+1} \cdot \Delta Y_{i,t+1}] \\
&= \frac{1}{2} \sum_{i=1}^N \left\{ \Delta X_{i,T} \cdot \Delta Y_{i,T} + \frac{1}{2} \sum_{t=0}^{T-1} [\nabla_p \mathcal{H}_i(P_{i,t}, \psi_t) - \nabla_p \mathcal{H}_i(P'_{i,t}, \psi'_t)] \cdot \Delta P_{i,t} \right\} \\
&= \frac{1}{2} \sum_{i=1}^N \left\{ \Delta X_{i,T} \cdot \Delta Y_{i,T} + \frac{1}{2} \sum_{t=0}^{T-1} [\nabla_p \mathcal{H}(P_{i,t}, \psi_t) - \nabla_z \mathcal{H}(P_{i,t}, \psi'_t)] \cdot \Delta P_{i,t} + \frac{1}{2} \sum_{t=0}^{T-1} \Delta P_{i,t} \cdot \nabla_z^2 \mathcal{H}(P_{i,t} + r_1(t) \Delta P_{i,t}, \psi_t) \Delta P_{i,t} \right\} \quad [82]
\end{aligned}$$

where in the last line, we used Taylor's theorem with  $r_1(t) \in [0, 1]$  for each  $t$ . Now, we can rewrite the terminal terms in Eq.81 and Eq.82 as follows:

$$\begin{aligned}
& (Y_{i,T} + \frac{1}{2} \Delta Y_{i,T}) \cdot \Delta X_{i,T} \\
&= -\frac{1}{N} \nabla \Phi(X_{i,T}) \cdot \Delta X_{i,T} - \frac{1}{2N} [\nabla \Phi(X_{i,T}) - \nabla \Phi(X_{i,T})] \cdot \Delta X_{i,T} \\
&= -\frac{1}{N} \nabla \Phi(X_{i,T}) \cdot \Delta X_{i,T} - \frac{1}{2N} \Delta X_{i,T} \cdot \nabla^2 \Phi(X_{i,T} + r_2 \Delta X_{i,T}) \Delta X_{i,T} \\
&= -\frac{1}{N} (\Phi(X_T) - \Phi(x_T)) - \frac{1}{2N} \Delta X_{i,T} \cdot [\nabla^2 \Phi(X_{i,T} + r_2 \Delta X_{i,T}) + \nabla^2 \Phi(X_{i,T} + r_3 \Delta X_{i,T})] \Delta X_{i,T}, \quad [83]
\end{aligned}$$

for some  $r_2, r_3 \in [0, 1]$ . Lastly, for each  $t = 0, 1, \dots, T-1$  we have

$$\begin{aligned}
& \mathcal{H}(P_{i,t}, \psi_t) - \mathcal{H}(P'_{i,t}, \psi'_t) \\
&= [\mathcal{H}(P_{i,t}, \psi_t) - \mathcal{H}(P_{i,t}, \psi'_t)] \\
&\quad + \nabla_p \mathcal{H}(P_{i,t}, \psi_t) \cdot \Delta P_{i,t} \\
&\quad + \frac{1}{2} \Delta P_{i,t} \cdot \nabla_p^2 \mathcal{H}(P_{i,t} + r_4(t) \Delta P_{i,t}, \psi_t) \Delta P_{i,t} \quad [84]
\end{aligned}$$

where  $r_4(t) \in [0, 1]$ .

Substituting Eq.80-84 into Eq.79 yields

$$\begin{aligned}
& \frac{1}{N} \sum_{i=1}^N \left[ \sum_{t=0}^{T-1} R_i(X_{i,t}, \psi_t) + \mathcal{V}(\Phi_i(\psi_T); \theta) \Phi_i(X_{i,T}) \right] - \frac{1}{N} \sum_{i=1}^N \left[ \sum_{t=0}^{T-1} R_i(X'_{i,t}, \psi'_t) + \mathcal{V}(\Phi_i(\psi'_T); \theta) \Phi_i(X'_{i,T}) \right] \\
&= -\sum_{i=1}^N \sum_{t=0}^{T-1} [\mathcal{H}_i(X_t, Y_{t+1}, \psi_t) - \mathcal{H}_i(X_t, Y_{t+1}, \psi'_t)] \\
&\quad + \frac{1}{2N} \sum_{i=1}^N \left\{ \Delta X_{i,T} \cdot \mathcal{V}(\Phi_i(\psi_T); \theta) [\nabla^2 \Phi_i(X_{i,T} + r_2 \Delta X_{i,T}) + \nabla^2 \Phi_i(X_{i,T} + r_3 \Delta X_{i,T})] \Delta X_{i,T} \right\} \\
&\quad + \frac{1}{2} \sum_{i=1}^N \sum_{t=0}^{T-1} [\nabla_p \mathcal{H}_i(P_{i,t}, \psi_t) - \nabla_p \mathcal{H}_i(P_{i,t}, \psi'_t)] \cdot \Delta P_{i,t} \\
&\quad + \frac{1}{2} \sum_{i=1}^N \sum_{t=0}^{T-1} \Delta P_{i,t} \cdot [\nabla_p^2 \mathcal{H}_i(P_{i,t} + r_1(t) \Delta P_{i,t}, \psi_t) - \nabla_p^2 \mathcal{H}_i(P_{i,t} + r_4(t) \Delta P_{i,t}, \psi_t)] \Delta P_{i,t} \quad [85]
\end{aligned}$$

Note that by summing over all  $s$ , the left hand side is simply  $\mathcal{L}(\psi) - \mathcal{L}(\psi')$ . Let us further simplify the right hand side. First, by Assumption 1, we have

$$\Delta X_{i,T} \cdot \mathcal{V}(\Phi_i(\psi_T); \theta) [\nabla^2 \Phi(X_{i,T} + r_2 \Delta X_{i,T}) + \nabla^2 \Phi(X_{i,T} + r_3 \Delta X_{i,T})] \Delta X_{i,T} \leq K \|\Delta X_{i,T}\|^2. \quad [86]$$

Next,

$$\begin{aligned}
& \left[ \nabla_z \mathcal{H}(P_{i,t}, \psi_t) - \nabla_z \mathcal{H}(P_{i,t}, \psi'_t) \right] \cdot \Delta P_{i,t} \\
& \leq \|\nabla_x \mathcal{H}(X_{i,t}, Y_{i,t+1}, \psi_t) - \nabla_x \mathcal{H}(X_{i,t}, Y_{i,t+1}, \psi'_t)\| \|\Delta X_{i,t}\| \\
& \quad + \|\nabla_y \mathcal{H}(X_{i,t}, Y_{i,t+1}, \psi_t) - \nabla_y \mathcal{H}(X_{i,t}, Y_{i,t+1}, \psi'_t)\| \|\Delta Y_{i,t+1}\| \\
& \leq \frac{1}{2N} \|\Delta X_{i,t}\|^2 + \frac{N}{2} \|\nabla_x \mathcal{H}(X_{i,t}, Y_{i,t+1}, \psi_t) - \nabla_x \mathcal{H}(X_{i,t}, Y_{i,t+1}, \psi'_t)\|^2 \\
& \quad + \frac{N}{2} \|\Delta Y_{i,t}\|^2 + \frac{1}{2N} \|\nabla_y \mathcal{H}(X_{i,t}, Y_{i,t+1}, \psi_t) - \nabla_y \mathcal{H}(X_{i,t}, Y_{i,t+1}, \psi'_t)\|^2 \\
& \leq \frac{1}{2N} \|\Delta X_{i,t}\|^2 + \frac{C^2}{2N} \|\nabla_x b(X_{i,t}, \psi_t) - \nabla_x b(X_{i,t}, \psi'_t)\|^2 \\
& \quad + \frac{1}{2N} \|\nabla_x R(X_{i,t}, \psi_t) - \nabla_x R(X_{i,t}, \psi'_t)\|^2 \\
& \quad + \frac{N}{2} \|\Delta Y_{i,t}\|^2 + \frac{1}{2N} \|b(X_{i,t}, \psi_t) - b(X_{i,t}, \psi'_t)\|^2, \tag{87}
\end{aligned}$$

where in the last line, we have used Lemma 5. Similarly, we can simplify the last term in Eq.85. Notice that the second derivative of  $\mathcal{H}$  concerning  $Y$  vanishes since it is linear. Hence, as in Eq.86 and using Lemma 5, we have

$$\begin{aligned}
& \Delta P_{i,t} \cdot \left[ \nabla_z^2 \mathcal{H}(P_{i,t} + r_1(t) \Delta P_{i,t}, \psi_t) - \nabla_z^2 \mathcal{H}(P_{i,t} + r_4(t) \Delta P_{i,t}, \psi_t) \right] \Delta P_{i,t} \\
& \leq \frac{2KC}{N} \|\Delta X_{i,t}\|^2 + 4K \|\Delta X_{i,t}\| \|\Delta Y_{i,t+1}\| \\
& \leq \frac{2KC}{N} \|\Delta X_{i,t}\|^2 + \frac{2K}{N} \|\Delta X_{i,t}\|^2 + 2KN \|\Delta Y_{i,t+1}\|^2 \tag{88}
\end{aligned}$$

Substituting Eq.86-88 into Eq.85, as follow

$$\begin{aligned}
& \frac{1}{N} \left[ \sum_{t=0}^{T-1} R_i(X_{i,t}, \psi_t) + \mathcal{V}(\Phi_i(\psi_T); \theta) \Phi_i(X_{i,T}) \right] - \frac{1}{N} \left[ \sum_{t=0}^{T-1} R_i(X'_{i,t}, \psi'_t) + \mathcal{V}(\Phi_i(\psi'_T); \theta) \Phi_i(X'_{i,T}) \right] \\
& = - \sum_{i=1}^N \sum_{t=0}^{T-1} \left[ \mathcal{H}_i(X_t, Y_{t+1}, \phi_t) - \mathcal{H}_i(X_t, Y_{t+1}, \psi'_t) \right] \\
& \quad + \frac{C}{N} \sum_{i=1}^N \sum_{t=0}^T \|\Delta X_{i,t}\|^2 + CN \sum_{i=1}^N \sum_{t=0}^{T-1} \|\Delta Y_{i,t+1}\|^2 \\
& \quad + \frac{C}{N} \sum_{i=1}^N \sum_{t=0}^{T-1} \|b(X_{i,t}, \psi_t) - b(X_{i,t}, \psi'_t)\|^2 \\
& \quad + \frac{C}{N} \sum_{i=1}^N \sum_{t=0}^{T-1} \|\nabla_x b(X_{i,t}, \psi_t) - \nabla_x b(X_{i,t}, \psi'_t)\|^2 \\
& \quad + \frac{C}{N} \sum_{i=1}^N \sum_{t=0}^{T-1} \|\nabla_x R_i(X_{i,t}, \psi_t) - \nabla_x R_i(X_{i,t}, \psi'_t)\|^2 \tag{89}
\end{aligned}$$

It remains to estimate the magnitudes of  $\Delta X_{i,t}$  and  $\Delta Y_{i,t}$ . Observe that  $\Delta X_{i,0} = 0$ , hence we have for each  $t = 0, \dots, T-1$

$$\begin{aligned}
\|\Delta X_{i,t+1}\| & \leq \|b(X_{i,t}, \psi_t) - b(X'_{i,t}, \phi_t)\| + \|b(X_{i,t}, \psi_t) - b(X'_{i,t}, \psi'_t)\| \\
& \leq K \|\Delta X_{i,t}\| + \|b(X_{i,t}, \psi_t) - b(X_{i,t}, \psi'_t)\|
\end{aligned}$$

Using Lemma 4, we have

$$\|\Delta X_{i,t}\| \leq C \sum_{i=1}^N \sum_{t=0}^{T-1} \|b(X_{i,t}, \psi_t) - b(X_{i,t}, \psi'_t)\| \tag{90}$$

Similarly,

$$\begin{aligned}
\|\Delta Y_{i,t}\| & \leq \|\nabla_x \mathcal{H}_i(X_{i,t}, Y_{i,t+1}, \psi_t) - \nabla_x \mathcal{H}_i(X'_{i,t}, Y'_{i,t+1}, \psi'_t)\| \\
& \leq 2K \|\Delta Y_{i,t+1}\| + \frac{C}{N} \|\Delta X_{i,t}\| \\
& \quad + \frac{C}{N} \|\nabla_x b(X_{i,t}, \psi_t) - \nabla_x b(X_{i,t}, \psi'_t)\| \\
& \quad + \frac{C}{N} \|\nabla_x R_i(X_{i,t}, \psi_t) - \nabla_x R_i(X_{i,t}, \psi'_t)\|,
\end{aligned}$$

and so by Lemma 4, Eq.90 and the fact that  $\|\Delta Y_{i,T}\| \leq \frac{K}{N} \|\Delta X_{i,T}\|$  by Assumption 1, we have

$$\begin{aligned}
\|\Delta Y_{i,t}\| &\leq \frac{C}{N} \sum_{i=1}^N \sum_{t=0}^{T-1} \|b(X_{i,t}, \psi_t) - b(X_{i,t}, \psi'_t)\| \\
&\quad + \frac{C}{N} \sum_{i=1}^N \sum_{t=0}^{T-1} \|\nabla_x b(X_{i,t}, \psi_t) - \nabla_x b(X_{i,t}, \psi'_t)\| \\
&\quad + \frac{C}{N} \sum_{i=1}^N \sum_{t=0}^{T-1} \|\nabla_x R(X_{i,t}, \psi_t) - \nabla_x R(X_{i,t}, \psi'_t)\|.
\end{aligned} \tag{91}$$

Finally, we conclude the proof of Theorem 3 by substituting estimates Eq.90 and Eq.91 into Eq.89.  $\square$

## 5. Proof of Our Data Valuation Method

**A. Proof of the Data State Utility Function.** In this subsection, we provide detailed proof of the data state utility function from the optimal state sensitivity.

**Theorem 3.** *Assume that a set of data points undergoes a single iteration of model training, yielding an optimal control strategy, the form of the utility function corresponding to these data points is then as follows*

$$U_i(S) = -X_{i,T} \cdot Y_{i,T},$$

*Proof.*  $\square$

**B. Proof of Dynamic Marginal Contribution.** In this subsection, we provide a detailed proof of dynamic marginal contribution in Proposition 1.

**Proposition 1.** *For arbitrary two data points  $(x_i, y_i)$  and  $(x_j, y_j)$ ,  $i \neq j \in [N]$ , if  $U_i(S) > U_j(S)$ , then  $\Delta(x_i, y_i; U_i(S)) > \Delta(x_j, y_j; U_j(S))$ .*

*Proof.* For  $i \neq j$ , if  $U_i(S) > U_j(S)$ , we have

$$\begin{aligned}
&\Delta(x_i, y_i; U_i(S)) - \Delta(x_j, y_j; U_j(S)) \\
&= \left[ U_i(S) - \sum_{i' \in \{1, \dots, N\} \setminus i} \frac{U_{i'}(S)}{N-1} \right] - \left[ U_j(S) - \sum_{j' \in \{1, \dots, N\} \setminus j} \frac{U_{j'}(S)}{N-1} \right] \\
&= [U_i(S) - U_j(S)] + \frac{1}{N-1} \left[ \sum_{j' \in \{1, \dots, N\} \setminus j} U_{j'}(S) - \sum_{i' \in \{1, \dots, N\} \setminus i} U_{i'}(S) \right] \\
&= [U_i(S) - U_j(S)] + \frac{1}{N-1} [U_i(S) - U_j(S)] \\
&= \frac{N}{N-1} [U_i(S) - U_j(S)] \\
&> 0.
\end{aligned} \tag{92}$$

Then, the proof is complete.  $\square$

**C. Proof of Dynamic Data Valuation.** In this subsection, we provide a detailed proof process demonstrating how our proposed dynamic data valuation metric satisfies the common axioms.

For the **efficiency** property, If there are no data points within the coalition, then no data states are presented. In this case, it still holds that

$$\begin{aligned}
\sum_{i \in N} \phi(x_i, y_i; U_i) &= \sum_{i \in N} \Delta(x_i, y_i; U_i) \\
&= \sum_{i \in N} \left[ U_i(S) - \sum_{j \in \{1, \dots, N\} \setminus i} \frac{U_j(S)}{N-1} \right] \\
&= -X_t \cdot \mathcal{V}(\Phi(X_t; \mu_T)) Y_T - 0 \\
&= U(N) - U(\emptyset),
\end{aligned} \tag{93}$$



For the **symmetry** property, the value to data point  $(x'_i, y'_i)$  is  $\phi((x'_i, y'_i); U'_i)$ . For arbitrary  $S \in N \setminus \{(x_i, y_i), (x'_i, y'_i)\}$ , if  $U(S \cup (x_i, y_i)) = U(S \cup (x'_i, y'_i))$ , the proof of this property as follow

$$\begin{aligned}
\phi(x'_i, y'_i; U'_i(S)) &= \Delta(x'_i, y'_i; U'_i(S)) \\
&= U'_i(S) - \sum_{j \in \{1, \dots, N\} \setminus \{i', i\}} \frac{U_j(S)}{N-1} \\
&= U_i(S) - \sum_{j \in \{1, \dots, N\} \setminus \{i, i'\}} \frac{U_j(S)}{N-1} \\
&= \phi(x_i, y_i; U_i(S)),
\end{aligned} \tag{94}$$

For the **dummy** property, since  $U(S \cup (x_i, y_i)) = U(S)$  for all  $S \in N \setminus (x_i, y_i)$  always holds, the value to the data point  $(x_i, y_i)$  is

$$\begin{aligned}
\phi(x_i, y_i; U_i(S)) &= \Delta(x_i, y_i; U_i(S)) \\
&= U_i(S) - \sum_{j \in \{1, \dots, N\} \setminus i} \frac{U_j(S)}{N-1} \\
&= 0,
\end{aligned} \tag{95}$$

For the **additivity** property, we choose the two utility functions  $U_1$  and  $U_2$  together, impacting the data point  $(x_i, y_i)$ . The value to it for arbitrary  $\alpha_1, \alpha_2 \in \mathbb{R}$  is

$$\begin{aligned}
\phi(x_i, y_i; \alpha_1 U_{1,i}(S) + \alpha_2 U_{2,i}(S)) &= \Delta(x_i, y_i; \alpha_1 U_{1,i}(S) + \alpha_2 U_{2,i}(S)) \\
&= [\alpha_1 U_{1,i}(S) + \alpha_2 U_{2,i}(S)] - \sum_{j \in \{1, \dots, N\} \setminus i} \frac{\alpha_1 U_{1,j}(S) + \alpha_2 U_{2,j}(S)}{N-1} \\
&= \alpha_1 \left[ U_{1,i}(S) - \sum_{j \in \{1, \dots, N\} \setminus i} \frac{U_{1,j}(S)}{N-1} \right] + \alpha_2 \left[ U_{2,i}(S) - \sum_{j \in \{1, \dots, N\} \setminus i} \frac{U_{2,j}(S)}{N-1} \right] \\
&= \alpha_1 \phi((x_i, y_i); U_{1,i}(S)) + \alpha_2 \phi((x_i, y_i); U_{2,i}(S)),
\end{aligned} \tag{96}$$

For the **marginalism** property, if each data point has the identical marginal impact in two utility functions  $U_1, U_2$ , satisfies  $U_1(S \cup (x_i, y_i)) - U_1(S) = U_2(S \cup (x_i, y_i)) - U_2(S)$ . The proof of this property is as follows

$$\begin{aligned}
\phi(x_i, y_i; U_{1,i}) &= \Delta(x_i, y_i; U_{1,i}(S)) \\
&= U_{1,i}(S) - \sum_{j \in \{1, \dots, N\} \setminus i} \frac{U_{1,j}(S)}{N-1} \\
&= U_1(S \cup (x_i, y_i)) - U_1(S) \\
&= U_2(S \cup (x_i, y_i)) - U_2(S) \\
&= U_{2,i}(S) - \sum_{j \in \{1, \dots, N\} \setminus i} \frac{U_{2,j}(S)}{N-1} \\
&= \phi(x_i, y_i; U_{2,i}).
\end{aligned} \tag{97}$$

Then, the proof of the five common axioms is complete.

It is evident that our proposed dynamic data valuation metric satisfies the common axioms. Then, we provide the following Proposition 2 to identify important data points among two arbitrarily different data points.

**Proposition 2.** For arbitrary two data points  $(x_i, y_i)$  and  $(x_j, y_j)$ ,  $i \neq j \in [N]$ , if  $U_i(S) > U_j(S)$ , then  $\phi(x_i, y_i; U_i(S)) > \phi(x_j, y_j; U_j(S))$ .

*Proof.* For  $i \neq j$ , if  $U_i(S) > U_j(S)$ , we have

$$\begin{aligned}
\phi(x_i, y_i; U_i(S)) - \phi(x_j, y_j; U_j(S)) &= \Delta(x_i, y_i; U_i(S)) - \Delta(x_j, y_j; U_j(S)) \\
&= \left[ U_i(S) - \sum_{i' \in \{1, \dots, N\} \setminus i} \frac{U_{i'}(S)}{N-1} \right] - \left[ U_j(S) - \sum_{j' \in \{1, \dots, N\} \setminus j} \frac{U_{j'}(S)}{N-1} \right] \\
&= [U_i(S) - U_j(S)] + \frac{1}{N-1} \left[ \sum_{j' \in \{1, \dots, N\} \setminus j} U_{j'}(S) - \sum_{i' \in \{1, \dots, N\} \setminus i} U_{i'}(S) \right] \\
&= [U_i(S) - U_j(S)] + \frac{1}{N-1} [U_i(S) - U_j(S)] \\
&= \frac{N}{N-1} [U_i(S) - U_j(S)] \\
&> 0.
\end{aligned} \tag{98}$$

Then, the proof is complete.  $\square$

Moreover, the following Proposition 3 shows that our proposed dynamic data valuation metric converges to the LOO metric.

**Proposition 3.** For arbitrary  $i \in [n]$  and error bound  $\varepsilon$ , if  $\|U_i(S) - U(S \cup (x_i, y_i))\| \leq \varepsilon$ , then  $\|NDDV - LOO\| \leq 2\varepsilon$ .

*Proof.* For arbitrary pair data points  $(x_i, y_i)$  and  $(x_j, y_j)$ ,  $i \neq j \in [N]$ . The LOO metric difference between those data points is

$$\begin{aligned} & \phi_{\text{loo}}(x_i, y_i; U(S)) - \phi_{\text{loo}}(x_j, y_j; U(S)) \\ &= [U(S \cup (x_i, y_i)) - U(S)] - [U(S \cup (x_j, y_j)) - U(S)] \\ &= U(S \cup (x_i, y_i)) - U(S \cup (x_j, y_j)), \end{aligned} \quad [99]$$

Then, call for Eq.92, we have

$$\phi_{\text{nddv}}(x_i, y_i; U_i(S)) - \phi_{\text{nddv}}(x_j, y_j; U_j(S)) = \frac{N}{N-1} [U_i(S) - U_j(S)] \quad [100]$$

In addition, the  $L_2$  error bound between the NDDV and LOO metric is

$$\begin{aligned} \|\text{NDDV} - \text{LOO}\| &= \|\phi_{\text{nddv}}((x_i, y_i), U_i(S)) - \phi_{\text{nddv}}((x_j, y_j), U_j(S)) - [\phi_{\text{loo}}((x_i, y_i), U(S)) - \phi_{\text{loo}}((x_j, y_j), U(S))]\| \\ &= \|\frac{N}{N-1} [U_i(S) - U_j(S)] - [U(S \cup (x_i, y_i)) - U(S \cup (x_j, y_j))]\| \\ &= \|[U_i(S) - U(S \cup (x_i, y_i))] - [U_j(S) - U(S \cup (x_j, y_j))]\| + \frac{1}{N-1} \|U_i(S) - U_j(S)\| \\ &\leq \|U_i(S) - U(S \cup (x_i, y_i))\| + \|U_j(S) - U(S \cup (x_j, y_j))\| + \frac{1}{N-1} \|U_i(S) - U_j(S)\| \\ &= 2\varepsilon, \quad N \rightarrow \infty. \end{aligned} \quad [101]$$

Concludes the proof.  $\square$

Finally, we also provide the  $L_2$  error bound between our proposed dynamic data valuation metric and Shapley value metric in the following Proposition 4.

**Proposition 4.** For arbitrary  $i \in [N]$  and error bound  $\varepsilon$ , if  $\|U_i(S) - U(S \cup (x_i, y_i))\| \leq \varepsilon$ , then  $\|NDDV - \text{Shap}\| \leq \frac{2\varepsilon N}{N-1}$ .

*Proof.* For arbitrary pair data points  $(x_i, y_i)$  and  $(x_j, y_j)$ ,  $i \neq j \in [N]$ . The Shapley value metric different between those data points is

$$\begin{aligned} & \phi_{\text{shap}}(x_i, y_i; U(S)) - \phi_{\text{shap}}(x_j, y_j; U(S)) \\ &= \frac{1}{N} \sum_{i'=1}^N \Delta_{i'}(x_i, y_i; U(S)) - \frac{1}{N} \sum_{j'=1}^N \Delta_{j'}(x_j, y_j; U(S)) \\ &= \sum_{S \in \mathcal{D} \setminus (x_i, y_i)} \frac{|S|!(N-|S|-1)!}{N!} [U(S \cup (x_i, y_i)) - U(S)] - \sum_{S \in \mathcal{D} \setminus (x_j, y_j)} \frac{|S|!(N-|S|-1)!}{N!} [U(S \cup (x_j, y_j)) - U(S)] \\ &= \sum_{S \in \mathcal{D} \setminus (x_i, y_i)} \frac{|S|!(N-|S|-1)!}{N!} [U(S \cup (x_i, y_i)) - U(S \cup (x_j, y_j))] \\ &\quad + \sum_{S \in \{T | T \in \mathcal{D}, (x_i, y_i) \notin T, (x_j, y_j) \in T\}} \frac{|S|!(N-|S|-1)!}{N!} [U(S \cup (x_i, y_i)) - U(S)] \\ &\quad - \sum_{S \in \{T | T \in \mathcal{D}, (x_i, y_i) \in T, (x_j, y_j) \notin T\}} \frac{|S|!(N-|S|-1)!}{N!} [U(S \cup (x_j, y_j)) - U(S)] \\ &= \sum_{S \in \mathcal{D} \setminus \{(x_i, y_i), (x_j, y_j)\}} \frac{|S|!(N-|S|-1)!}{N!} [U(S \cup (x_i, y_i)) - U(S \cup (x_j, y_j))] \\ &\quad + \sum_{S' \in \mathcal{D} \setminus \{(x_i, y_i), (x_j, y_j)\}} \frac{(|S'|+1)!(N-|S'|-2)!}{N!} [U(S' \cup (x_i, y_i)) - U(S' \cup (x_j, y_j))] \\ &= \sum_{S \in \mathcal{D} \setminus \{(x_i, y_i), (x_j, y_j)\}} \left[ \frac{|S|!(N-|S|-1)!}{N!} + \frac{(|S|+1)!(N-|S|-2)!}{N!} \right] [U(S \cup (x_i, y_i)) - U(S \cup (x_j, y_j))] \\ &= \frac{1}{N-1} \sum_{S \in \mathcal{D} \setminus \{(x_i, y_i), (x_j, y_j)\}} \frac{1}{C_{N-2}^{|S|}} [U(S \cup (x_i, y_i)) - U(S \cup (x_j, y_j))]. \end{aligned} \quad [102]$$

Then, call for Eq.92, we have

$$\phi_{\text{nddv}}(x_i, y_i; U_i(S)) - \phi_{\text{nddv}}(x_j, y_j; U_j(S)) = \frac{N}{N-1} [U_i(S) - U_j(S)] \quad [103]$$

In addition, the  $L_2$  error bound between the NDDV method and Shapley value metric is

$$\begin{aligned}
\|\text{NDDV} - \text{Shap}\| &= \|\phi_{\text{nddv}}(x_i, y_i; U_i(S)) - \phi_{\text{nddv}}(x_j, y_j; U_j(S)) - [\phi_{\text{shap}}(x_i, y_i; U(S)) - \phi_{\text{shap}}(x_j, y_j; U(S))]\| \\
&= \left\| \frac{N}{N-1} [U_i(S) - U_j(S)] - \frac{1}{N-1} \sum_{S \in \mathcal{D} \setminus \{(x_i, y_i), (x_j, y_j)\}} \frac{1}{C_{N-2}^{|S|}} [U(S \cup (x_i, y_i)) - U(S \cup (x_j, y_j))] \right\| \\
&= \left\| \frac{N}{N-1} [U_i(S) - U_j(S)] - \frac{1}{N-1} \sum_{k=0}^{N-2} C_k^{N-2} \frac{1}{C_{N-2}^{|S|}} [U(S \cup (x_i, y_i)) - U(S \cup (x_j, y_j))] \right\| \\
&\leq \frac{N}{N-1} \left\| [U_i(S) - U_j(S)] - \min \left\{ \sum_{k=0}^{N-2} C_k^{N-2} \frac{1}{NC_{N-2}^{|S|}} \right\} [U(S \cup (x_i, y_i)) - U(S \cup (x_j, y_j))] \right\| \\
&= \frac{N}{N-1} \left\| [U_i(S) - U_j(S)] - 2^{N-2} \frac{1}{NC_{N-2}^{\frac{N-2}{2}}} [U(S \cup (x_i, y_i)) - U(S \cup (x_j, y_j))] \right\| \\
&\leq \frac{N}{N-1} \|U_i(S) - U(S \cup (x_i, y_i))\| + \|U_j(S) - U(S \cup (x_j, y_j))\| \\
&= \frac{2\varepsilon N}{N-1}, \quad N \rightarrow \infty. \tag{104}
\end{aligned}$$

Concludes the proof.  $\square$

## 6. Experiments Details

In this section, we provide details of the experiment. Our Python-based implementation codes are publicly available at <https://github.com/liangzhangyong>.

**A. Datasets.** In the subsection, six distinct datasets were utilized, detailed in Tab.S1, encompassing a pair of datasets across three categories: tabular, textual, and image.

**Table S1. A summary of six classification datasets used in our experiments.**

Dataset	Sample Size	Input Dimension	Number of Classes	Minor Class Proportion	Data Type	Source
pol	15000	48	2	0.336	Tabular	(57)
electricity	38474	6	2	0.5	Tabular	(58)
2dplanes	40768	10	2	0.499	Tabular	(57)
bbc	2225	768	5	0.17	Text	(59)
IMDB	50000	768	2	0.5	Text	(60)
STL10	5000	96	10	0.01	Image	(61)
CIFAR10	50000	2048	10	0.1	Image	(62)

**B. Hyperparameters for Data Valuation Methods.** In this subsection, we explore the impact of hyperparameters for marginal contribution-based data valuation methods.

- For LOO (5), we do not need to set arbitrary parameters, maintaining the default parameter values. For the utility function, we choose the test accuracy of a base model trained on the training subset.
- For Data Shapley (7) and Beta Shapley (30), we use a Monte Carlo method to approximate the value of data points. Specifically, the process begins by estimating the marginal contributions of data points. Following this, the Shapley value is computed based on these marginal contributions, serving as the data's assigned value. Accordingly, we configure the independent Monte Carlo chains to 10, the stopping threshold to 1.05, the sampling epoch to 100, and the minimum training set cardinality to 5.
- For DataBanzhaf (31), we set the number of utility functions to be 1000. Moreover, We use a two-layer MLP with 256 neurons in the hidden layer for larger datasets and 100 neurons for smaller ones.
- For InfluenceFunction (32), we also set the number of utility functions to be 1000. Subsequently, the cardinality of each subset is set to 0.7, indicating that 70% of it consists of data points to be evaluated.
- For KNN Shapley (10), we set the number of nearest neighbors to be equal to the size of the validation set. This is the only parameter that requires setting.
- For AME (12), we set the number of utility functions to be 1000. We consider the same uniform distribution for constructing subsets. For each  $p \in \{0.2, 0.4, 0.6, 0.8\}$ , we randomly generate 250 subsets such that the probability that a datum is included in the subset is  $p$ . As for the Lasso model, we optimize the regularization parameter using 'LassoCV' in 'scikit-learn' with its default parameter values.
- For Data-OOB (13), we set the number of weak classifiers to 1000, corresponding to utility function. These weak classifiers are a random forest model with decision trees, and the parameters are set to the default values in 'scikit-learn'.

- Our method, we set the size of the meta-data set to be equal to the size of the validation set. The meta network’s hidden layer size is set at 10% of the meta-data size. For the training parameters, we set the max epochs to 50. Both base optimization and meta optimization use Adam optimizer, with the initial learning rate for out-optimization set at 0.01 and for in-optimization at 0.001. For base optimization, upon reaching 60% of the maximum epochs, the learning rate decays to 10% of its initial value, and at 80% of the maximum epochs, it further decays by 10%. For meta optimization, only one epoch of training is required. To maintain the original training step size, weights of all examples in a training batch are normalized to sum up to one, enforcing the constraint  $|\mathcal{V}(\ell; \theta)| = 1$ , and the normalized weight

$$\eta_i^k = \frac{\mathcal{V}^k(\Phi_i; \theta)}{\sum_j \mathcal{V}^k(\Phi_j; \theta) + \delta(\sum_i \mathcal{V}^k(\Phi_j; \theta))},$$

where the function  $\delta(a)$ , set to  $\tau > 0$  if  $a = 0$  and 0 otherwise, prevents degeneration of  $\mathcal{V}^k(\Phi_j; \theta)$  to zeros in a mini-batch, stabilizing the meta weight learning rate when used with batch normalization.

**C. Pseudo Algorithm.** We provide a pseudo algorithm in Alg 3.

---

**Algorithm 3** Pseudo-code of NDDV training

---

**Input:** Training data  $\mathcal{D}$ , meta-data set  $\mathcal{D}'$ , batch size  $n, m$ , max iterations  $T$ .

**Output:** The value of data points:  $\phi(x_i, y_i; U(S))$ .

- 1: **Initialize** The base optimization parameter  $\psi^0$  and the meta optimization parameter  $\theta^0$ .
  - 2: **for**  $t = 0$  **to**  $T - 1$  **do**
  - 3:    $\{x, y\} \leftarrow \text{SampleMiniBatch}(\mathcal{D}, n)$ .
  - 4:    $\{x', y'\} \leftarrow \text{SampleMiniBatch}(\mathcal{D}', m)$ .
  - 5:   Formulate the base training function  $\hat{\psi}^k(\theta)$  by Eq.17.
  - 6:   Update the base optimization parameters  $\theta^{k+1}$  by Eq.17.
  - 7:   Update the meta optimization parameters  $\psi^{k+1}$  by Eq.17.
  - 8:   Update the weighted mean-field state  $\mu_t^k$  by Eq.32.
  - 9:   Compute the data state utility function  $U_i(S)$  by Eq.38.
  - 10:   Compute the dynamic marginal contribution  $\Delta(x_i, y_i; U_i)$  by Eq.39.
  - 11:   Compute the value of data points  $\phi(x_i, y_i; U(S))$  by Eq.40.
- 

**D. Convergence Verification for The Training Loss.** To validate the convergence results obtained in Theorem 1 and 2 in the paper, we plot the changing tendency curves of training and meta losses with the number of epochs in our experiments, as shown in Fig.S1-S2. The convergence tendency can be easily observed in the figures, substantiating the properness of the theoretical results in proposed theorems.

**E. Data Points Removal and Addition Experiment.** In this section, we consider analyzing the evolution of data points removal and addition in six datasets.

**F. Results on Data State Trajectories.** In this section, we consider analyzing the evolution of data state trajectories in six datasets.

**G. Results on Data Value Trajectories.** In this section, we consider analyzing the evolution of data state trajectories in six datasets.

**H. Additional Results on Elapsed Time Comparison.** In this section, we present comparing the elapsed time of our method with LOO, DataShapley, BetaShapley, and DataBanzhaf in small dataset sizes. A set of data sizes  $n$  is  $\{5.0 \times 10^2, 7.0 \times 10^2, 1.0 \times 10^3, 3.0 \times 10^3, 5.0 \times 10^3\}$ .

**I. Additional Results on The Impact of Adding Various levels of Label Noise.** In this section, we explore the impact of adding various levels of label noise. Here, we consider the six different levels of label noise rate  $p_{\text{noise}} \in \{5\%, 10\%, 20\%, 30\%, 40\%, 45\%\}$ .

**J. Additional Results on The Impact of Adding Various levels of Feature Noise.** In this section, we explore the impact of adding various levels of feature noise. Here, we consider the six different levels of feature noise rate  $p_{\text{noise}} \in \{5\%, 10\%, 20\%, 30\%, 40\%, 45\%\}$ .

**K. Ablation Study.** We perform an ablation study on the hyperparameters in the proposed NDDV method, where we provide insights on the impact of setting changes. We use the mislabeled detection use case and the plc dataset as an example setting for the ablation study.

For all the experiments in the main text, the impact of re-weighting data points on the NDDV method is initially explored. As shown in Fig.S12, the NDDV method enhanced with data point re-weighting demonstrates superior performance in detecting mislabeled data and removing or adding data points. Additionally, in the same experiments, Fig.S13 shows the impact of mean-field interactions parameter  $a$  at 1, 3, 5, 10. It is observed that when  $a = 10$ , the NDDV method exhibits poorer model performance, whereas, for the other values, it shows similar performance. Furthermore, we explore the impact of the diffusion constant  $\sigma$  on the NDDV method. Specifically, we set  $\sigma$

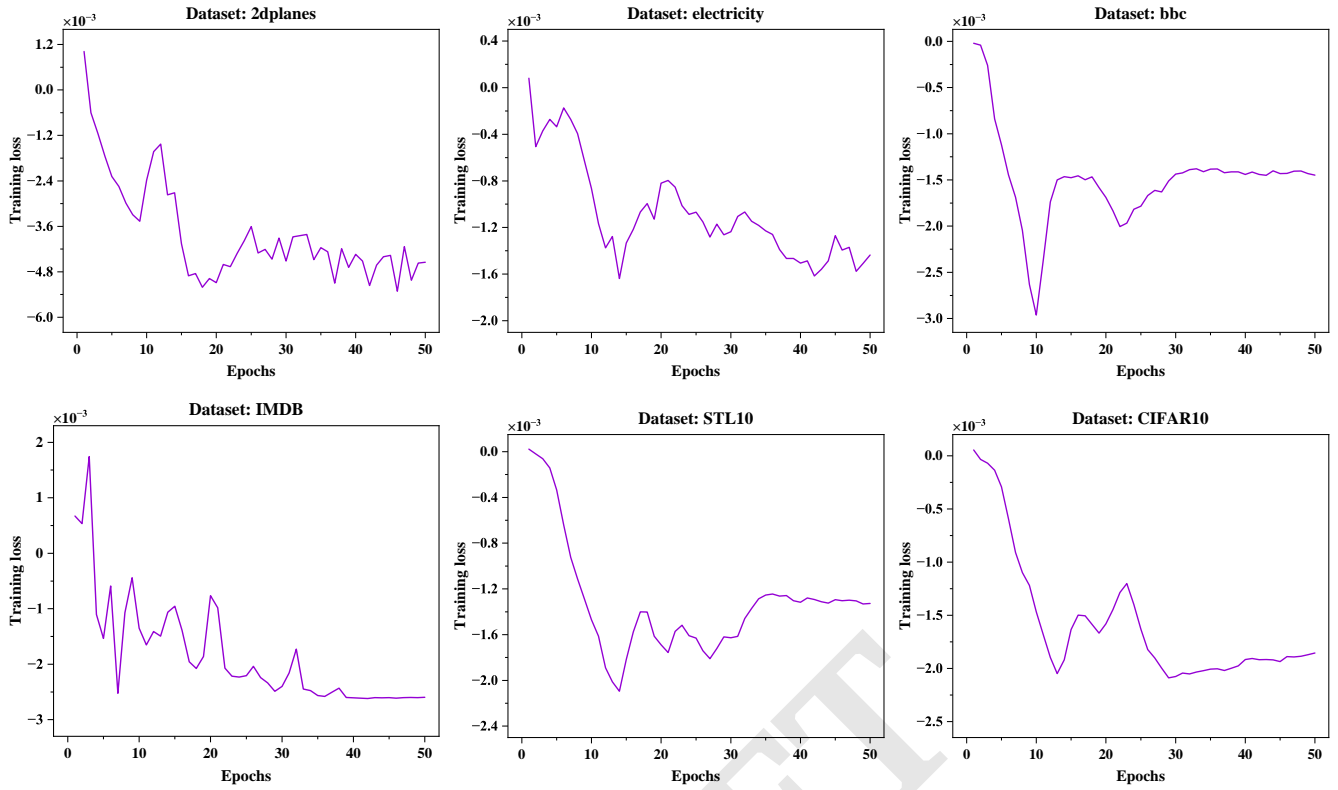


Fig. S1. Training loss tendency curves on six datasets.

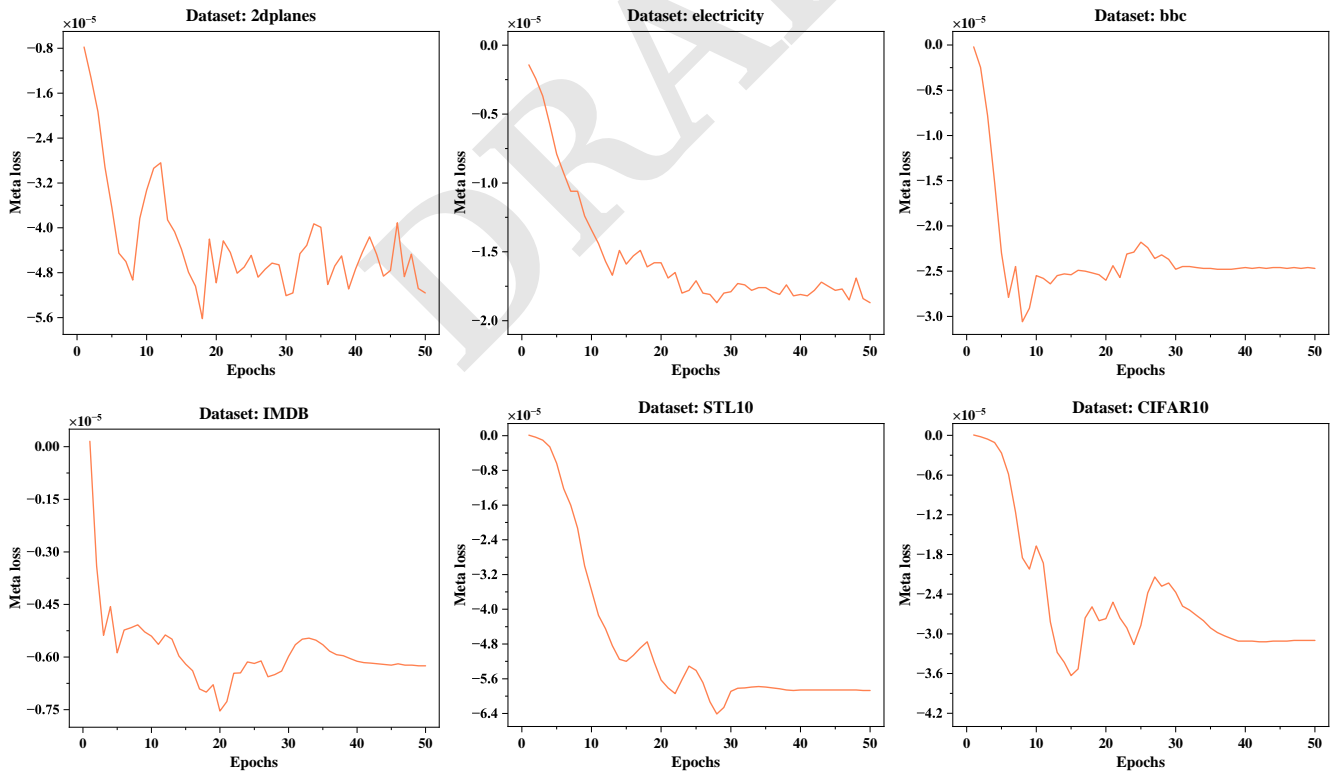


Fig. S2. Meta loss tendency curves on six datasets.

at 0.001, 0.01, 0.1, 1.0 to compare model performance. As shown in Fig.S14, the model performance significantly deteriorates at  $\sigma = 1.0$ . It can be observed that excessively high values of  $\sigma$  increase the random dynamics of the data points, causing the model performance to

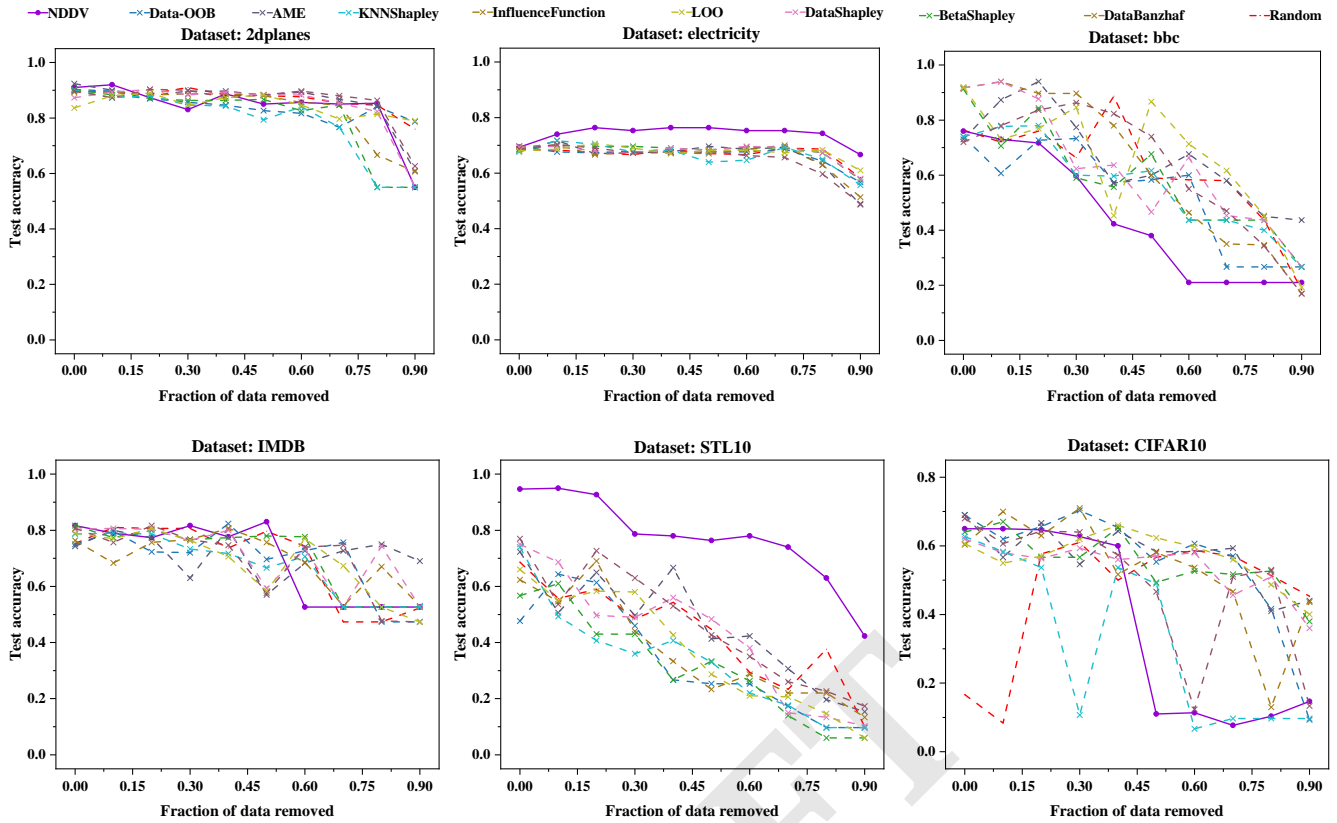


Fig. S3. Removing low value data experiment on six datasets with 10% label noisy rate. Test accuracy curves show the trend after removing the least valuable data points.

randomness. Then, we use the meta-dataset of size identical to the size of the validation set. Naturally, we want to examine the effect of the size of the metadata set on the detection rate of mislabeled data. We illustrate the performance of the detection rate with different metadata sizes: 10, 100, and 300. Fig.S15 shows that various metadata sizes have a minimal impact on model performance. Finally, we analyzed the impact of the meta hidden points on model performance. As shown in Fig.S16, it is an event in which the meta hidden points are set to 5, and there is a notable decline in the performance of the NDDV method. In fact, smaller meta hidden points tend to lead to underfitting, making it challenging for the model to achieve optimal performance.

Table S2. F1-score of different data valuation methods on the different label noise rates. The mean and standard deviation of the F1-score are derived from 5 independent experiments. The highest and second-highest results are highlighted in bold and underlined, respectively.

Noise Rate	LOO	Data Shapley	Beta Shapley	Data Banzhaf	Influence Function	KNN Shapley	AME	Data -OOB	NDDV
5%	0.09±	0.12±	0.11±	0.09±	0.11±	0.17±	0.01±	0.62±	<b>0.74±</b>
	0.003	0.007	0.008	0.004	0.003	0.003	0.009	0.002	0.003
10%	0.16±	0.19±	0.19±	0.18±	0.18±	0.30±	0.18±	0.74±	<b>0.76±</b>
	0.007	0.010	0.009	0.005	0.003	0.003	0.010	0.002	0.003
20%	0.30±	0.25±	0.25±	0.31±	0.31±	0.45±	0.010±	<b>0.79±</b>	<u>0.77±</u>
	0.005	0.008	0.008	0.002	0.002	0.004	0.009	0.001	0.001
30%	0.39±	0.52±	0.51±	0.42±	0.42±	0.55±	0.46±	<b>0.80±</b>	<u>0.78±</u>
	0.003	0.012	0.010	0.002	0.008	0.002	0.011	0.001	0.004
40%	0.54±	0.55±	0.56±	0.48±	0.46±	0.60±	0.58±	0.73±	<b>0.74±</b>
	0.008	0.008	0.008	0.003	0.004	0.002	0.010	0.001	0.002
45%	0.55±	0.55±	0.62±	0.48±	0.48±	0.56±	0.27±	0.63±	<b>0.67±</b>
	0.007	0.008	0.009	0.003	0.001	0.004	0.009	0.001	0.004

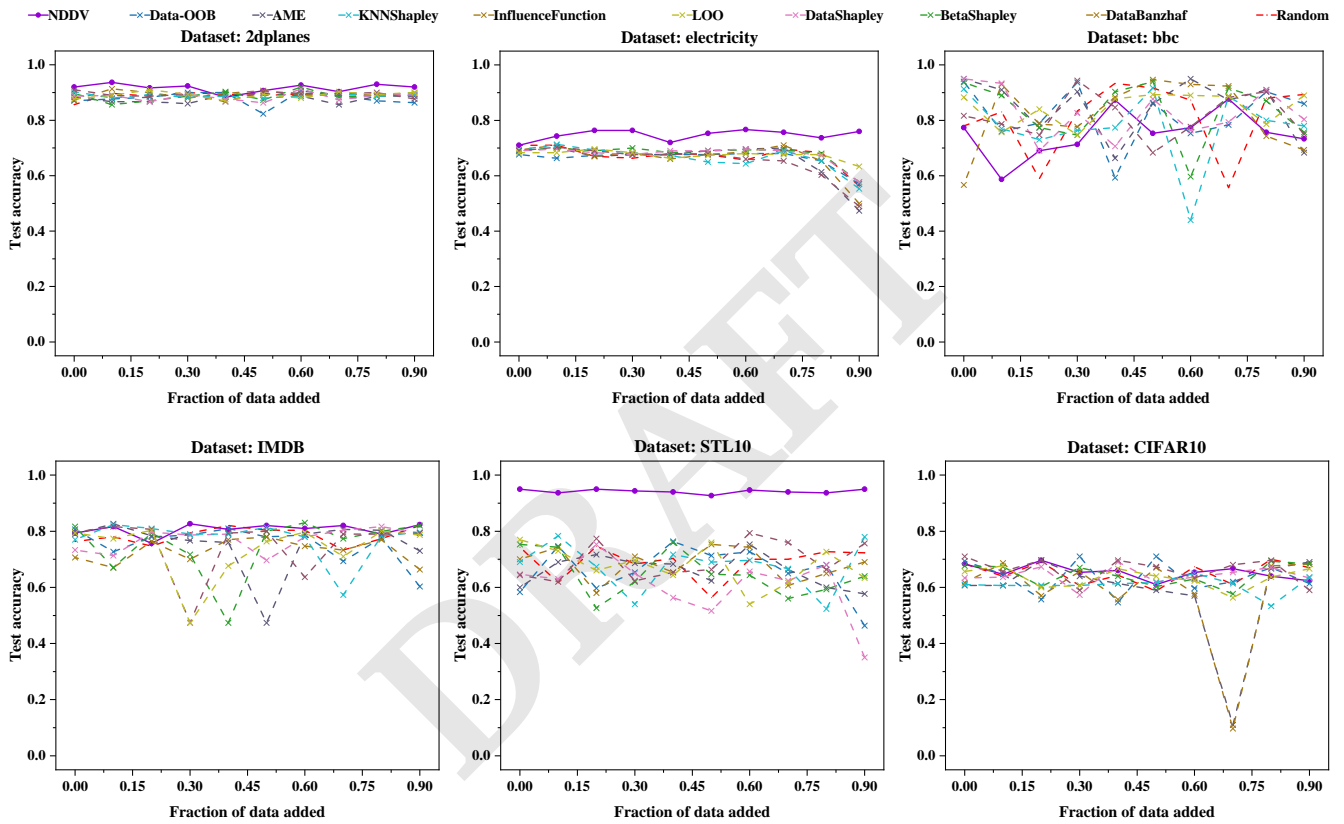


Fig. S4. Adding high value data experiment on six datasets with 10% label noisy rate. Test accuracy curves show the trend after removing the most valuable data points.

**Table S3. F1-score of different data valuation methods on the different feature noise rate. The mean and standard deviation of the F1-score are derived from 5 independent experiments. The highest and second-highest results are highlighted in bold and underlined, respectively.**

Noise Rate	LOO	Data Shapley	Beta Shapley	Data Banzhaf	Influence Function	KNN Shapley	AME	Data -OOB	NDDV
5%	0.09±	0.10±	0.10±	0.07±	0.10±	0.17±	0.09±	0.15±	<b>0.30±</b>
	0.007	0.009	0.007	0.004	0.003	0.003	0.012	0.002	0.006
10%	0.18±	0.18±	0.18±	0.15±	0.15±	0.15±	0.18±	0.21±	<b>0.46±</b>
	0.007	0.010	0.009	0.005	0.003	0.003	0.010	0.002	0.003
20%	0.33±	0.01±	0.01±	0.28±	0.30±	0.27±	0.01±	0.32±	<b>0.34±</b>
	0.005	0.008	0.008	0.002	0.002	0.002	0.010	0.001	0.003
30%	0.43±	0.01±	0.01±	0.33±	0.35±	0.35±	0.01±	0.37±	<b>0.45±</b>
	0.008	0.012	0.010	0.002	0.008	0.002	0.012	0.001	0.005
40%	0.51±	0.01±	0.01±	0.01±	0.37±	0.40±	0.01±	0.43±	<b>0.57±</b>
	0.008	0.010	0.008	0.003	0.004	0.002	0.010	0.001	0.004
45%	0.53±	0.01±	0.01±	0.50±	0.47±	0.39±	0.01±	0.46±	<b>0.62±</b>
	0.007	0.011	0.009	0.003	0.001	0.002	0.012	0.001	0.006



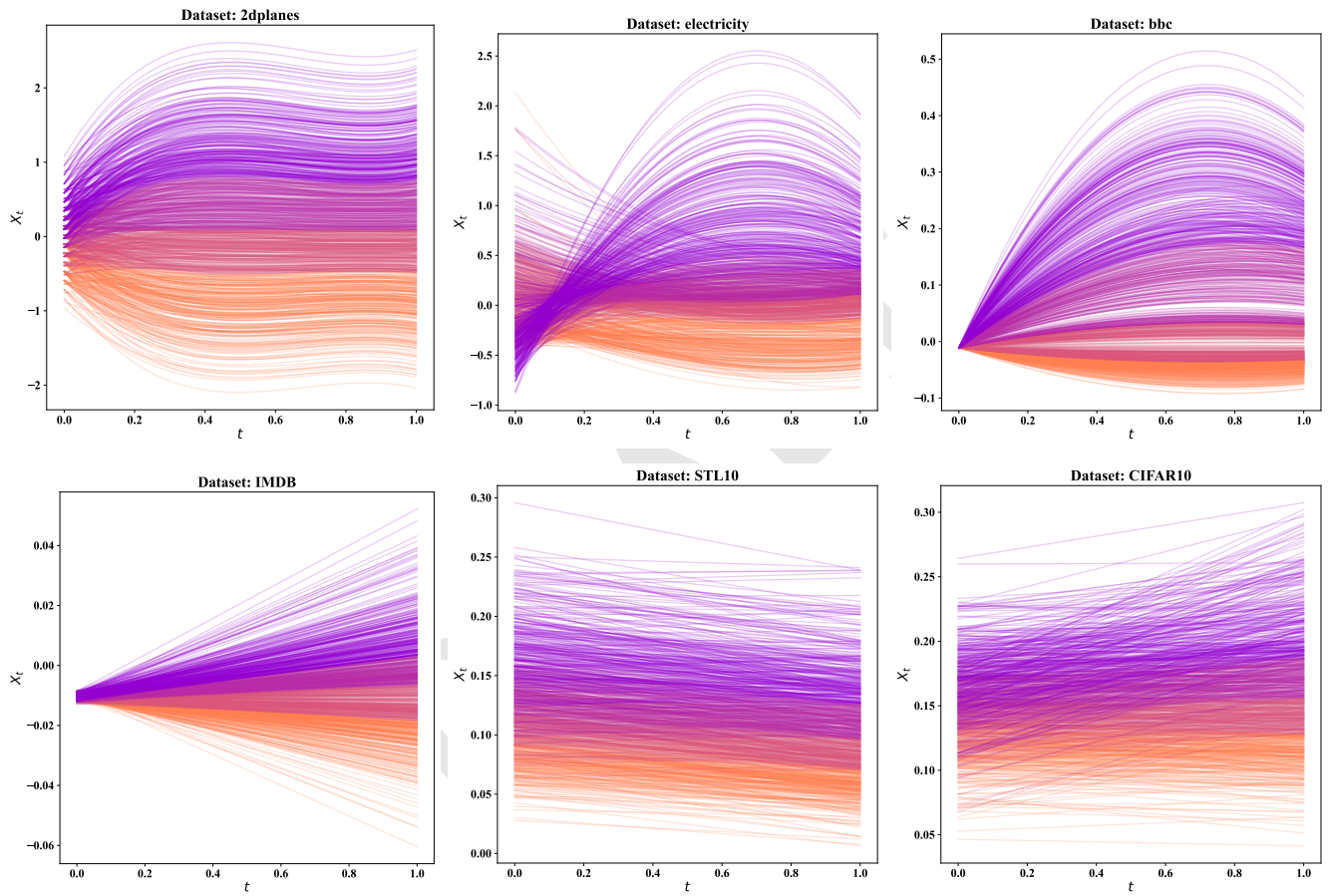


Fig. S5. Data State Trajectories on six datasets.

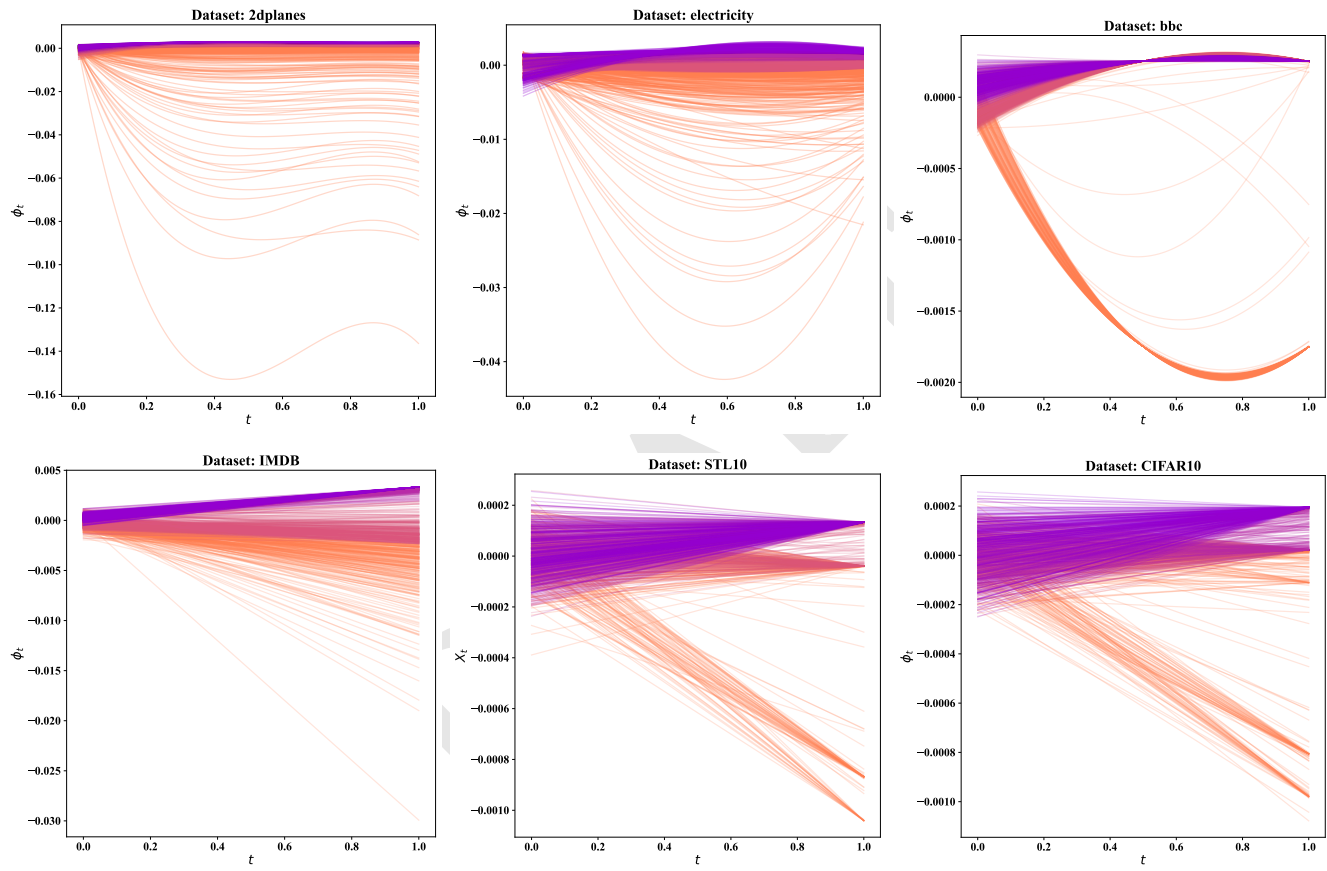
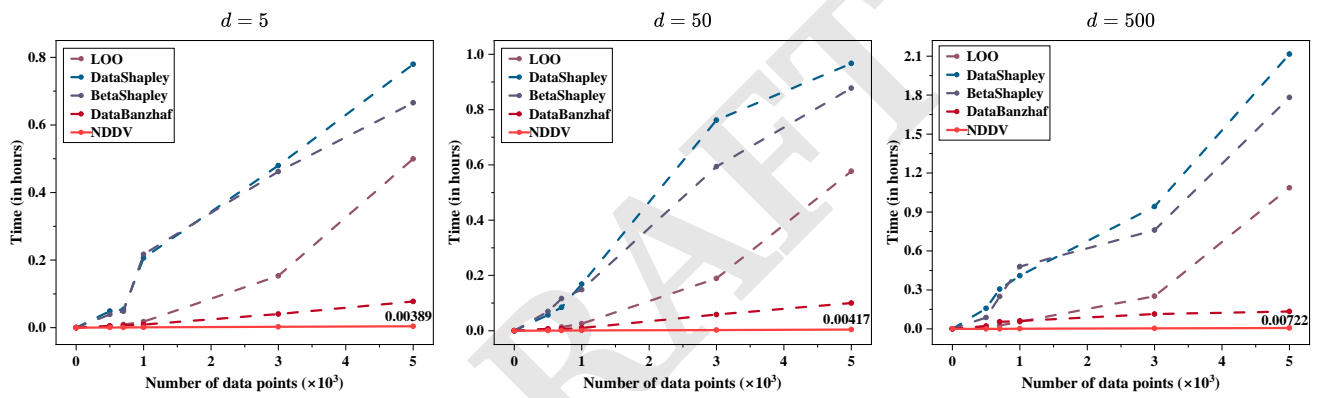


Fig. S6. Data value Trajectories on six datasets.



**Fig. S7. Elapsed time comparison between LOO, DataShapley, BetaShapley, DataBanzhaf, and NDDV.** We employ a synthetic binary classification dataset, illustrated with feature dimensions of (left)  $d = 5$ , (middle)  $d = 50$  and (right)  $d = 500$ . As the number of data points increases, our method exhibits significantly lower elapsed time compared to other methods.

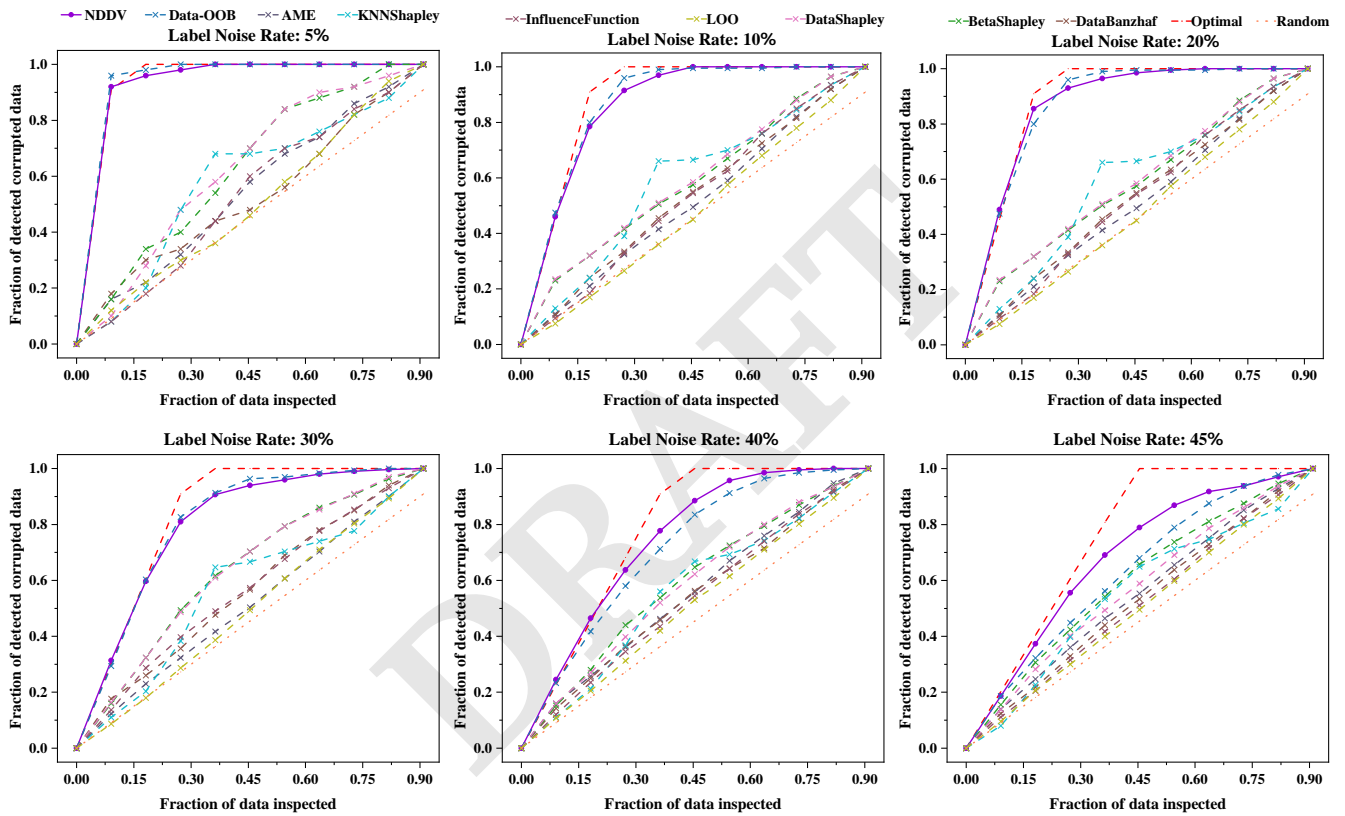


Fig. S8. Discovering corrupted data on the six different levels of label noise rate.

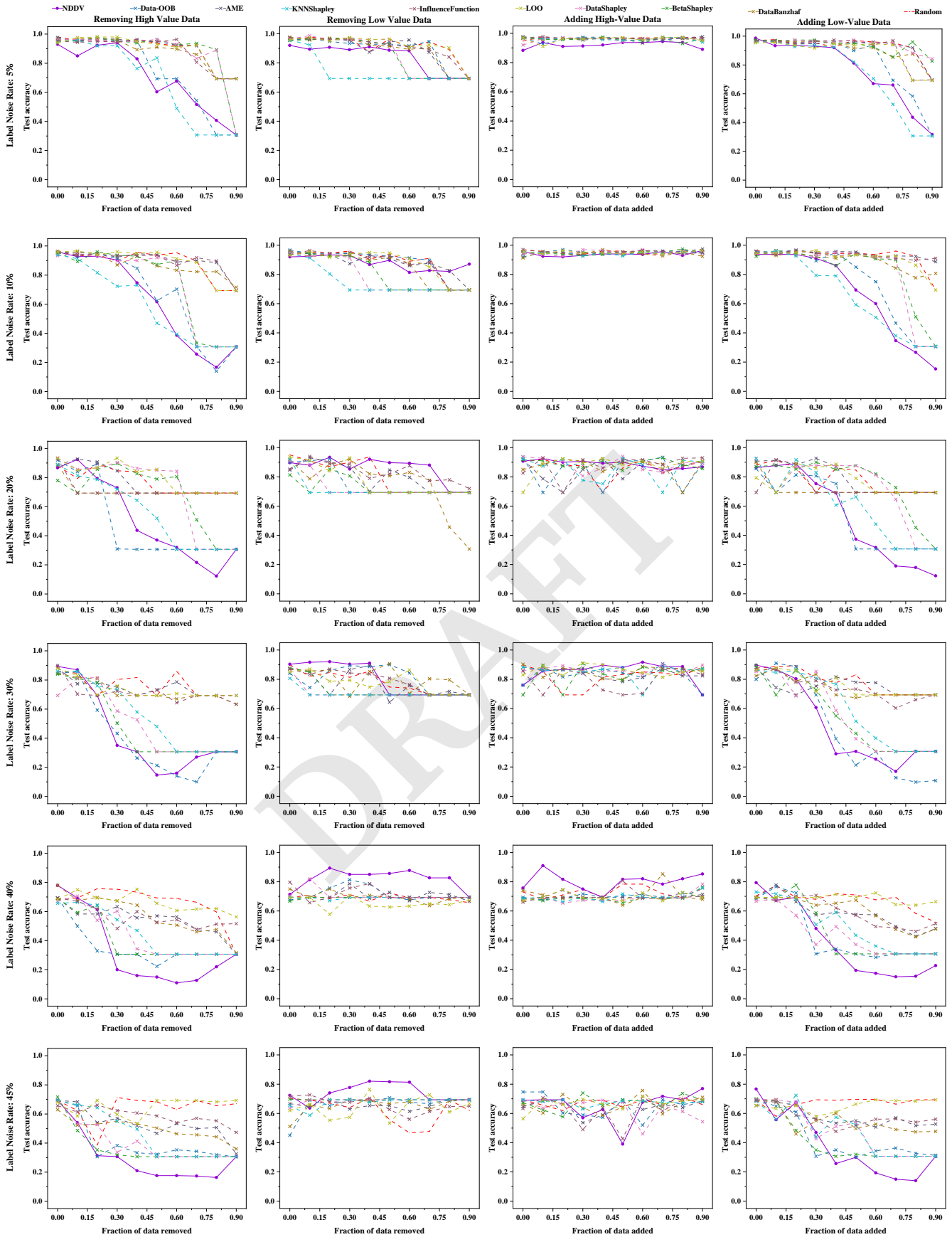


Fig. S9. Data points removal and addition experiment on six different levels of label noise rate. (First column) Removing high value data experiment. (Second column) Removing low value data experiment. (Third column) Adding high value data experiment. (Fourth column) Adding low value data experiment.

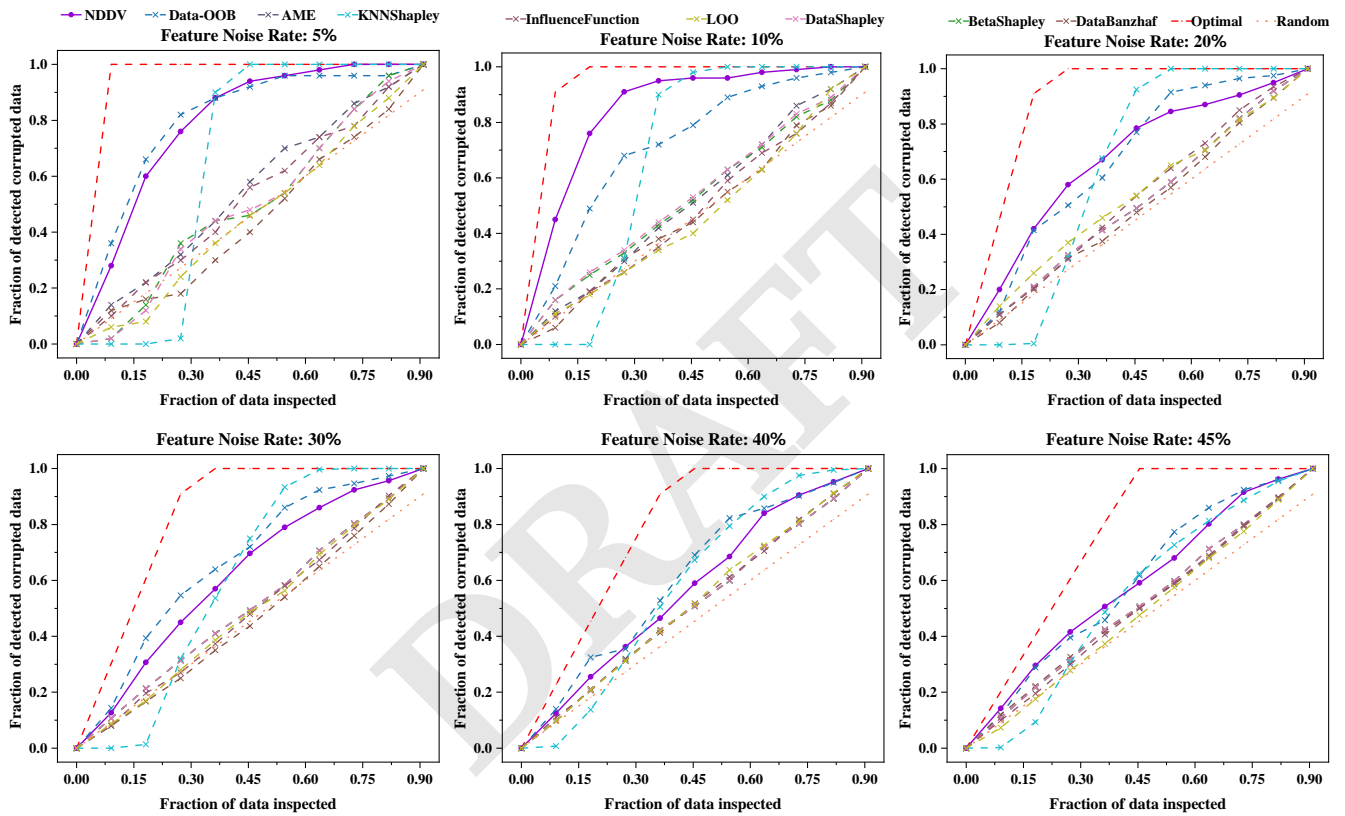


Fig. S10. Discovering corrupted data on the six different levels of feature noise rate.

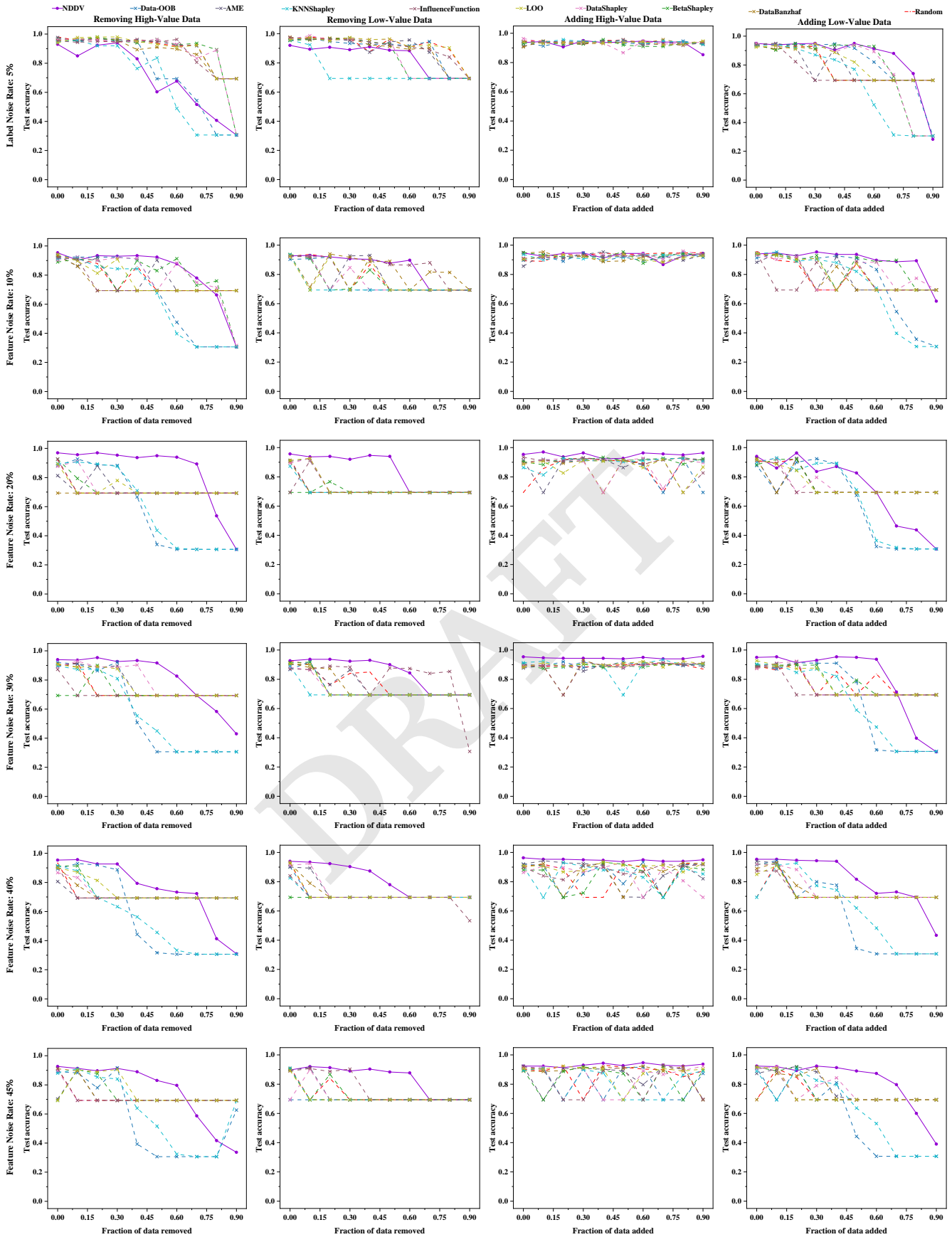


Fig. S11. Data points removal and addition experiment on six different levels of feature noise rate. (First column) Removing high value data experiment. (Second column) Removing low value data experiment. (Third column) Adding high value data experiment. (Fourth column) Adding low value data experiment.

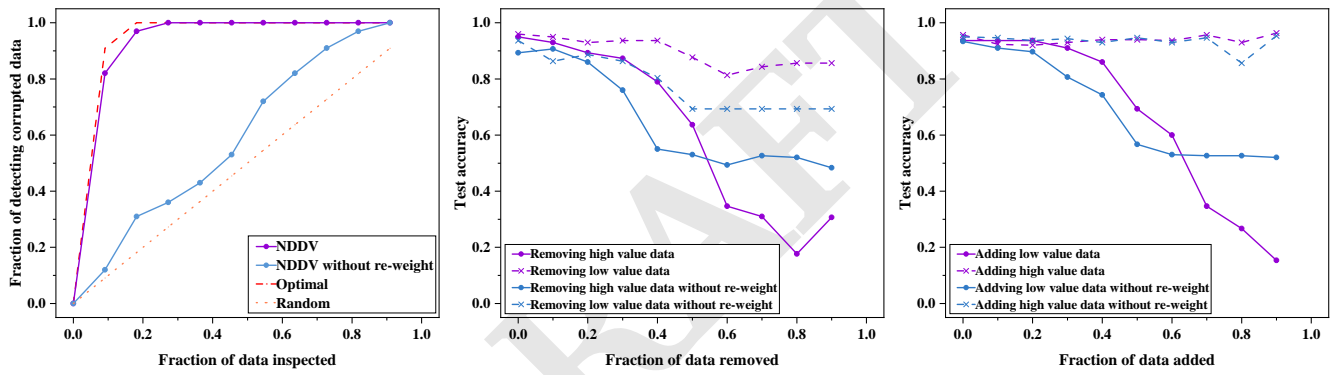


Fig. S12. Impact of data points re-weighting.



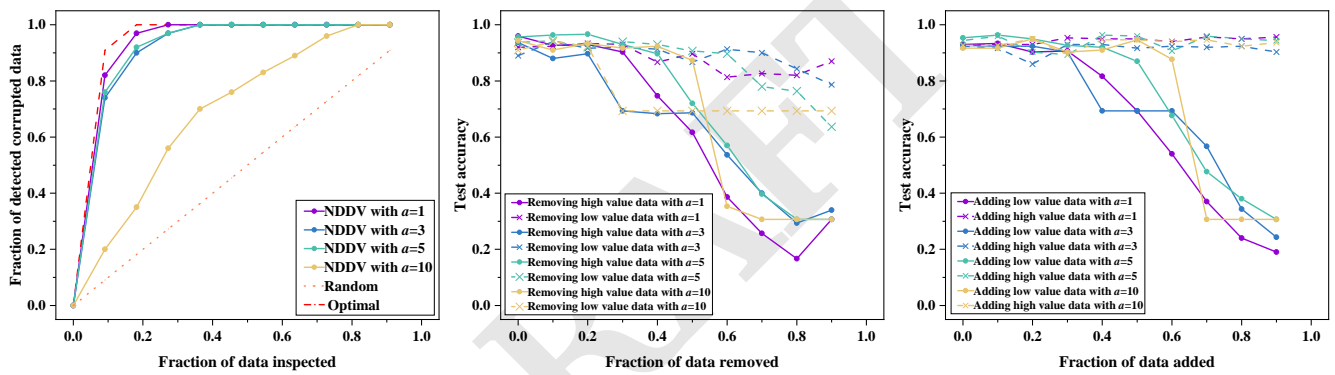


Fig. S13. Impact of the mean-field interactions.

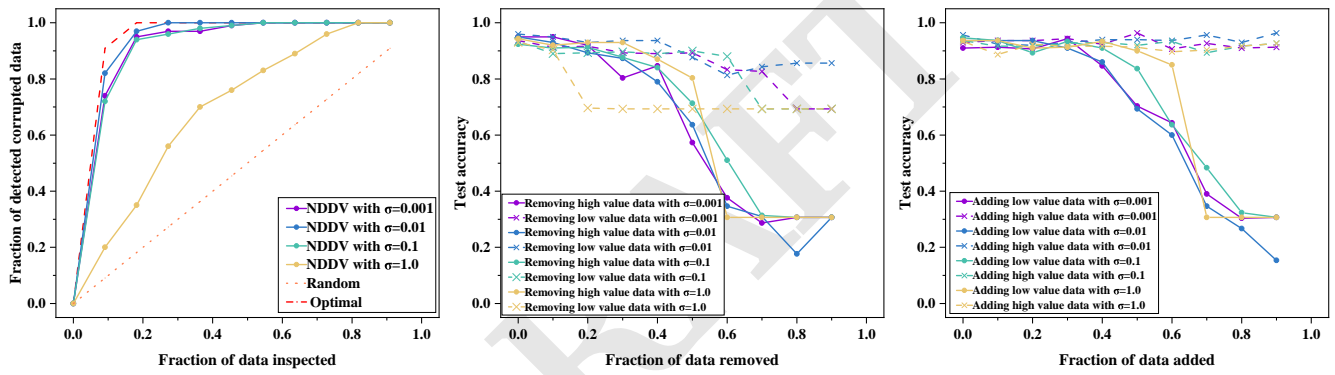


Fig. S14. Impact of the diffusion constant.

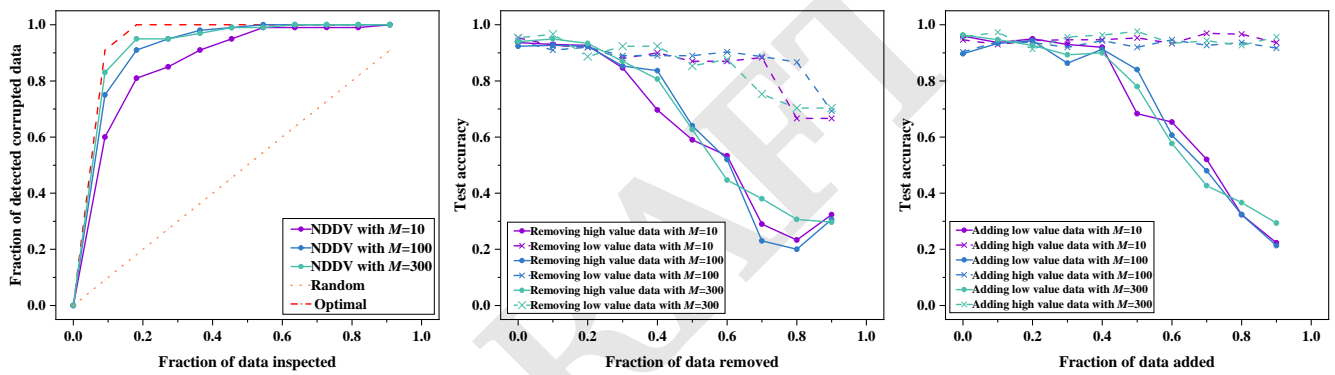


Fig. S15. Impact of the metadata sizes.

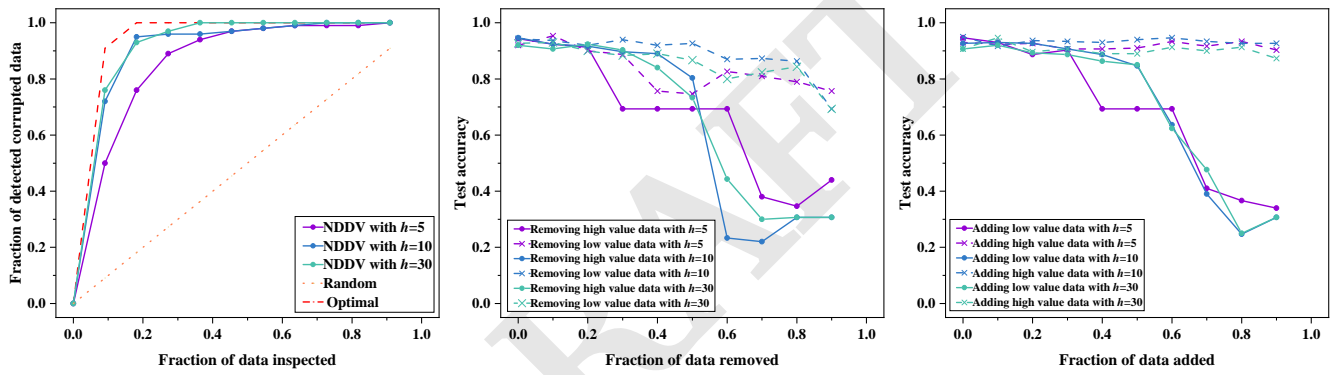


Fig. S16. Impact of the meta hidden points.